Compatibility design of retrofit T5 LED tube

Passive and active methods

TUDelft

Compatibility design of retrofit T5 LED tube
Passive and active methods

by

Fanyu Kong

to obtain the degree of Master of Science
at the Delft University of Technology,
to be defended publicly on Wednesday July 26, 2017 at 14:00 PM.

An electronic version of this thesis is available at `http://repository.tudelft.nl/`.

ŤUDelft

Summary

LED lamps become more and more economically attractive in the lighting market, primarily thanks to their great energy saving, long lifetime and ever decreasing cost compared with the conventional lighting solutions, such as incandescent or fluorescent ones. A traditional fluorescent lighting system consists of a fluorescent lamp(s) and a magnetic/electronic ballast. A direct replacement of a fluorescent lamp by a LED lamp with the same form factor and pin connection avoids any rewiring or removal of the ballast, which is known as the retrofit concept. The retrofit LED lamps further guarantee a minimal total cost of ownership.

This work investigates the compatibility issues between the T5 Retrofit LED lamps and the legacy electronic ballasts. The compatibility design focuses on the following points: 1. The LED lamps should generate stable light output at the specified lumen level; 2. The lifetime and reliability of the LED lamps and ballasts fulfill the given specifications; 3. The driver design should fit into the T5 tubes.

Two methods to ensure the compatibility have been studied, a passive method and an active method. The passive method utilizes inductance and capacitance to increase the load impedance seen by the ballasts so as to reduce the ballast output current and control the ballast thermal issues. Four structures with inductance and capacitance haven been analyzed by means of mathematical analysis and simulations. The active method realizes the LED current control that is absent in the passive method. Efforts are conducted to reduce the size of the two proposed active circuits. After the simulation analysis of each designs, a demonstration board has been built for experimental verification.

Combining the passive methods with the active ones, four possible solutions that satisfy the design requirements are found. The comparisons between these solutions and the design suggestions are given in the last chapter.

Acknowledge

Fanyu Kong
Delft, July 2017

I would like to show my gratitude to my supervisors, Dr. Ir. Yi Wang and Prof. dr. eng. Pavol Bauer, who have provided me with valuable guidance in every stage of my thesis. Their enlightening instructions and patience enlighten me not only in this thesis but also in my future study.

I shall also extend my thanks to the committee member Dr.ir. Jose L. Rueda Torres and Dr. Zian Qin for attending my thesis defense and evaluating my thesis work.

Thanks to my colleagues in R&D department (Philips Lighting) for their impressive kindness and help. It is a great pleasure to work with them. I am also appreciated my friends being there for me. With their support and company, I overcame many difficulties during the past nine months. I have learned a lot from their positive attitude to life as well as study.

Thanks for my parents, their selfless love is the most precious gift in my life.

Contents

List of Figures

<div align="right">

1

</div>

Introduction

1.1. Background

Light-emitting diode (LED) is becoming a compelling alternative to replace traditional light source such as incandescent lamps, halogen lamps and fluorescent lamps in terms of lifetime and energy saving.

With a long history, incandescent lamps still have been used in indoor system now. However, the most energy (about 95 %) of incandescent lamps is consumed by heat, leading to a low efficiency. Thus for incandescent lamps the luminous efficacy is around 12-18 Lm/W (Lumens per watt) and lifetime is only about 2000 hours [1]. Therefore, the incandescent lamp is getting out of phase. The halogen lamp is a type of incandescent lamps, but it is filled with halogen gas, which brings tungsten particles back to the filament. This circulation creates longer lifetime, higher luminance and higher energy efficiency (about 10-20% higher than traditional incandescent lamps [2]).

The fluorescent lamp relies on the low-pressure mercury vapor discharging to produce visible light. Although works with cool light and slow start-up time, the fluorescent lamp still owns many domestic lighting applications. The luminous efficacy of fluorescent lighting is more than 55 Lm/W and the lifetime is around 8000-15000 hours [3]. However, toxic material in this lamp needs to be disposed carefully and ballasts are indispensable for current control.

As a semiconductor light source, LED produces light when they are forward-biased. With more than 30000-hour lifetime and typically 80-100 Lm/W luminous efficacy (for new mid-power LED products, 180 Lm/W), the performance of LEDs is attractive in the market. Compared with other lighting options, LED is more expensive. However, due to the high energy saving and long lifetime, the payback time of LEDs is accepted by customers. Therefore, LED lamps become more popular.

1.2. TL fluorescent lamp and TLED retrofit lamp

1.2.1. TL fluorescent lamp system

The TL fluorescent lamp is welcomed in indoor lighting applications including offices, hotels, cabinets, showcase and furniture. "TL" stands for "Tube Luminescent" and the number following "TL" represents the diameter of the lamp in eights of an inch. For example, TL5 lamps have a "5/8" inch diameter, which means this type of lamp is smaller than the TL8 lamp and TL12 lamp. Besides, miniature bi-pin sockets can fit TL5 lamps, while TL8 lamps need medium bi-pin sockets. These characteristics have made TL5 lamps cannot be used to replace other types of lamps and vice versa.

The smaller lamp diameter increases optical control efficiency and flexibility of luminaries, and the higher optimal temperature may lead TL5 to be precise in closed luminaries than open luminaries. Besides, the smaller diameter makes it easier to design optical part: distributing light in the intended directions. For above reasons, TL5 lamps are more desirable for indirect lighting, high-bay applications, and wall-washing applications. TL5 lamps provide standard output and high output(HO). The standard power levels of TL5 lamps are 14, 21, 28, and 35 watts, and the high output TL5 lamps are available in 24, 39, 54, and 80 watts. The high light output produces a same illuminance level with fewer luminaries than other fluorescent lamps, while the TL5 HO lamp may have a slightly lower efficiency than the standard TL5 lamp due to more losses from the high ballast current.

A typical fluorescent lamp system is illustrated in Fig.1.1. The basic working principle of fluorescent lamps is the discharge of low-pressure. Fluorescent lamps usually require a high voltage to ignition and will exhibit a negative impedance after the current flows in (increasing of free electrons lowers conduction resistance of the fluorescent lamp), which means the more current goes in will lead to a lower voltage drop over the fluorescent lamp. Therefore, it cannot connect to the AC mains directly. Because of the characteristic of fluorescent lamps, a ballast is needed to achieve current limiting, preheating of filaments and providing start voltage. Besides, the operation frequency needs to be high enough (8-10 times higher than the mains frequency) to prevent from restarting in each cycle.
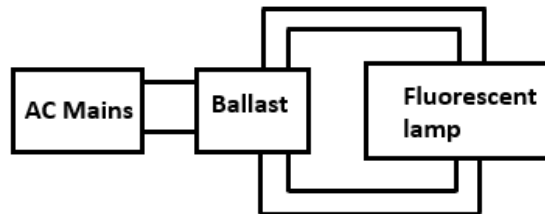
Figure 1.1: A typical fluorescent system

Generally, fluorescent ballasts can be classified into electronic ballast (high frequency) and magnetic ballast (50/60 Hz) which are introduced in details in Chapter 2. Basically, the magnetic ballast uses bulky transformers or inductors (especially in T5 and T8 system due to the small tube size) to regulate current and works in the AC mains frequency. This ballast may cause visible flickers due to the low operation frequency. Electronic ballasts work with tens of kHz frequency and more complex structure (including the PFC circuit, current regulation and control circuit and etc.) which leads to a higher efficiency. With small size, flicker eliminated and high efficiency, the electronic ballast is more competitive in the market. In this thesis, all designs focus on electronic ballasts based on the fluorescent lamp system.

1.2.2. TLED retrofit lamp system

TLED, as known as tubular LED, is one type of the LED, applied in wide applications. The TLED retrofit lamp is a direct replacement product of TL fluorescent lamps, which means no rewiring or fixture open is required by retrofit lamps. Besides, the form factors and connection pins of retrofit lamps are the same as fluorescent lamps. Thus the need to replace and recycle fluorescent tubes is reduced. Compared with 100 lm/W Luminous efficacy of TL fluorescent lamps, the typical efficacy of TLED system can reach 150 lm/W. In Fig.1.2 the TLED retrofit lamp with an electronic ballast is shown[4]. The pin safety circuit and the LED driver with filament emulation are located on PCB-A and PCB-B respectively. Besides, designs in later chapters should be fitted in PCB-B. The filament emulation simulates the filament in fluorescent lamps to match the starting character of ballasts. The typical filament circuit is consist of a string of SMD resistors, a current limiting element (eg.

a thermal fuse in Fig. 1.3) and a voltage limiting element in parallel with filament resistors. In a fluorescent lamp, there is a conductive path only after the ignition happens, therefore the tube is safe when disconnected from the mains. But in the LED case, two ends of the tube are conductive and safety issue should be reconsidered. A pin safety circuit is added to solve this problem. An efficient method is the mechanical based relay pin safety circuit. The relay inside the tube is closed when both ends of the lamp are powered on and keeps open when only one end is energized [4]. The main function of the LED driver is to regulate and control the LED current, and in this thesis all designs will focus on this driver block.
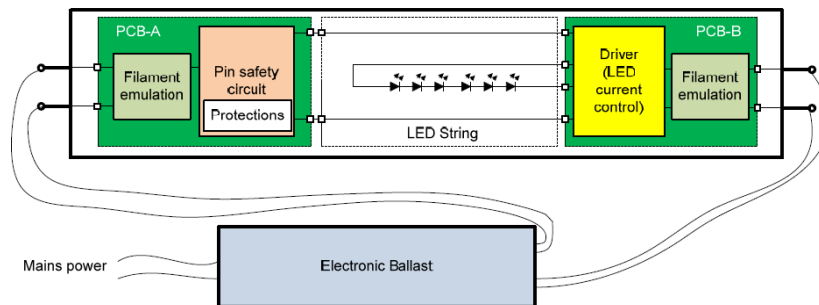
Figure 1.2: TLED driver architecture with two separate PCBs on bothe ecaps[4]

The LED is a p-n junction diode, while the ballast output is an AC current. Therefore, the rectification part is needed, which can be achieved by a rectifier and large capacitor between the ballast and LED load. Fig. 1.3 presents the practical driver PCB. The filament emulation, thermal fuses and output capacitor of the T5 driver are shown on the top side. On the bottom side, the rectifier is settled. The schematic of this simplest driver is shown in 1.4.

Figure 1.3: A practical driver PCB's on both ends of a TLED tube

1.3. Problem statement

A LED driver in the simplest form that can connect with a fluorescent ballast consists of a diode rectifier and a buffer capacitor as shown in 1.4.
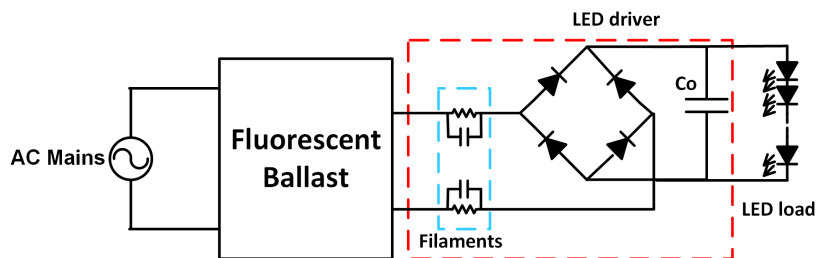
Figure 1.4: The LED driver in the simplest form

The problems of the simple and cheap driver are as follows: Firstly, the ballast current becomes higher than the fluorescent load condition, which may lessen the lifetime of ballasts. It is because that the impedance of fluorescent lamp changes during the start stage, output circuit will make

the impedance match and lead the output of inverter stage change to a certain operation point. That makes the ballast work as a load-dependent current source. Different from a fluorescent lamp, the input impedance of an LED load is highly non-linear. When facing the LED load, the input impedance is relatively low, resulting in a higher ballast current compared with fluorescent case. Five TL5 HO 80W ballasts are tested with the LED load and related electrical parameters are shown in Table1.1. The first ballast is dimmable, and others are non-dimmable. For TL5 HO 80W ballasts, the test current of the reference ballast is 550 mA, only one ballast in the table meets this requirement with the LED load. Furthermore, for the power feedback ballast, the operation frequency is not fixed. The LED load needs relatively lower power than the fluorescent lamp, which means this type ballast tends to reduce the frequency resulting in a higher the ballast current [5].

Table 1.1: Parameters of different types of ballast

80W ballast overview	Type of ballast	Charateristic	L_r [mH]	C_r [nF]	f_r [kHz]	$f_{operation}$ [kHz]	Ballast current with LED load [mA]
Helvar	EL1x80Sc	Dimmable	1.34	3.9	69	35.6	680.12
Helvar	EL1x80ngn5	Non-Dimmable	1.1	3.3	83.6	41	713.31
BAG	BCS80.1FX-11/220-240	Non-Dimmable	1.3	4.7	64.4	42	592.96
Philips	HF-P 180 TL5/PL-L3	Non-Dimmable	1.3	5.6	59	44.8	556.86
Vossloh	ELXc180.866	Non-Dimmable	1.24	5.6	60	46.2	566.03

Secondly, the LED current is uncontrolled. The ballast output current is not a constant value even in the same power level. Besides, due to the luminous efficacy difference between LED and fluorescent lamp, the power rating needs to be taken into account in substitution. For example, the light output of 80W T5 HO fluorescent lamp is 7000 lm, while in TLED system, only 5600 lm (power is only 35W) is needed because the cost of the LED is high and human eyes cannot distinguish the slight difference of the light. The power intake of LED tubes should be reduced compared to fluorescent tubes (lamp power reduction by up to 50% compared to fluorescent tubes). Therefore the LED current should be controlled to match the power requirement by the LED driver when connected to different ballasts. Only through a diode rectifier and a output capacitor, apparently the LED cannot be controlled.

Another problem regarding to the design is that the required functions should be realized in a small T5 form factor. And the PCB size in the T5 LED tube is $40 \times 10 mm^2$. Hence the size of the design is limited.

The existing literature related to the compatibility design is limited, because the technique is still immature. One possible solution is based on controlling input impedance of the rectifier next to the output stage of ballasts [6]. While the passive component cannot be changed to other different ballasts, the compatibility of this solution may be effected. Also, the available volume for LED driver in TL5 tube is smaller than TL8 tube in which the existing design fitted.

1.3.1. Requirements definition
Based on the described problems, the requirements of this project are given as follows.

Compatibility
The compatibility of the LED driver contains three concerns. Firstly, the stable light level is required, which means no visible flicker exists in the system; Secondly, thermal and electrical stress of both ballasts and TLED lamps should be controlled within an acceptable range for a guaranteed reliability and lifetime of the products; Thirdly, the ballast current with LED loads should be limited less than 120% compared with the fluorescent situation.

Light consistency

For different ballasts, even at the same power level the output current could be different. The current through the LED needs to maintain a stabilized illumination. Power control and current regulation are required in LED drivers.

Size limitation

The TL5 fluorescent lamp is the smallest in dimension (diameter=16.8 mm) compared to other commonly seen linear fluorescent lamps, but the power to be processed is not smaller. The dimension of PCB for the LED driver and filament emulation is $40 \times 10mm^2$. The retrofit LED lamp with the integrated electronic driver is primarily challenged with limited area and high lamp power, in other words, high power density.

The main requirements are mentioned above. There are some other requirements which should be concerned. The efficiency of the added solution should be as high as possible. Meanwhile, it is also reasonable to take the cost and the effect on ballast current into consideration.

1.4. Research goals and Approaches

Focusing on the compatibility of TLEDs and TL5 fluorescent ballasts, the goals of this thesis are defined as follows:

1. Analyze various TL5 ballast structures and working principles.

2. Explore the appropriate passive matching solutions which improve the compatibility of retrofit T5 tubes.

3. Explore the possibility of active solutions that further reduces the driver volume and regulates the LED current compared to the passive solution.

4. Experimental verification and validation of the active solutions, and develop a form-fit demo of the best solution.

The research approaches are given as below:

1. Investigate the ballast working principle and define the reasons why the ballasts are not compatible with the LED drivers in the simplest form.

2. Develop analytical and simulation models to optimize the parameters of the passive matching network.

3. Build SPICE simulation models to analyze the possible active concepts.

4. Experimental validation of the active methods and compare them with the passive method.

1.4.1. Passive method

Shown in Fig.1.5, the basic concept of this method is to use lossless passive components to change the load impedance seen by the ballast, which components will influence the ballast current.
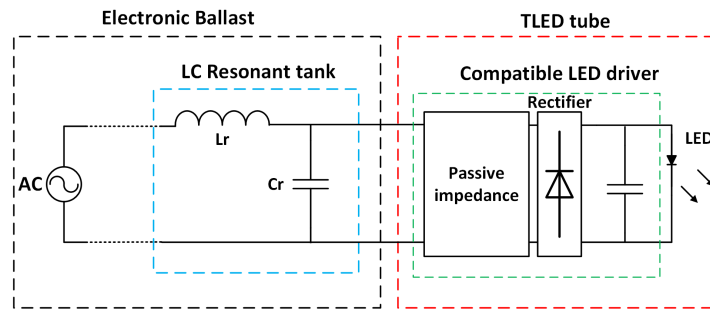
Figure 1.5: The block diagram of the passive method applied in the LED driver

Compared to existing solutions[6], this project will deal with a smaller available volume (the TL5 tube) to setup the components. Besides, more than one type of ballasts should be considered. In order to match different 80W ballasts by the added components, the trade-off analysis of different ballasts should be conducted.

Because no active component is applied in this method, the design is an open loop system. In order to improve the compatibility and stability of the T5 system with different ballasts, active components should be contained in the design. Because only with those components can a system become a closed loop system, which system is more likely to have higher compatibility and stability than that of an open loop system. In this thesis, more attention will be given to the active methods.

1.4.2. Active method

By adding a closed-loop switch mode power supply (SMPS) module into a LED driver, the LED current can be regulated. This method is mainly investigated in this thesis. The start point of this method is similar to the DC-DC converter case in [9].
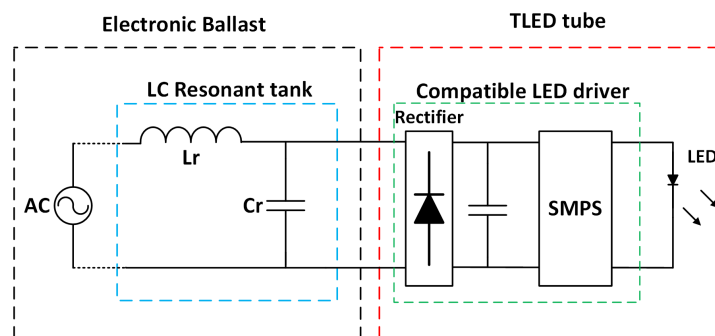
Figure 1.6: The block diagram of the SMPS method applied in the LED driver

The basic concept is shown in Fig. 1.6. It can be seen from the figure that the output of ballast is generally an AC current source. In order to apply the DC-DC converter topology a rectifier is needed at the input of the SMPS circuit. To make sure the ballast sees a resistive impedance at the ballast output frequency, the switching frequency of the SMPS circuit should be 5 to 10 times higher than the ballast frequency.

Besides, a current charge pump concept (see Fig. 1.7) is proposed. The circuit size could shrink further through this method.
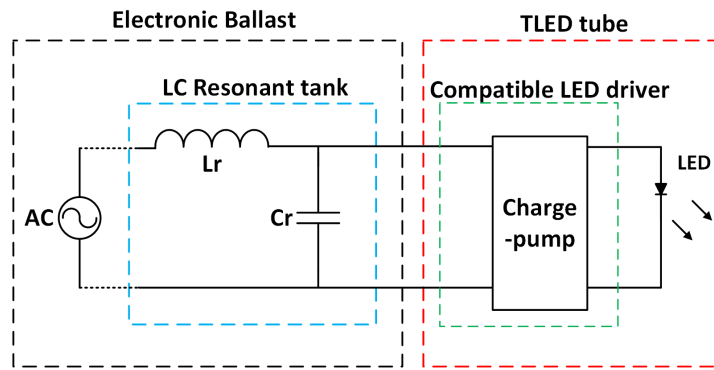
Figure 1.7: The block diagram of the Charge-pump method applied in the LED driver

1.5. Structure of this thesis

Chapter 2 consists of the overview of ballast structures and ballast applications in fluorescent and LED systems. Moreover, related information about ballast LC resonant circuit structures and parameter ranges are introduced as well.

In Chapter 3, the passive approach is presented in details with mathematical analysis and simulations of the circuit.

Chapter 4 presents active approaches with conceptual designs and validations.

Chapter 5 includes the evaluation of all approaches, and the suggestions for the future work.

2

Overview of the fluorescent lamp and ballast structures

2.1. Working principle of fluorescent lamps

The tubular fluorescent lamp works on the low-pressure mercury discharge principle.
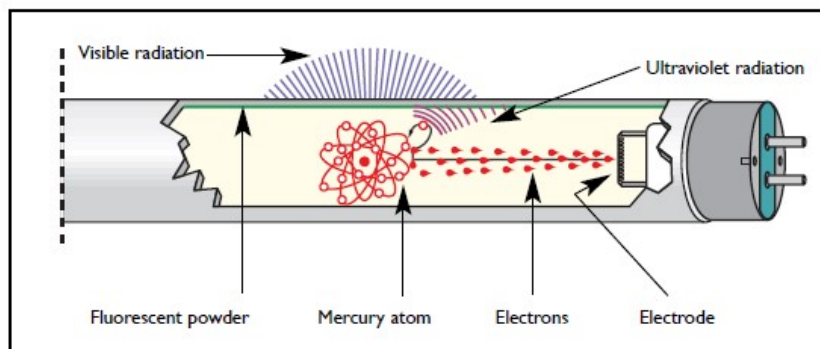
Figure 2.1: Fluorescent lamp working principles[7]

As shown in Fig. 2.1[7], electrodes are placed in each side of the tube. Inside the tube the inert gas and mercury (present in liquid and vapor states) are filled. The inner wall of the tube is coated with fluorescent powders, by which the ultraviolet radiation of the mercury discharges into light. There are many different fluorescent powders used for this purpose to produce light in different color temperature by mixing together. The efficacy of fluorescent lamps is better than other traditional light sources especially producing white light.

2.1.1. TL5 lamps with cold chamber (cold-spot technology)

The luminous flux of TL5 lamps is determined by the mercury vapor pressure which depends on the temperature of the coldest spot in the lamp. In terms of T5 tubes, the cold spot also named as cold chamber is situated behind the electrode at the stamp side. [7].

The TL5 lamp was designed to reach its maximum flux at 35 °C ambient temperature in draught-free air when operated on gear without additional heating of the electrodes. A ballast which realizes such characteristics is called a cut-off ballast. 35 °C is the common ambient temperature within luminaires. Any deviation from these nominal conditions for operation will influence the light output of a TL5 lamp. Deviations can come from: 1.A design of the luminaire allows an ambient temperature near the lamp(s) deviating from 35 °C; 2.The nominal specifications of gear include a lamp

current deviating from the nominal value and/or include heating of the electrodes during operation. Once the above undesirable cases happen, the additional power dissipation will heat the cold spot behind the electrodes and so will result in a shift of the curve of the output of the luminous flux. The highest luminous flux will be reached at lower ambient temperatures, so that the use of ballasts with low additional heating is recommended with T5 lamps [7].

2.1.2. SoS dimming

Dimming can be described as the reduction of the luminous flux of a lamp, either continuously or in steps, by current or power control. The lifetime of a fluorescent lamp depends on the lifetime of the electrode which is related to the temperature. If the temperature is above a specific value, the electrodes will be too hot, resulting in over evaporation of emissive material. If the temperature is below a certain value, then the sputtering of the emitter occurs. Therefore the temperature of the electrode should be limited in a reasonable range. To achieve this, additional filament heating is generally given to the electrode especially during low dimming levels. The temperature of an electrode mainly relies on three currents (see Fig. 2.2) [7].
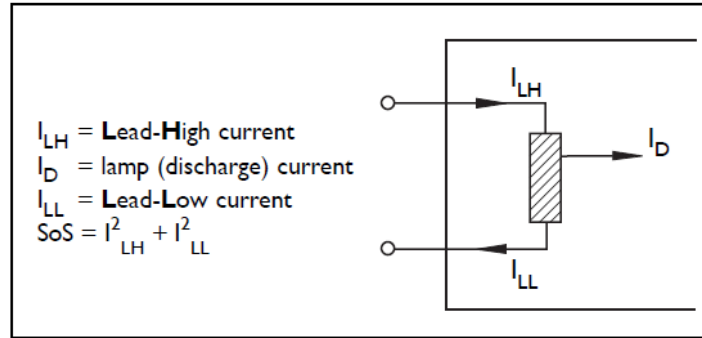
Figure 2.2: A Lamp electrode[7]

I_{LH} and I_{LL} present two currents, the higher one of the two currents and the lower one respectively. Both of them can be measured by a current probe around the lead-in wire. The definition of SoS is the sum of squares of I_{LH} and I_{LL}. I_D can be measured when use one current probe to test two wires together, and named as discharge current.

The value of the additional heating current depends on the lamp current and the ballast circuit layout. If the circuits include a capacitor in parallel or in other layouts, a phase shift may exist. These effects can be described by measuring the currents I_{LH}, I_{LL} and I_D, and calculating SoS_{min}, SoS_{max} and SoS_{target}. The SoS_{min} keeps the cathode at the lowest sufficient temperature, and it can be related to the discharge current.

$$SoS_{min} = I_{LH}^2 + I_{LL}^2 = X_1 - Y_1 \times I_D \qquad (2.1)$$

X_1 and Y_1 can be given as the critical conditions in this equation to get SoS_{min}, thus preventing cathode sputtering (get to a very low temperature). The highest value of temperature can be limited by the value of a SoS_{max} line. In the overheating condition, the bare tungsten and the coat part can be protected by $I_{LH,max}$ and $I_{LL,max}$ respectively. The "hot spot" region is protected by SoS line.

$$SoS_{max} = I_{LH}^2 + I_{LL}^2 = X_2 - Y_2 \times I_D \qquad (2.2)$$

Where X_2 and Y_2 are similar as for low temperature. Consider both SoS boundaries, the target SoS line is defined:

$$SoS_{target} = I_{LH}^2 + I_{LL}^2 = X_1 - z \times Y_2 \times I_D \tag{2.3}$$

The factor z defines the slope of this line. At normal operation the electrode also needs to be protected for overheating through setting a limitation of $I_{LH,max}$ and $I_{LL,max}$.

2.2. Ballast structure overview

As mentioned in chapter 1, the basic functions of ballast are: 1. Convert mains into a desirable current source for the fluorescent lamp operating. 2. Provide filament heating and ignite the fluorescent lamp.

Generally, ballasts can be classified into magnetic ballasts and electronic ballasts. The magnetic ballast consists of a transformer for current regulation and a starter for ignition. The conventional magnetic ballast structure is shown in Fig. 2.3. The transformer is known as a "choke", and a starter is located in parallel to the lamp [8]. The transformer elements has such a feature that when more current flows through the transformer, more magnetic field will be generated to slow down the increasing current. While it should be noticed that this magnetic field cannot stop current increasing. However, the magnetic ballast operates at AC mains which is constantly reversing itself, the transformer only needs to deal with the current increment in a particular direction and also in a short time (1/50s). The starter behaves like a timed switch and lowers down the ignition voltage to 230 V. During the starting transition, the switch is closed and the filaments are heated. The lamp therefore can be seen as an open circuit. After one or two seconds delay, the starter is open, and electrons start to flow across the tube and the mercury vapor will be ionized.

As only passive components are used, the operation frequency of magnetic ballasts is synchronized with the AC mains frequency. In such low frequency (50Hz or 60Hz), flickering and a large amount reactive power will lead to a low luminous efficacy. The bulky size and rarely effective method for regulating power are mainly disadvantages of magnetic ballast.
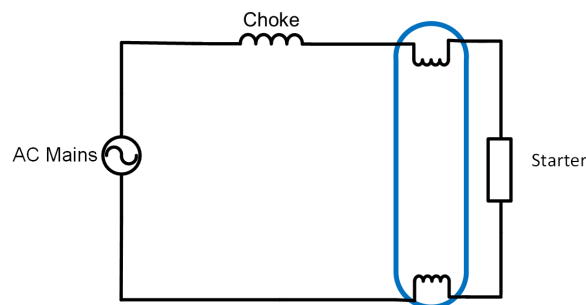
Figure 2.3: The simplified model of the conventional magnetic ballast

Compared with magnetic ballasts, electronic ballasts usually operate at high frequency (tens of kHz frequency). The electronic ballasts can be classified as constant current source and constant power source. Majority of the ballasts in the lighting market is constant current source, which means the ballast delivers constant current to the lamp. To reduce the power intake of this type of ballasts for LED lamps, reducing the amplitude or duty cycle of the lamp voltage is concerned in general. However, most of the Tridonic ballasts are designed with constant power output and a typical feature of those ballasts is that they usually limit the bottom frequency. Above the bottom frequency, the ballast outputs a constant power. While at a fixed bottom frequency, the ballast control loop is saturated. Therefore, the output power of this type of ballasts can be reduced from this perspective [9].

In general, several stages are cascaded in the electronic ballast as shown in Fig. 2.4. There are numerous implementations for each stage, while the basic functions are similar. The input stage can be realized by various structures such as a rectifier with electrolytic capacitors, a valley-fill PFC, an active PFC or a power feedback PFC. In the output stage, half bridge LC resonant circuit is broadly applied in the electronic ballast. Besides, a push-pull circuit or current-fed half bridge can also be an option in self-oscillating control ballasts [9].

The input stage of electronic ballasts converts the AC mains voltage to a DC voltage, and shapes the input current to comply with harmonics and EMI regulations.
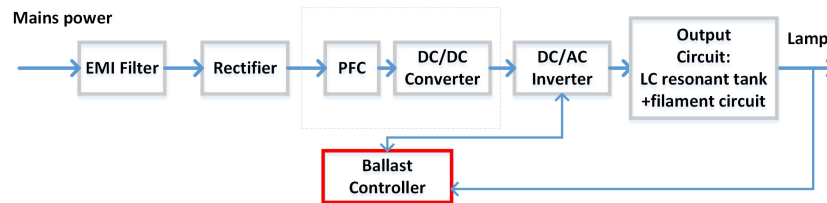
Figure 2.4: The block diagram of electronic ballasts

Power factor (PF) is an important parameter in AC power system, and it is defined as the ratio of the real power over the apparent power[10].

$$Power\,factor = \frac{Average\,power}{Apparent\,power} = \frac{P_{av}}{V_{rms}I_{rms}} \tag{2.4}$$

Where the apparent power is the product of root mean square (RMS) voltage and RMS current at the input stage. With a low power factor, the system needs more power to achieve required active power (load power) due to the large reactive power. A PFC circuit regulates the input current in phase with the voltage, to increase the real power close to the apparent power. In addition, the output DC voltage from this stage will be fed to the next stage. The output stage converts the DC energy from the input stage into a high frequency AC current for driving the fluorescent lamp. The implementations of the output circuit can be various according to different starting methods. A DC/AC inverter together with the resonant tank is chosen in most electronic ballasts (in Fig. 2.5). After the LC resonant tank, the pre-heating (filament circuit) is shown in Fig. 2.7. The resonant tank only works in resonance during the ignition stage, after current flows through filaments, the capacitor is open. Therefore, no starter is required in electronic ballasts.
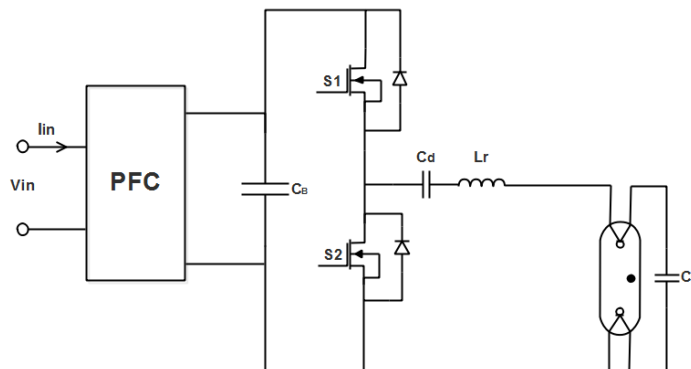
Figure 2.5: A typical output stage of electronic ballasts

Moreover, the control method of ballasts also can be realized by various options. For minimal cost requirement, self-oscillating control is a good choice. While in high-end ballasts, IC controlled with

fix frequency, IC controlled with power regulated, high-end uC and ASIC are available according to different starting methods. In steady state some ballasts operate at a fixed frequency like Philips C2E IC based ballasts, and other ballasts control the lamp power by a flexible operation frequency which is named as the power controlled ballast[4]. The LED tubes need mostly need less power compared to the fluorescent lamps because of the luminous efficacy difference between those two lighting sources. Power controlled ballasts may deliver more current (also power) to the LED tubes than fixed frequency ballasts due to the changeable operation frequency. The fixed frequency control sometimes is more popular because of lower cost and predictable characteristic.

The compatibility design in this project will focus on the LED driver part, which means the characteristic of the ballast output stage has most significant impact on the design. More precisely, the LC resonant circuit and filament circuit connected directly to the LED driver need more attention.

2.2.1. Starting characteristics of electronic ballasts
All fluorescent lamps have electrodes with some emissive material facilitating ignition, which electrodes require a sufficiently high temperature for heating.

a. The ballast operation frequency during each operation stage   b. Voltage ration during each operation stage
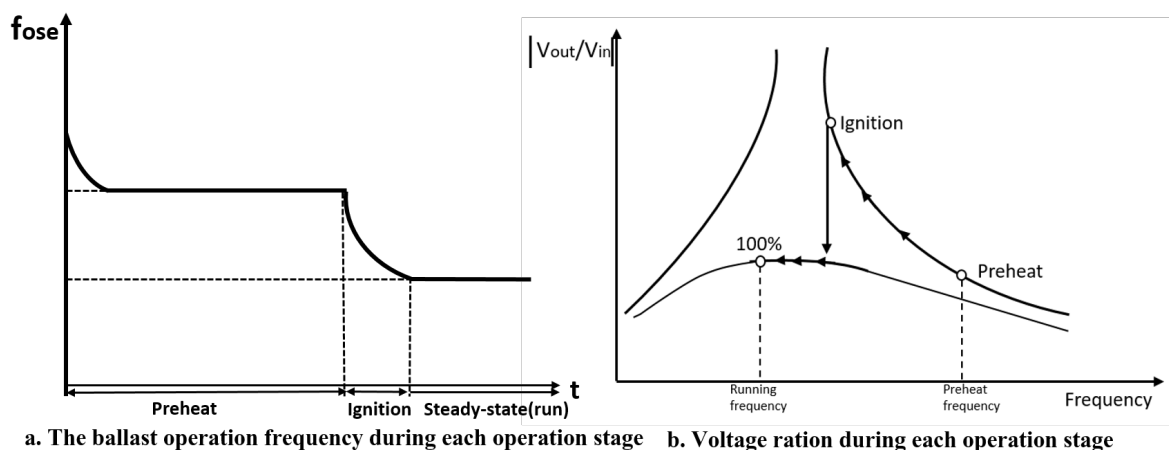
Figure 2.6: The ballast working process

The operation frequency of ballasts during each operation stage is shown in Fig. 2.6(a). At the first, the ballast controller starts at its maximum frequency (f_{start}) typically 100 - 120 kHz. Then drops quickly to the preheat frequency around 70 kHz to 80 kHz (resonance), waiting for the preheat time to pass (typically 0.8 s to 1.5 s). Later the frequency reach to the steady state operation frequency around 40 kHz (f_{min}). The lamp voltage also changes during starting. The transition is shown in Fig. 2.6(b) [11]. At the high frequency, the lamp voltage is at a low level, and increases rapidly near the resonant frequency. Through this process, the ignition can be achieved. In the steady state, the lamp current will be regulated by the inductor of the LC tank. When the lamp comes into steady state, electronic ballasts will operate at a fixed frequency or variable frequency (e.g. power feedback ballast)

In general, many starting methods such as instant start, rapid start, preheat start and programmed start are adopted in electronic ballasts, according to different ballast designs or requirements [12]. Instant start allows operation prior to electrode heating, and higher open circuit voltage strikes the lamp soon after the power delivered to the ballast. Rapid start is by means of secondary low voltage to heat the electrodes. Preheat start needs preheating current to preheat the electrodes. Programmed start offers precise time for each step by programming, which means this method can better eliminate the time errors compared to other methods.

2.2.2. The filament heating methods

The starting methods also can be classified into cold start (often used in self-oscillating ballasts) and warm start. The cold start ballast is lack of the filament heating process and starts the lamp through the high ignition voltage (see Fig. 2.7). While warm ignition needs to preheat the filament. Per-heating methods like current mode heating and voltage mode heating (see Fig. 2.8) are realized through various structures. This ignition type enables the lamps to be switched on and off without reducing lifetime, and suitable in a high switching frequency applications.
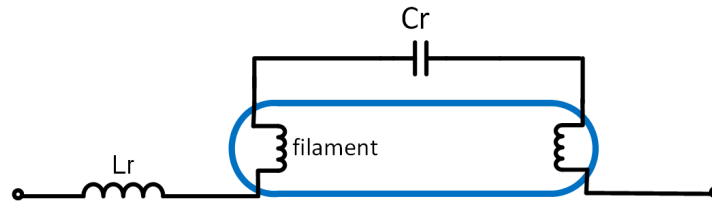
Figure 2.7: The filament circuit of cool ignition

During the pre-heating stage, the lamp behaves like an open circuit. In terms of the voltage mode heating, the current flows through L_1 and C_r. The voltage on L_1 is induced on $L_{1'}$, leading to a heating current in cathodes. The frequency of current in L_1 is decided by previous half bridge operation frequency [13]. In current mode heating, the basic method is also producing a heating current, while the current is the same as the current flows in resonant inductor (in the LC tank).
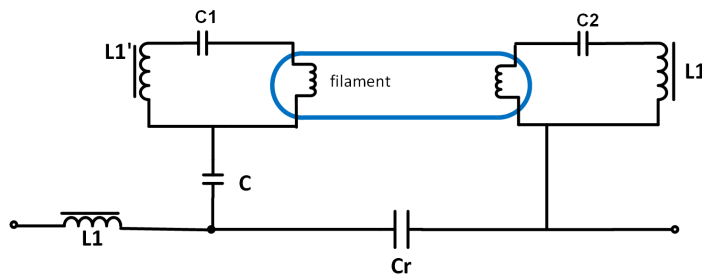
Figure 2.8: The filament circuit of voltage mode heating

In self-oscillating ballasts, a positive temperature coefficient (PTC) resistor is used for current mode heating. At first, the lamp is cold, the PTC resistor can be seen as a short circuit. In the preheating stage, the current heats electrons and PTC together. When the temperature of electrons and PTC is high enough, the PTC becomes an open circuit. The current will go into series capacitor and achieve ignition. At the end, the capacitor with PTC can be considered as a large impedance in parallel to the tube. When the lamp comes into steady state, ballasts can operate at a fixed frequency or variable frequency for power control.

When the fluorescent tube is replaced by the retrofit TLED tube where no filaments exist, the filament emulation is added to the LED driver. Thus the LED tube can match to the ignition feature of the ballast.

2.2.3. Practical overview of electronic ballasts

In order to design the compatible LED driver, the operation frequency, the LC tank parameters and different filament circuits of widely used ballasts are summarized. Those information of ballasts will influence the later design, practical overview of typical electronic ballasts will be shown in this section. The 35W TL5 ballast is chosen because of the various types and available amount in lab, and also two 49W TL5 ballasts are added.

Table 2.1: Parameters of different types of ballast

Characteristic of ballast	Type of ballast	$C_{dc}(nF)$	$C_r(nF)$	$L_r(mH)$	$f_r(kHz)$
Self-oscillating	EB-C 228 TL5	100	1.95	4.8	52.02
Dimmable ballast	HF-R Es 114-35 TL5	220	2.2	3.5	57.36
Dimmable ballast	HF-R Es 214-35 TL5	220	4.7	1.8	54.72
Non-dimmable	PC 1/49 T5 PRO LP -Tridonic	180	5.6	2.4	43.41
Non-dimmable	EL1x49s-u-Helva r	150	3.3	2	61.95
Non-dimmable	HF-P 2 14-35 TL5 HE III IDC	220	3.9	3	46.53
Non-dimmable	HF-P 1 14-35 TL5 HE III IDC	220	3.3	3.57	46.37
Non-dimmable	QTP5 1x14-35 - Osram	150*2	2.7	3.9	49.05
Non-dimmable	QTP5 2x14-35 - Osram	68*2	3	2.8	48.16

From Table. 2.1, the conclusion of each parameter is as follows:
1. The basic range of the LC resonant frequency is 40 kHz to 65 kHz.
2. The parameters of LC tanks are also in a range. For instance, the resonant capacitor is around 1.95 nF to 4 nF.
3. The DC block capacitor is 220 nF in most conditions.

For low cost application, the self-oscillating ballast is rather popular in the market. As shown in Fig. 2.9(a), the half-bridge transistors are driven by a ring core (T1). Three windings (T11, T12, T13) are set in one ring core. This circuit will oscillate itself once it is triggered. The operating frequency of the half-bridge is determined by the LC tank resonant frequency, turns ratio of the ring core and transistor parameters (storage time). The ignition method is similar as the mentioned methods.

a. Low-cost self-oscillating ballast output stage   **b. Tridonic PC 49W PRO LP ballast output stage for 1 lamp**
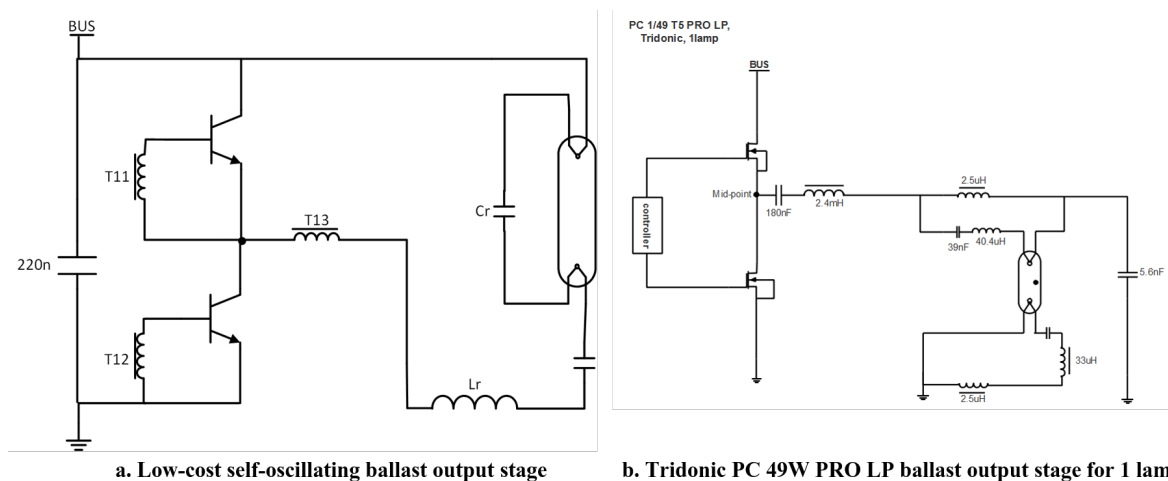
Figure 2.9: Two types of electronic ballasts

For non-dimmable ballast, a Tridonic PRO 49 W ballast is shown in Fig.2.9(b). In this ballast, warm ignition is employed. When the ballast starts, current first goes through the resonant inductor. Later current is delivered to the filament secondary side to finish preheating and ignition. The resonant capacitor is 5.6 nF and the DC block capacitor (180nF) is connected to the half bridge.

For dimmable ballast, there is a function part for dimming in the structure. Take Philips HF (high frequency) as an example. The operating principles are the same in one lamp and two lamp bal-

lasts. The simplified ballast structure of one lamp is shown in Fig. 2.10 According to the filament circuit, this ballast applies warm start, preheating the lamp electrodes. Transformers coupled in the filament part and the dimmable part can adjust the current through the filament when dimming is needed. A voltage dependent resistor(VDR) in the filament circuit is for over-voltage protection. The half bridge part and resonant LC tank are same as non-dimmable ballasts shown in Fig. 2.9.
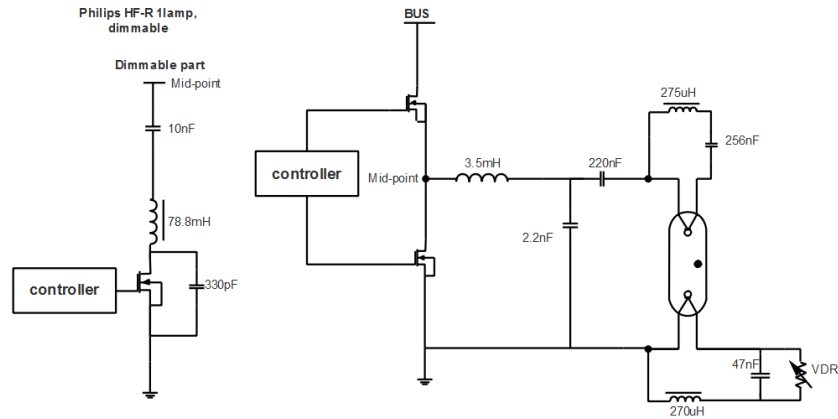
Figure 2.10: The Philips HF-R dimmable ballast output stage for 1 lamp

In this thesis, the compatibility design of retrofit TLED tube is based on 80W electronic ballasts. In Table.1.1, five ballasts and related electrical parameters are shown. The first ballast is dimmable, and others are non-dimmable. For TL5 HO 80W ballasts, the test current of the reference ballast is 550mA, which means the preferable ballast current is around 550mA. Therefore, Philips HF-P-180 TL5 ballast can be seen as a reference ballast in the simulation and practical tests. For other four ballasts, the ballast current with LED lamp should be reduced by compatible LED drivers.

2.3. Electronic Ballasts with LED driver

The general high frequency compatible LED driver contains the following elements: "1. a series capacitor placed between the ballast and the LED load, providing pin safety; 2. a matching network consisting of capacitors and/or for adjusting LED current; 3. a diode rectifier bridge for converting AC current to DC; 4. a capacitor connected across the LED string for smoothing out the ripple current; 5. An over-voltage protection circuit placed across the output of the rectifier, consisting of a thyristor, trigger circuit, etc. 6. a thermal or over-current protection circuit, for example a thermal fuse or over-current protection circuitries"[9]. To simulate the behavior of the electronic ballast with the LED lamp system, a LTspice model is setup in Fig. 2.11. As mentioned in the introduction, ballasts cannot be connected to LED lamps directly, therefore the start point from existing designs includes a rectifier and a filter capacitor.

The AC voltage source is the inverter output, a square wave with the ballast operation frequency. The DC block capacitor is connected to the AC voltage source and the LC tank. The filament can be simulated as a resistor and a large capacitor in parallel. Before ignition, the filament behaves like a large resistance, when AC current flows (conduction condition), the current will only go through the capacitor and will not change the ballast current. Then the rectifier and filter capacitor are connected to the filament. The LED load is modeled as a diode and a DC voltage source with dynamic resistance. The dynamic resistance is related to the value of the LED voltage.
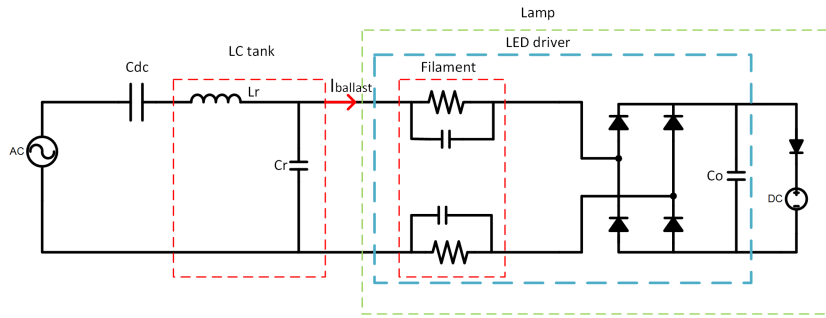
Figure 2.11: The simulation model of the ballast output stage with the LED load

Choose the parameters of the reference ballast, Philips HF-P 180 TL5 to build the initial simulation model. The output power is about 37W which is satisfied the power the LED lamp needs to produce almost same luminance as the 80W fluorescent lamp.
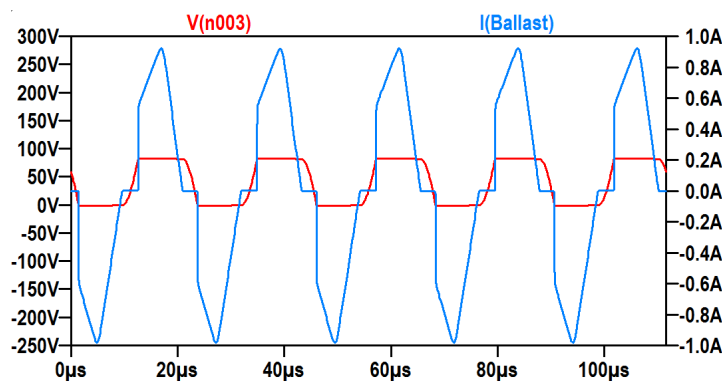
Figure 2.12: The ballast current and the resonant capacitor voltage of the simulation

The LED voltage is set to 80 V. In Fig. 2.12 the resonant capacitor voltage and ballast current are shown. The blue line is ballast current, and the red line is the capacitor voltage. The ballast current is tested between the resonant capacitor and Lamp. The red line represents the voltage on capacitor, which shows that the voltage is limited by 80 V LED voltage at the end of resonance.
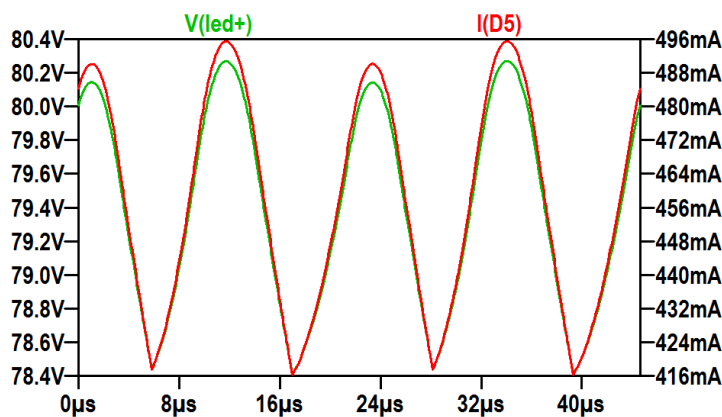
Figure 2.13: The LED current and voltage of spice model

In Fig. 2.13, the LED current and voltage are shown in green and red respectively. The LED voltage is limited around 80V, since the voltage drop on the diode is added in the model. The average LED

current is 464 mA, therefore, the output power is about 36.5 . The LED current ripple is about 120 mA which can be reduced to a lower level through the later work.

In order to examine the simulation model, the practical test result of the ballast current (yellow line) and LED current (green line) are shown in Fig.2.14. The RMS value of ballast current is 550 mA (from power meter) and the average LED current is about 451 mA. In the practical setup the LED voltage is 80V, and the output power is about 36W. Besides, the operation frequency of the ballast is 44 kHz in the test, which frequency matches the reference ballast operation frequency.
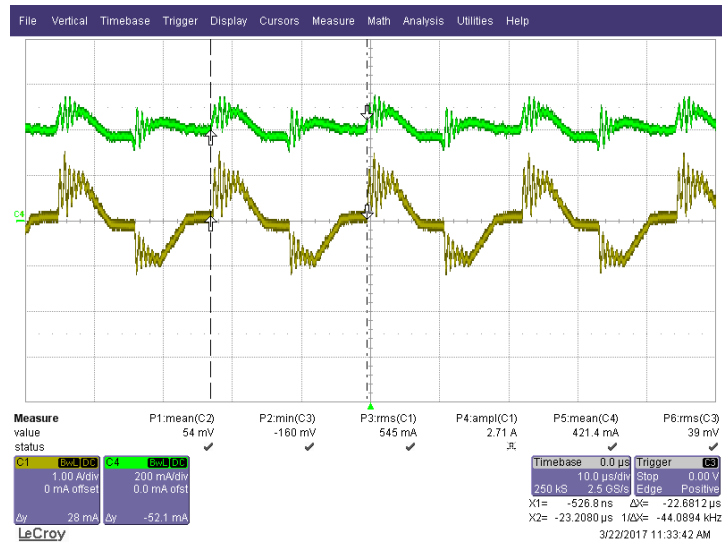
Figure 2.14: Test results of the ballast current and the LED current

In a conclusion, the test results match the simulation results. Therefore, the simulation part of Chapter 3 will base on this model.

<div style="text-align: right; font-size: 3em;">3</div>

The passive approach

This chapter will focus on the passive method. The basic principle is to increase the load impedance of a ballast so as to reduce the ballast current when faced a LED load. Normally, the impedance network can consist of resistors, inductors and capacitors. In order to avoid the extra loss on the added elements only inductors and capacitors are considered in the network design. The research model considered in this chapter is presented in Fig. 3.1 in which a rectifier and an output capacitor with the LED load are connected to the LC tank of the ballast.

The load impedance seen by the ballast is defined as Z_{load} in Fig. 3.1. The non-linear characteristic of this system comes from the blanking time of rectifier diodes. The definition of blanking time is related to the diode of the rectifier in Fig. 3.1. The conduction of diodes needs to wait for the voltage on the resonant capacitor (C_r) reaching the LED voltage, resulting in a blanking time. During the blanking time, four diodes are not conducting and the current only goes through the LC tank. Therefore, this system has a non-linear load behavior. The LED voltage (V_{LED}) and the resonant tank determines the blanking time. Normally, the blanking time will be extended when the operation frequency is much higher than the LC resonant frequency. It is because the resonant tank needs relatively more time to reach the LED voltage as the voltage from the inverter changes direction faster.
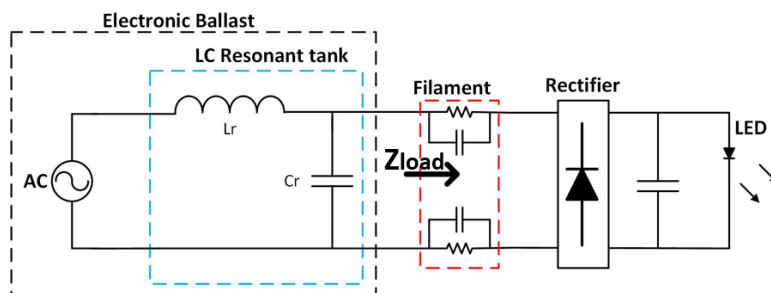
Figure 3.1: The basic structure of the research model

When dealing with such a system, the first harmonic analysis[14] is not accurate. Especially under the situation where the operation frequency and the LC resonant frequency differs a lot. To describe this system in details, the time domain analysis is adopted. In later sections, several impedance matching networks will be investigated based on the time domain analysis and simulations. From the time domain analysis, the load impedance can be described as well as the ballast current. When it is difficult to derive the time domain equations of each variables, the simulation is a potential alternative to simplify the problem. Through the relations between the ballast current and other

variables such as the LED current and the resonant inductor/capacitor current, the variation trend of the ballast current still can be presented. After all impedance network structures studied, a design solution based on this method will be concluded at the end of this chapter.

3.1. Parallel capacitor

This section will discuss the possibility of increasing the load impedance by the parallel capacitor. The reason for choosing this topology as a starting point is that the structure is rather simple compared to other typologies and it is always of convince to start from an easy level to get an initial concept then implement it to a difficult level. This impedance network is a second order resonance system because of the added capacitor is in parallel with the resonant capacitor during the blanking time. A mathematical model is built to analyze and conclude the system behavior. The system then contains a resonant inductor and a capacitor which is the sum of the resonant capacitor and the added capacitor. Together with the initial conditions of the inductor current and the capacitor voltage, equations of those parameters derived from the second order series resonant circuit, are applicable in this matching network. Besides, in order to fulfill a comprehensive mathematical model which matches the different practical circuit behaviors, the variables which decide the value of parameters should be involved in the expressions. The LED voltage (V_{LED}) and the operation frequency have effects on the blanking time, and the resonant frequency depends on the parallel capacitor together with the resonant inductor. Therefore, those three variables are chosen to realize the flexibility of this model.

Based on the expressions of the inductor current and the capacitor voltage, the ballast current and the LED power are presented as $I_{Ballast}(V_{LED}, C_p, f_s)$, and $P_{LED}(V_{LED}, C_p, f_s)$. As a famous software tool for mathematical modeling, verification, and reutilization of engineering calculations, Mathcad is applied to derive the mathematical model.

The operation points of this system can be mainly classified into three modes (different operation modes) according to the relation between the resonant frequency and the ballast operation frequency: The capacitance voltage can/cannot reach the V_{LED} from -V_{LED} at the end of the half positive operation period. The typical range of ballast operation frequency is 40 kHz to 120 kHz. When the operation frequency is higher than the resonant frequency, there will be two resonant states in one period. It is because that the voltage source changes the direction during the blanking time. In this situation, it is difficult to derive the ballast current in time-domain directly, therefore the state plane analysis is considered to solve this problem. Dividing the behavior of the resonant tank into the resonant stage and the linear stage, each stage will contribute an arc or a line part which consist of the trajectory on the state plane. Moreover, if the operation frequency goes to higher than the twice of the resonant frequency (usually happens during the ballast starting transition), no current will flow to the LED load. Because the voltage on the capacitor cannot reach the LED voltage during each half operation period, the current only circulates in the inductor and capacitors. Based on above analysis, the first operation mode is defined as the operation frequency is lower than the resonant frequency. The operation frequency is higher than the resonant frequency but lower than the resonant frequency is named as the second operation mode. Furthermore, the third operation mode happens when the operation frequency is higher than twice of the resonant frequency.

Fig. 3.2 describes the simulation model of the ballast output stage with the parallel capacitor LED driver and related variables. Considering the steady state, the filaments behave like a short circuit and the current flows to the load through the large capacitors. Therefore the filaments actually can be skipped in the steady state model.
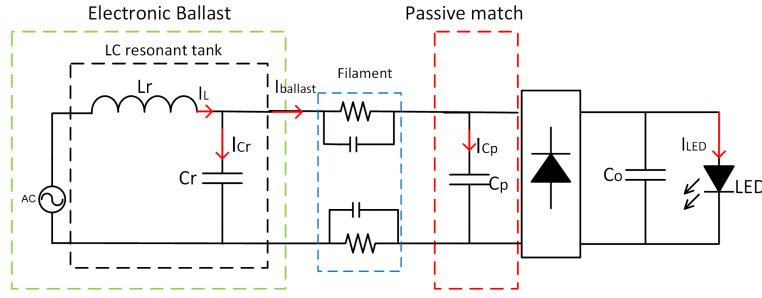
Figure 3.2: Add a capacitor in parallel to the ballast output stage

The resonance frequency of the LC tank with the parallel capacitor is:

$$f_r = \frac{1}{2\pi\sqrt{L_r(C_r + C_p)}} \tag{3.1}$$

Where L_r and C_r correspond to the resonant inductor and capacitor in the ballast output stage, and C_p is the parallel capacitor added next to the ballast. The angular frequency is defined as:

$$\omega_0 = \frac{1}{\sqrt{L_r(C_r + C_p)}} \tag{3.2}$$

The ballast current from the Fig. 3.2 is:

$$I_{Ballast} = I_L - I_{Cr} \tag{3.3}$$

The two boundary conditions between three operation modes are shown in Fig.3.3. The square wave in black is the input voltage, the inductor current and voltage on C_r and C_p is shown in the blue and red respectively.

a. The boundary condition *of $i_L(t)$ and $u_c(t)$* between the first mode and second mode

b. The boundary condition *of $i_L(t)$ and $u_c(t)$* between the second mode and the third mode
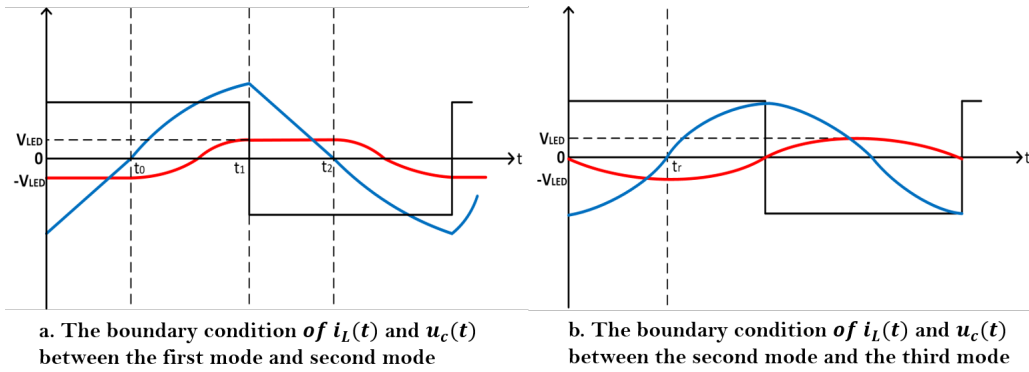
Figure 3.3: The boundary conditions of $i_L(t)$ and $u_{c(t)}$

In Fig.3.3(a), the capacitor voltage can reach the LED voltage (V_{LED}), before the voltage source changes the direction. The time-domain analysis of this transition can be derived as below. During 0 to t_0 interval:

$$u_c(t) = -V_{LED} \tag{3.4}$$

$$i_L(t) = \frac{V_{LED} + V_s}{L_r}t - i_L(0) \tag{3.5}$$

Where V_{LED} is the LED voltage and V_s is the input voltage. End point of this interval: $u_c(t_0) = -V_{LED}$; $i_L(t_0) = 0$

During t_0 to t_1 interval, the initial state and the second order differential equation are given:

$$u_c(t) = V_s - (V_s - u_c(t_0))cos(\omega_0(t - t_0)) \tag{3.6}$$

$$i_L(t) = \omega_0 C_r(V_s - u_c(t_0))sin(\omega_0(t - t_0)) \tag{3.7}$$

End point of this interval: $u_c(t_1) = V_{LED}$; $i_L(t_1) = \omega_0 C_r(V_s - u_c(t_0))sin(\omega_0(t_1 - t_0))$
During t_1 to t_2 interval:

$$u_c(t) = V_{LED} \tag{3.8}$$

$$i_L(t) = -\frac{V_{LED} + V_s}{L_r}(t - t_1) + i_L(t_1) \tag{3.9}$$

End point of this interval: $u_c(t_2) = V_{LED}$; $i_L(t_2) = 0$
The no-linear time is $t_1 - t_0$ and from equation 3.6 this time interval can be derived:

$$t_1 - t_0 = t_r = \frac{acos\frac{V_s - V_{LED}}{V_s + V_{LED}}}{\omega_0} \tag{3.10}$$

The linear time is $t_2 - t_1$ and from equation 3.9 this time interval can derived:

$$t_2 - t_1 = t_L = \frac{L_r}{V_s + V_{LED}}\omega_0(C_r + C_p)(V_s + V_LED)sin(\omega_0 t_r) \tag{3.11}$$

Therefore, the boundary frequency of the first operation mode is:

$$f_{limit1} = \frac{1}{2(t_r + t_L)} \tag{3.12}$$

The second boundary frequency is defined when the system keeps resonant and no linear part anymore(see Fig3.3(b)).

$$f_{limit2} = \frac{1}{4t_r} \tag{3.13}$$

When the ballast operation frequency is higher than f_{limit1} but lower than f_{limit2}, this situation is quiet complex. The capacitor voltage can reach the LED voltage until voltage source changes direction for a while. This condition is shown in Fig. 3.4. The time-domain analysis is shown as below:
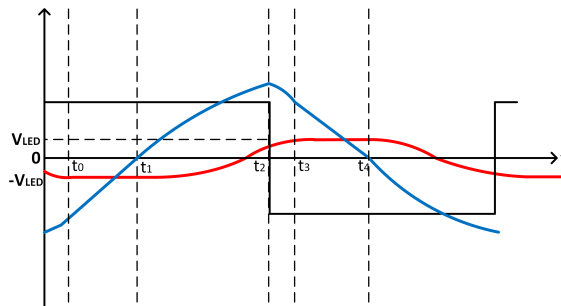
Figure 3.4: $i_L(t)$ and $u_{c(t)}$ when the operation frequency between f_{limit1} and f_{limit2}

t_1 to t_2 interval:

$$u_c(t) = V_s - (V_s - u_c(t_1))cos(\omega_0(t - t_1)) \tag{3.14}$$

$$i_L(t) = \omega_0 C_r(V_s - u_c(t_1))sin(\omega_0(t - t_1)) \tag{3.15}$$

End point of this interval: $u_c(t_2) = V_s - (V_s - u_c(t_1))cos(\omega_0(t_2 - t_1))$
$i_L(t_2) = \omega_0 C_r(V_s - u_c(t_1))sin(\omega_0(t_2 - t_1))$
$V_c(t_1) = -V_{LED}$

t_2 to t_3 interval:

$$u_c(t) = -V_s + (V_s + u_c(t_2))cos(\omega_0(t - t_2)) + Z_0 i_L(t_2)sin(\omega_0(t - t_2)) \tag{3.16}$$

$$i_L(t) = i_L(t_3)cos(\omega_0(t - t_2)) - \omega_0 C_r(V_s + u_c(t_2))sin(\omega_0(t - t_2)) \tag{3.17}$$

End point of this interval:
$u_c(t_3) = -V_s + (V_s + u_c(t_2))cos(\omega_0(t_3 - t_2)) + Z_0 i_L(t_2)sin(\omega_0(t_3 - t_2))$
$i_L(t_3) = i_L(t_3)cos(\omega_0(t_3 - t_2)) - \omega_0 C_r(V_s + u_c(t_2))sin(\omega_0(t_3 - t_2))$

t_3 to t_4 interval:

$$u_c(t) = V_{LED} \tag{3.18}$$

$$i_L(t) = -\frac{V_{LED} + V_s}{L_r}t + i_L(t_3) \tag{3.19}$$

End point of this interval:
$u_c(t_4) = V_{LED}; i_L(t_4) = 0$
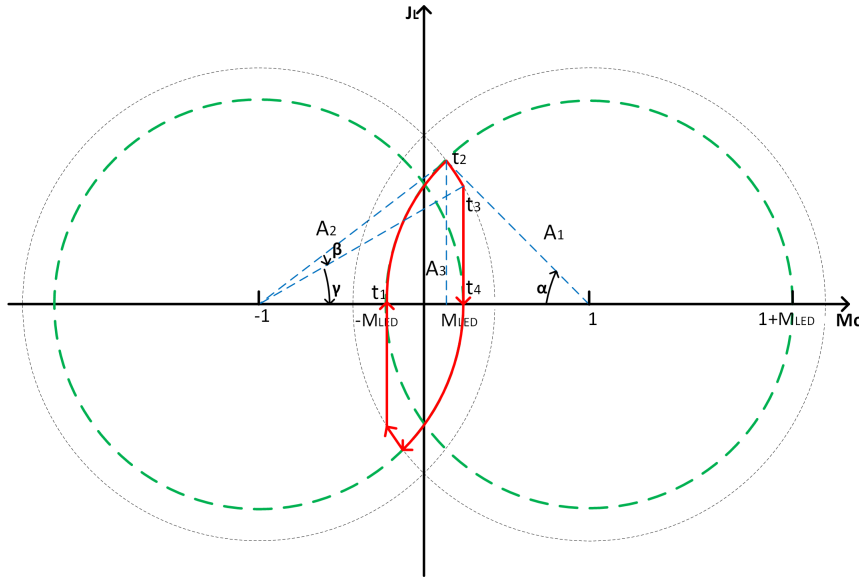
Figure 3.5: State plane analysis when the operation frequency between f_{limit1} and f_{limit2}

To analyze steady and dynamic features of the system, state-plane method is considered. In the state plane analysis, the radius is related to the initial values of the previous stages. After the normalization of each values, and transfer from time-domain to state-plane M-J figure. The trajectory of M_c and J_c is shown in Fig.3.5. There are several parameters need to be defined before analysis. Total voltage on capacitor is nominalized:

$$M_c = \frac{V_c}{V_s} \tag{3.20}$$

The LED voltage is nominalized:

$$M_{LED} = \frac{V_{LED}}{V_s} \tag{3.21}$$

The resonant impedance:

$$Z_0 = \omega_0(C_r + C_p) \tag{3.22}$$

The inductor current is nominalized:

$$J_L = \frac{I_L Z_0}{V_s} \tag{3.23}$$

ω_s is operation angular frequency.

$$\omega_N = \frac{\omega_s}{\omega_0} \tag{3.24}$$

The green circle and black circle are named as circle 1 and circle 2, representing two operation stages. In t_1 to t_2 interval, the non-linear part can be shown in circle 1:

$$J_L^2 + (M_c - 1)^2 = (1 + M_{LED})^2 \tag{3.25}$$

In t_2 to t_3 interval the non-linear part can be shown in circle 2, the radius is related to the end point t_3:

$$J_L^2 + (M_c - 1)^2 = J_L(t_3)^2 + (M_C(t_3) + 1)^2 \tag{3.26}$$

In order to solve the end point value of t_2 and t_3, the geometric relationship need to be considered.

$$\alpha + \beta + \gamma = \pi/\omega_N \tag{3.27}$$

$$cos(\pi/\omega_N - \alpha - \frac{A_3}{A_1}) = 1 - \frac{A_2^2 + (1 - M)^2 - 2A_1(sin(\alpha)A_3 + cos(\alpha)A_3(1 - M)))}{2A_2^2} \tag{3.28}$$

Where A_1 is the radius of circle 1, and A_2 is the radius of circle 2. A_3 presents the linear part in the transition. Once α is confirmed, the radius of circle 2 can be derived. Therefore, t_2 and t_3 can be solved. After all initial conditions and time intervals in each operation modes are gained. Transfer the equations into Mathcad through which the curves of $I_{Ballast}(V_{LED}, C_p, f_s)$, and $P_{LED}(V_{LED}, C_p, f_s)$ will be shown when V_{LED}, C_p and f_s are given.

The validation of Mathcad model is as follows. The example is based on Philips HF-P 80W ballast, which works at 44.8 kHz in steady state. The comparison of results between the simulation model(right) and the mathematical model(left) is illustrated at 44.8 kHz (Fig.3.6) and 120kHz (Fig.3.7). The related parameters $i_{Ballast}(V_{LED}, C_p, f_s, t)$, $i_L(V_{LED}, C_p, f_s, t), t)$, $u_c(V_{LED}, C_p, f_s, t)$, and $u_s(t)$ are given. The details of the Mathcad model are given in Appendix. A.1.
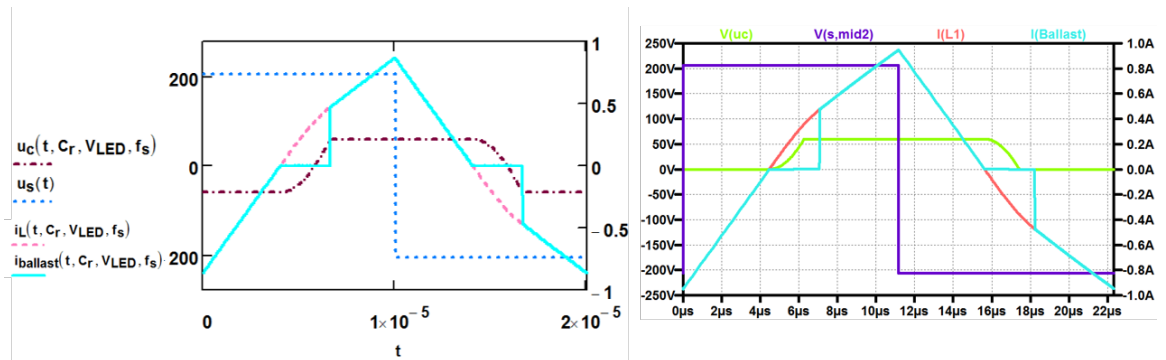
Figure 3.6: Curves of Mathcad model and LTspice model at 44.8 kHz

The third operation mode happens when the operation frequency is higher than f_{limit1}, which is 108.5 kHz from the calculation. Therefore, 120 kHz is chosen for validation. For a higher operation frequency, where the system keeps resonant and no current flows through the load, the results are also matched to each other while this condition is not a normal operation point and not presented in this section.
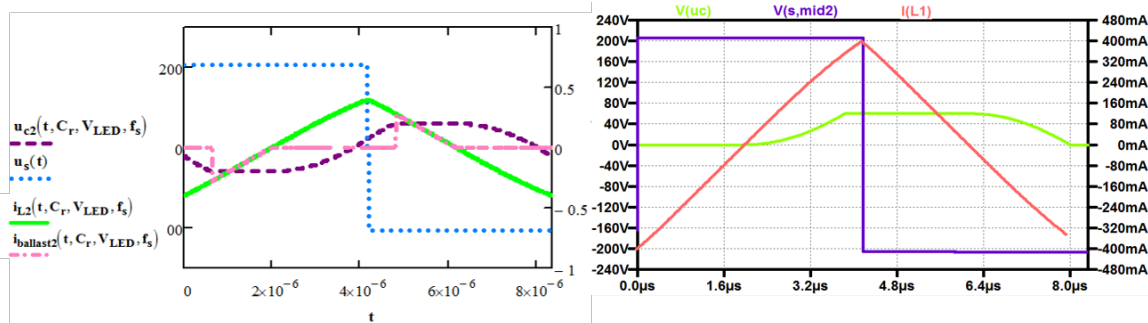
Figure 3.7: Curves of Mathcad model and LTspice model at 120 kHz

The Mathcad model matches the LTspice model in every operation mode from above figures. For most HO 80 W ballasts, the steady state operation frequency is below the resonant frequency. Based on the overview of ballasts in Chapter 2, normally 45 kHz - 60 kHz is designed as the steady state operation frequency. Take the rated operation frequency 44.8 kHz as an example. The ballast current can be simply derived from the inductor current and ratio of C_p and C_r.
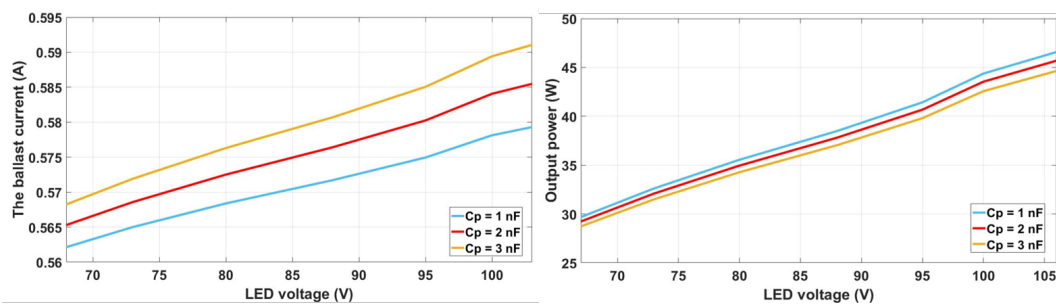
Figure 3.8: The ballast current and output power with different parallel capacitors

Fig. 3.8 shows the ballast current and the output power change along the different LED voltages in different parallel capacitors. The result apparently shows that adding a capacitor in parallel actually reduce the load impedance and leads to a higher ballast current.

3.2. Parallel inductor

In this section, the parallel inductor structure is built in Fig. 3.9 and the positive direction of the current of each variables is described as well. The inductor has different impedance character from the capacitor, there is always a current though the inductor not only during the blanking time. When the voltage on the inductor has opposite direction to the current, the current tends to prevent the change. This feature causes a delay of the inductor current direction change. Therefore, the inductor current may prevent the ballast current increase during a certain time interval (around the LED voltage switching directions), which transition may lead to a higher load impedance. Similar with the previous analysis method, a simulation model and a mathematical method are combined to investigate this situation.
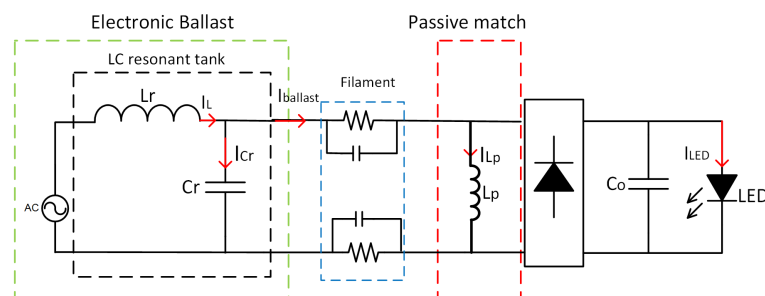
Figure 3.9: Add an inductor in parallel to the ballast output stage

According to the previous section, 1 mH inductor is added in parallel to the rectifier. The current through each components at the ballast operation frequency is shown in Fig. 3.10. The blanking time presents in A interval, all diodes are off thus no current flows to the load. After the supply voltage switches to positive from negative at t = 0 s, the resonant inductor current (I_{Lr}) tends to change the direction as well. The voltage on the parallel inductor at that time is - V_{LED}, so the parallel inductor current (I_{Lp}) is negative. This resonance stage starts when I_{Lr} equals I_{Lp}. Voltage on the resonant capacitor (V_{Cr}) changes from - V_{LED} to + V_{LED}, during this transition:

$$I_{Lr} = I_{Lp} + I_{Cr} \tag{3.29}$$

Stage A ends at V_{Cr} reaching V_{LED}, where the diodes are conducting again. Then the system steps into the linear stage B where supply voltage and V_{Cr} keep positive increasing I_{Lr} and I_{Lp} respectively. Later the system goes into the linear stage C, when supply voltage changes the direction from positive to negative. I_{Lr} is decreasing while I_{Lp} stays increasing due to the + V_{LED}. This stage ends until I_{Lr} equals I_{Lp}, and then the similar process circulates in the rest half period.
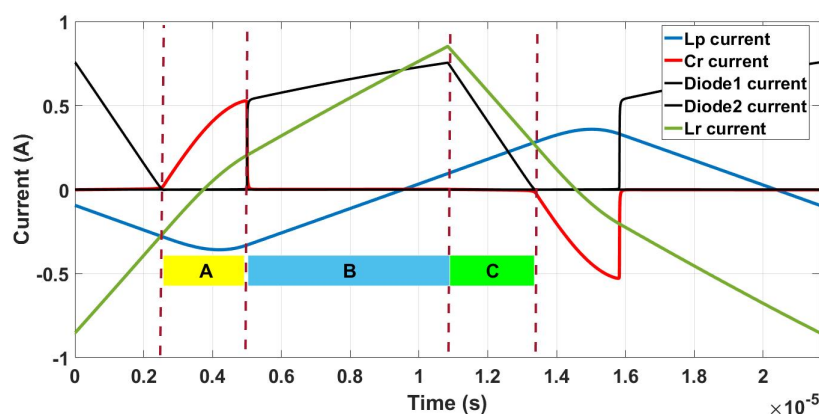
Figure 3.10: System behavior with 1 mH inductor in parallel @46.2 kHz

This system is simplified by Thévenin's theorem, and the transformation is shown in Fig. 3.11. The ballast and the added inductor seen from the rectifier are transferred from the initial structure (left in Fig. 3.11) to the simplified circuit (right in Fig. 3.11). The voltage source (V_s) from the inverter and the inductance from two inductors are equalized to V_{eq} and L_e.
V_{eq} and L_e are defined as follows.

$$V_{eq} = \frac{L_p}{L_p + L_r} V_s \tag{3.30}$$
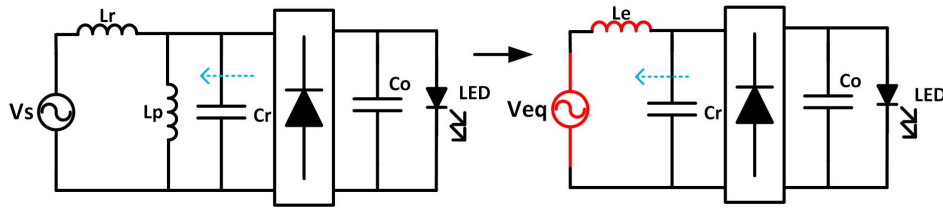
Figure 3.11: Transfer to simple structure based on Thévenin's theorem

$$L_e = \frac{L_p L_r}{L_p + L_r} \tag{3.31}$$

The mathematical model in the previous section therefore can be transferred to this situation after changing V_s and L_r into V_{eq} and L_e. The parallel inductor value becomes one of variables. Then the relation between the LED current, the LED power, and the LED voltage can be derived based on the Mathcad model.
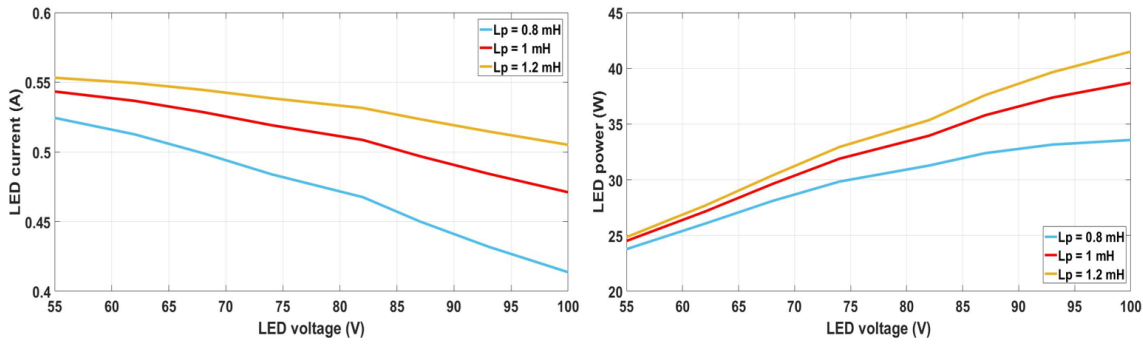
Figure 3.12: The LED current and power with different inductor in parallel @ operation frequency

Fig. 3.12 introduces the function of parallel inductors to the compatibility system at the steady state operation frequency. As the LED voltage increases, the LED power apparently goes up even though the LED current becomes lower. The LED current decreases because the higher LED voltage results in a longer resonant time (Equation.3.10) in same LC parameters. The current effect on the power is less than the voltage, due to the difference of the resonant time is relatively smaller than the voltage change. Besides, higher inductor value leads to higher output current as the resonant time decreases. Normally, keeping the output power around 35 - 40 W can meet the luminance requirement of 80 W ballasts. If the LED voltage is higher than 70 V, change of LED strip structures (combination of parallel and series) can shunt the current, in case the high current in LEDs causing the additional losses. Although through the simplified model the relation of L_p and the LED current can be gained, the relation between the ballast current and L_p is still difficult to derive. The simplified model cannot be employed to express the ballast current (see Equation. 3.32).

$$I_{ballast} = I_{Lr} - I_{Cr} \tag{3.32}$$

Only the initial model presents this parameters. However, the initial conditions of each variables except the resonant capacitor, are difficult to solve. Thus consider using the simulation model to describe the system. The LED load is simulated as an ideal diode series with a DC voltage source and dynamic resistance. When increases the LED voltage the dynamic resistance also increases according to a factor N. First set the system in operation frequency to observe the relation between added inductors and ballast current. In Fig. 3.13(a), the ballast current and LED current vary along with different parallel inductors at the operation frequency are shown. The ballast current can be

seen as a current source because the ballast output impedance is much higher than the impedance of the LED load. In order to reduce the ballast current, the load impedance seen by the ballast should be increased to a value where this load impedance is close to the impedance of the LC tank. The value of the added inductor is then settled according to the ballast output stage impedance. The LED current is rising by an increasing parallel inductor. Facing to a higher parallel inductor value means a less current flowing through the inductor (see Equation 3.31). Therefore, more current will go to the LED load. Although the ballast current grows up as the parallel inductor increases, it is still below the initial current without the parallel inductor. As a result, the load impedance is increased by L_p. Different from the parallel capacitor structure, there is always a current flowing through the parallel inductor. During the non-resonant time interval, the ballast output current always has the opposite direction to the current through the parallel inductor. Because the inductor current tends to flow against the change of the input current. Beside, from the relation between the inductor current and voltage, if the inductance increases, the inductor current decreases under the same inductor voltage. Therefore, the reduction effect on the ballast current decreases as the parallel inductor increases (shown in Fig. 3.13(a).

Fig. 3.13(b) shows that the peak current of parallel inductors increases as the inductor value decreases. It is reasonable because the current goes up when the same voltage added to a smaller impedance. Besides, the output power also decreases since more current flows back through the smaller parallel inductor. The output power under different parallel inductors is shown in Table. 3.1. Therefore, if a lower value of the added parallel inductor, a higher LED voltage is required to fulfill a certain output power level.
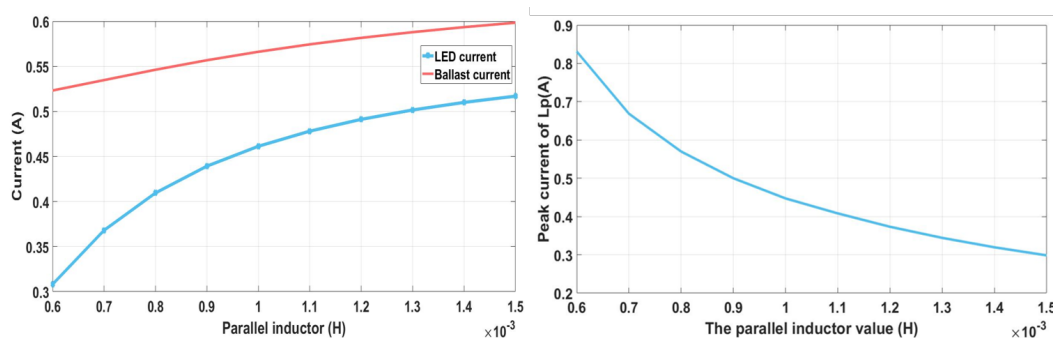
Figure 3.13: The LED current, the peak current of L_p and the ballast current with different inductors in parallel

Parallel inductor [mH]	0.9	1.2	1.5
P_{out} [W]	31	38	42
I_{LED} [mA]	391	475	530

Table 3.1: Output power in different parallel inductor added to the system

In order to study the relation of the ballast current, the peak current of the parallel inductor with the LED voltage, set L_P at 1 mH. The result shows in Figure. 3.14. The ballast current and the peak current of the parallel inductor show negative and positive correlation with the LED voltage respectively. A high LED voltage is equal to a high impedance (Based on the above equations and explanations, the LED current will decrease when LED voltage increases), the current through the resonant inductor will be lower when faced to a higher impedance. The load impedance of ballast mainly decides the inductor current and the LED current. In general, a higher output impedance corresponds to a lower LED current. Besides, to low down the ballast current to a value where the output power still meets the HO 80 W ballasts, the operation frequency also should be considered.
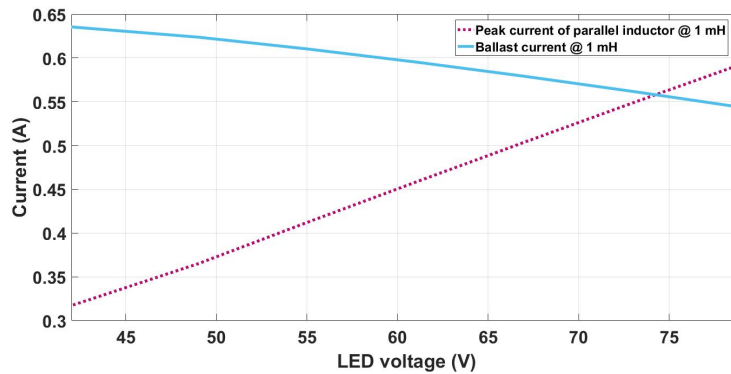
Figure 3.14: The peak current of parallel inductor and ballast current with different LED voltages @1mH

From Fig. 3.15, the relation between the operation frequency and the ballast current is shown with and without a parallel inductor. The scan frequency range is decided by the typical operation frequency of ballasts (for higher frequency, the ballast current still keeps the downtrend). Add a 1 mH inductor in parallel to the EL1x80sc ballast output stage as an example. Around the operation frequency the ballast current is effectively reduced compared to the initial ballast current. If the frequency is increased to a relatively high value (60 kHz in Fig. 3.15), the voltage on capacitor cannot reach the LED voltage due to the increasing ratio of resonant time and period. Therefore, the ballast current will decrease to an unacceptable value which cannot generate the enough power for the LED load.
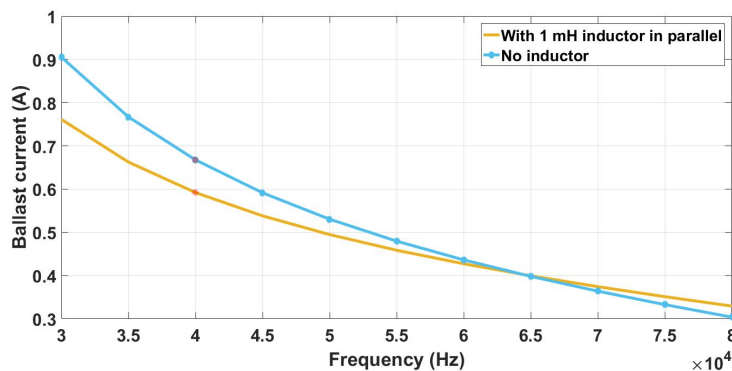
Figure 3.15: The ballast current in different frequency with and without L_p= 1 mH

As a conclusion, the parallel inductor structure has a high potential to raise the load impedance and reduce the ballast current. The elements such as the LED voltage, the peak parallel inductor current, and the LED power need to be taken into consideration, for choosing a suitable parallel inductor value for a range of ballasts. The details of the parallel inductor selection is given in section. 3.4.

3.3. Series inductor and capacitor

When considering series inductor and capacitor situations, the system transfers into the third order system. The series capacitor C_s structure is given in Fig. 3.16 (for the series inductor case, just replace the capacitor C_s by an inductor). The concept of the series structure is adding the impedance directly to the load impedance. The mathematical analysis could be complex and not necessary. The conclusion of this section will be generated from the observation of SPICE simulation results which is more straightforward and simple, but not mathematical analysis.
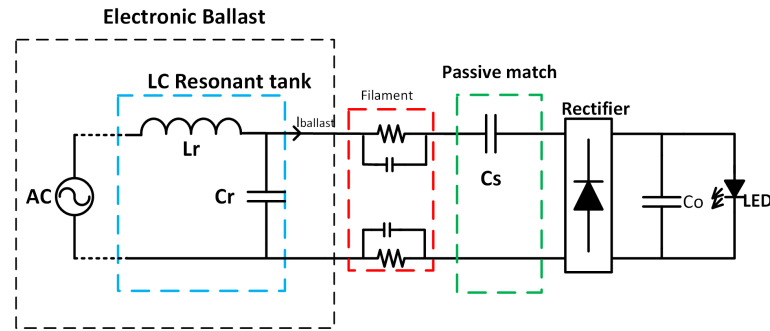
Figure 3.16: Add a capacitor in series to the ballast output stage

The simulation is built up according to Fig. 3.9 in LTspice. A capacitor or an inductor is added in series between the filament and the rectifier. "step" and "meas" functions are applied to scan the whole system in the different frequencies and parallel inductors. For example, function ".step param fosc 30kHz 70kHz 1kHz" means change the operation frequency from 30 kHz to 80 kHz with step of 1 kHz. ".step param Cs 2 nF 25 nF 5 nF" gives the series capacitor range and step. The sentence ".meas trans Iballast RMS I(ballast)" measures the ballast current. Besides, all measurements should start after the system reaches the stable condition. Therefore, the sample time is starting from 4 ms and lasting four operation periods.
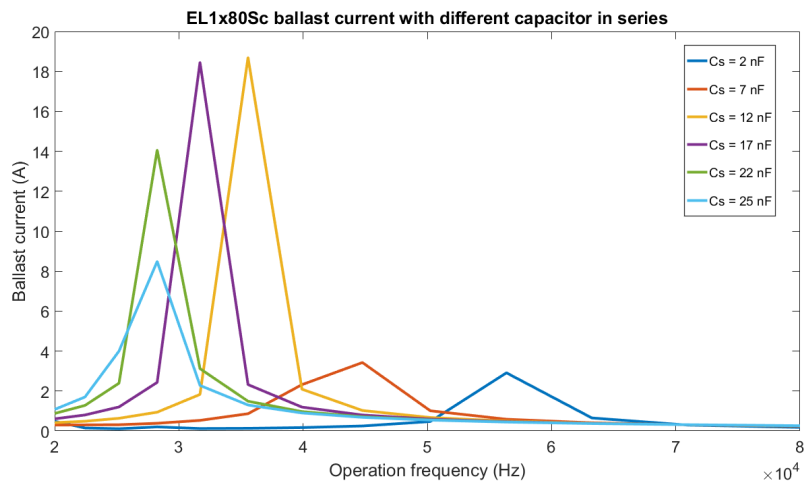
Figure 3.17: EL1x80Sc ballast current with different capacitors in series

In terms of the series capacitor structure, an unstable system behavior is caused by the added capacitor (C_s). From Fig. 3.17, C_s together with other passive components may lead to other series resonant points which are close to the operation frequency. In this situation, the system keeps resonance, producing a high voltage and current. For example, when a 12 nF capacitor is added in series to the system, a resonant point(34.5 kHz) which is close to the operation frequency (35.6 kHz) of EL1x80Sc causes a high ballast current. As a conclusion, the series capacitor structure cannot fit the compatibility requirements.

From Fig.3.18, this method does reduce the ballast current. However, the unstable behavior of the series inductor network with different operation frequencies is also observed. The frequency range in this simulation is between 30 kHz and 70 kHz, and the inductor value varies from 0.5 mH to 1.5 mH, which is enough to show the trend of the ballast current variation. The 1.5 mH inductor can match to the ballast when it is working in 33 kHz. However, there are two reasons showing the series

inductor method is not very desirable. Firstly, if the ballast current is less than 550 mA, for 80 W HO ballasts, the LED voltage needs to be increased to meet the power requirement. Basically, when the operation frequency is higher than 35 kHz, the ballast current is lower than 550 mA and not stable under all series inductor values. The operation frequency of ballast has a range, mostly in 40 kHz to 60 kHz. The scopes of other two lines are steeper and not monotonous, which means the ballast current varies in a large range though changes the series inductor value slightly. Above discussion shows that it will be difficult to choose a certain LED voltage which fulfills the power requirement in the most of the ballasts. Secondly, the series inductor may also added other resonant points which may result in an unstable system behavior. Besides, considering the peak current and the size of the series inductor, this structure has no size advantages (has the same inductor size as the parallel inductor) compared to the parallel inductor structure which is more stable.
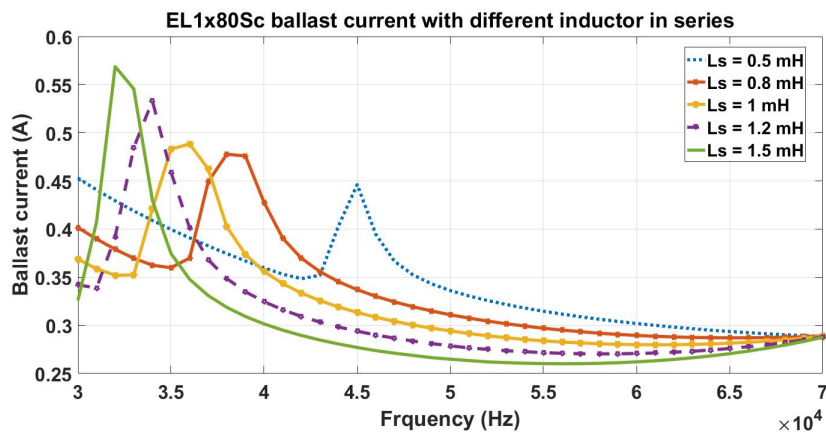
Figure 3.18: EL1x80Sc ballast current with different inductors in series

3.4. Design suggestions of T5 LED driver

From the discussion in previous sections, the ballast current can be reduced by adding an inductor in parallel. For different power level of ballasts, the standard LED voltage level is different. Usually a higher power output equals to a higher LED voltage, while the exception is the LED voltage of 49 W ballasts is higher than 80 W ballasts. The combination of the LED power and ballast current reduction can find a suitable parallel inductor value.

L_p [mH]	$I(L_{p,peak})$ [mA]	$I(L_{p,rms})$ [mA]	$Iballast_{rms}$ [mA]
0.5	889.78	563.77	507.79
0.7	684.78	418.53	538.46
0.9	531.85	325.65	565.17
1.1	435.47	266.5	584.76
1.3	368.01	225.51	599.09
1.5	319.34	195.41	609.87
Without L_p	/	/	680.99

Table 3.2: EL1x80Sc ballast connected to an inductor in parallel

Take the 80 W ballast as an example. Table. 3.2 and Table. 3.3 introduce the simulation results of two type of 80 W ballasts based on 70 V LED voltage. It should be noticed that if the parallel inductor is too small then at this LED voltage level the power will decrease below 35 W. Besides, the peak current of parallel inductor will increase, which limits the selection of the parallel inductor in the practical. Therefore, the trade-off between the parallel inductor, the LED voltage, the ballast

current (output power) and the peak current of the parallel inductor will be considered when choose a suitable solution for the ballast in a certain power level.

L_p [mH]	$I(L_{p,peak})$ [mA]	$I(L_{p,rms})$ [mA]	$Iballast_{rms}$ [mA]
0.5	740.6	461.59	478.97
0.7	527.36	329.76	495.7
0.9	409.64	256.37	509.68
1.1	334.73	209.7	519.57
1.3	282.82	177.34	526.64
1.5	244.84	153.69	531.93
Without L_p	/	/	562.99

Table 3.3: Exlc 180 ballast connected to an inductor in parallel

One of the reference ballasts for choosing inductor value is EL1x80Sc with relatively high ballast current in 80W ballasts. In order to avoid the ballast current is lower than required current 550 mA, Exlc 180 ballast with relatively low ballast current should be added to the investigation. The results of the two ballast are based on each ballast's operation frequency, shown in Table 3.2 and 3.3. Under a given LED voltage level, trade-off between reduction of ballast current, peak current of added inductor, and volume of the added inductor needs to be achieved. Based on Table. 3.2and 3.3, Fig.3.19 can be drawn.
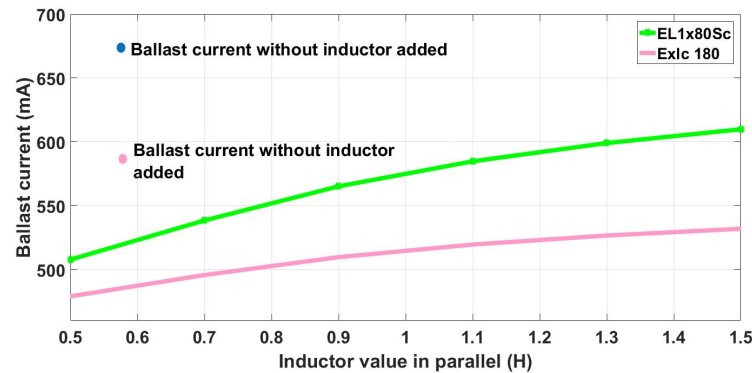
Figure 3.19: The ballast current of two types of ballasts when add different inductors

From Fig.3.19, a selected 1.2 mH inductor provides superior effects on the ballast current and the output power in a range of HO 80 W ballasts. The verification results are given in Table. 3.4 and Table. 3.5. The size in LED driver for TL5 tube is limited in 10 mm^2, thus WE-PD2 HV SMD Power Inductor (High Voltage)[15](10 mm×9 mm) from MOUSER is a good choice for the practical implementation. From Table 3.3 and 3.4, in two typical conditions, the output power is around 35 W which is acceptable for 80 W ballasts and the ballast current can be reduced to a reasonable value by the added inductor.

1.2(mH) in parallel	Test value [mA]	Datasheet [mA]
$i_{L,peak}$ of added inductor	301	350
$i_{Ballast,rms}$	629	WE-PD2 HV 1060
Current reduction	8 [%]	/

Table 3.4: EL1x80Sc ballast connected to chosen inductor in parallel

1.2(mH) in parallel	Test value [mA]	Datasheet [mA]
$i_{L,peak}$ of added inductor	223	350
$i_{Ballast,rms}$	542.7	WE-PD2 HV 1060
Current reduction	4.2 [%]	/

Table 3.5: Exlc 180 ballast connected to chosen inductor in parallel

The power loss of this method is mainly on the added inductor in this solution, so it is necessary to get RMS current of the inductor and AC resistance under the operation frequency. Due to the limitation of material in the lab, use EE1010-471 and 221 inductors to do the validation as the initial impression. The value of inductor is not exactly 1.2 mH but 1.16 mH in the practical. Based on Table. 3.6, take the EL1x80Sc ballast for instance, the RMS current of this inductor is 252 mA, and the loss of the inductor is 0.133 W.

Inductor value [mH]	Test inductor value	AC resistance
1.16	1.16	2.1

Table 3.6: Inductor parameters tested in 45 kHz

The drawback of this method is that only passive components are applied to the system which means the LED current cannot be regulated and controlled. Therefore, the active approach is mainly focused and introduced in the next chapter.

4

The active approach

The previous chapter introduces the passive method to improve the compatibility of the LED driver. However, the LED current cannot be regulated and controlled only through passive components. This chapter proposes two active methods for the retrofit T5 LED tube compatibility design. The first topology is a rectifier together with a boost converter, which is the SMPS method mentioned in the Chapter 1. The second topology named as the charge pump, also facilitates the compatibility design of the LED driver. Investigations on those two circuits will be shown and compared later.

4.1. The switch mode power supply (SMPS) method

A power supply is defined as "A device for the conversion of available power of one set of characteristics to another set of characteristics to meet specified requirements. Typical application of power supplies include to convert raw input power to a controlled or stabilized voltage and/or current for the operation of electronic equipment"[16]. The switch mode power supply, namely means supplying power by means of switch-on and switch-off states together with passive components such as inductors and capacitors to store and release power. The low power loss on switches and good capability of power conversion make it (SMPS) as a potential solution for the compatibility design.

4.1.1. The design principle

As mentioned in the previous section, the output of the ballast is an AC current. To apply SMPS method to the system, the input voltage should be first rectified and filtered by the rectifier and the capacitor. The regulated DC voltage is then fed to the SMPS. According to the requirements in Chapter 1, the LED output power should be around 35 W, and maintain the LED current below 300 mA to avoid high temperature thus enhance the lifetime of LEDs. Then considering that the ballast output current is around 550 mA, so the LED voltage should be almost twice higher than the input voltage. And there is no isolation required by the output. Furthermore, the size of the T5 tube limits the topology choices. Therefore, the boost topology is a good choice to realize the power conversion in the LED driver.

The control methods of the boost converter are various according to different proposals and applications. In order to have the less influence on the ballast, the LED driver should behave as resistive as possible. The output voltage of the ballast divided by output current should be a constant in this design (The LED is a constant voltage load and the LED current should be controlled). The on - time (T_{on}) control method which controls the switch-on time according to the feedback from the load current can achieve required behavior. It should be noticed that the input stage of this design is a current source rather than a voltage source and the control result is to keep output power constant instead of only keeping output voltage constant (a general situation of boost converters). The

basic principle of the on-time control is: When the load current increases, the switch-on time will prolong, leading to a lower input voltage. As a consequence the input and output power keeps constant with both the LED voltage and the input current stable. The basic block diagram (Fig. 4.1) to be discussed below, introduces the basic control principle and the gate signal generation. For the T_{on} control method, the available control chips in the market have relative large sizes which sizes are not acceptable in T5 applications. Besides, the operation frequency also limits the chip selection. The switch frequency is chosen to be higher than 250 kHz, based on following reasons:(1) For reducing the circuit size, the higher frequency leads to a smaller inductor. (2) The switching frequency should be much higher than the ballast operation frequency (tens of kHz), which makes the input voltage can be considered constant and the SMPS load resistive in a ballast switching cycle. Therefore, the gate signal is generated by a discrete circuit rather than chips. The gate driver voltage (V_{cc}) is normally gained from a zener diode with capacitors. Combining the control principle and
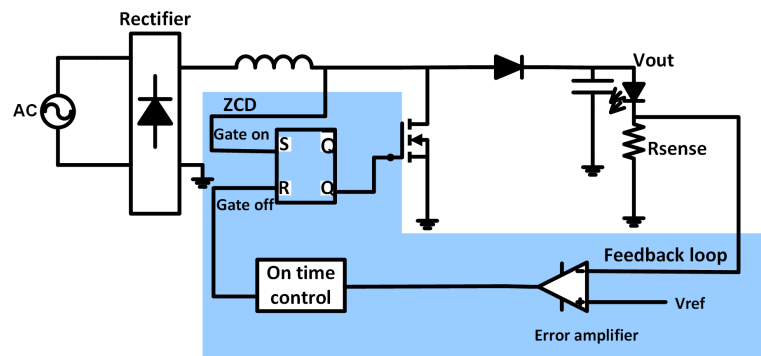
Figure 4.1: The basic block diagram of the SMPS method

the block diagram, the behavior of the control part can be described as: When the output current goes up, a control voltage generated by an error amplifier leads to a long on-time of the switch which means a lower load impedance seen by the ballast. The V_{in} is reduced and the output current will go back to the nominal value. The implementation of the on-time control part is realized by the RC oscillation circuit and two transistors which structure is low-cost and space saving. The control voltage from the output of the amplifier is regarded as the voltage source of the RC oscillating circuit (timing part). If the oscillation voltage reaches the turn-on voltage of the transistor, this transistor then short the gate voltage of the MOSFET resulting in a turn-off transition. Apparently the on-time of the MOSFET therefore depends on the oscillation time decided by the feedback loop. The detail of implementation is given later.

4.1.2. Basic knowledge of boost converter

Boost (Step-up) converters, as the name mentions, the output voltage is always higher than the input voltage. The basic structure is shown in Fig.4.2(left). When switch is on, the current flows through the switch, and the diode is reversed biased, isolating the output stage. The energy stored in output capacitor provides the load power during the switch - on time[17]. When switch is off, since the inductor current cannot change instantaneously, the output capacitor is charged and the load also gains power through the stored energy of the inductor. The boost converter can work in three operation modes. Continuous-conduction mode (CCM) means that the inductor current is continuously during every switching cycle, and discontinuous-conduction mode (DCM) as the name implies, the inductor current flows discontinuously. The boundary between continuous and discontinuous conduction is so-called boundary-conduction mode(BCM)[17]. Although the BCM operation brings a higher ripple current to the inductor and the switch compared to the CCM, it fulfills zero voltage switching (ZVS) during the turn-on transition of the switch and diode reverse

recovery is eliminated. For DCM, the current ripple in the inductor is high and not suitable for the on time control. Thus BCM is chosen in this design. The inductor current goes to zero at the end of every switch - off interval, shown in Fig.4.2(right)[17]. The red line is the inductor current. If the
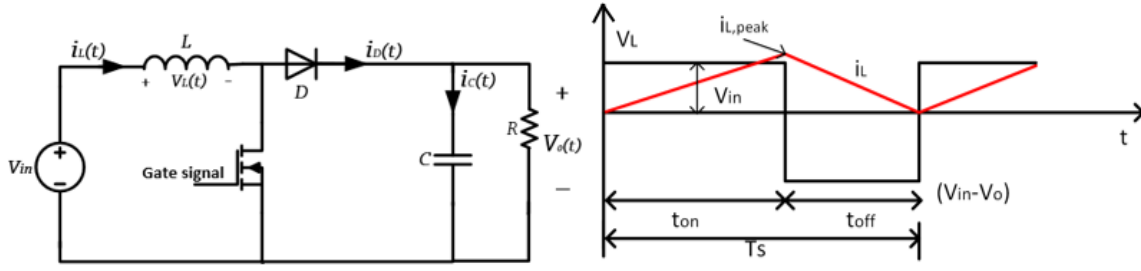
Figure 4.2: Boost topology and the inductor current with voltage in BCM

switch turns on for a fixed time, the peak inductor current is proportional to the input voltage. The duty cycle (D) corresponds to the on time of the switch, decided by the desirable output voltage in general case (while in this design the on-time depends on the LED current (power)).

$$\frac{V_o}{V_{in}} = \frac{1}{1-D} \tag{4.1}$$

The switch - on time (T_{on}) is defined as:

$$T_{on} = DT_s \tag{4.2}$$

Where T_s represents the operation period. The peak inductor current can be represented as:

$$\frac{V_{in}t_{on}}{L} = \frac{(V_{out} - V_{in})t_{off}}{L} = i_{L,peak} \tag{4.3}$$

The switching frequency of BCM boost converter is:

$$f_s = \frac{1}{t_{on} + t_{off}} \tag{4.4}$$

The power transferred through the inductor, the i_{Lpeak} is given in Equation 4.3:

$$P_L = \frac{1}{2}Li_{Lpeak}^2 f_s \tag{4.5}$$

The voltage-second balance equation for the inductor is:

$$V_{in}t_{on} = (V_{out} - V_{in})t_{off} \tag{4.6}$$

The average inductor current of BCM is specified as half of peak inductor current:

$$I_{LB} = \frac{1}{2}i_{L,peak} \tag{4.7}$$

From above equations, the switching frequency of boost converter depends on the input voltage, selected output voltage and power, and inductor value[18]. As the f_s needs to be higher than 250 kHz(introduced in the design principle) and output power requirements, the converter electrical specifications are as follows:
1. The output voltage: 150 V DC
2. The output power: 35 W
3. The switch frequency: higher than 250 kHz

4. The load is LED load

5. The design should provide a stable LED current with different brands of ballasts, which means the output current of ballast may vary around 550 mA. Therefore, a close - loop control in this system is needed.

6. Confronting the size limitation of T5 tube and the switching frequency, the gate signal generation of MOSFET will be realized by a discrete circuit instead of IC chips.

4.1.3. The implementation of the SMPS design

Based on the design concept and requirements above, the initial schematic is shown in Fig. 4.3.

Figure 4.3: The basic schematic of the design SMPS method

4.1.4. The on-time control

The principle of the T_{on} control is described in the concept design as the switch-on time will be controlled to fulfill the output power requirement. In this circuit, the T_{on} control is realized by R_2 as a sense resistor, C_3, R_8, R_3 and C_6 as a RC oscillation circuit, TS431 as an error amplifier, and R_{11}, D_3, R_{13} as the start circuit. The fundamental idea of T_{on} control method in the case of this current source input boost circuit is: when the output current decreases, T_{on} will be shortened by the control loop. As the input impedance increases, brings a higher input voltage. The output current therefore grows back to the initial value. Moreover, when the input current increases (by different type of ballasts), prolonging T_{on} keeps output current constant. From the other perspective, more current goes to the switch rather than the diode, eliminating the effect to the load current from the increasing input current. The T_{on} time is determined by RC oscillation time in this circuit, which can be derived as follow:

During the oscillation, C_6 and C_7 are in parallel with R_3. The control voltage can be seen as the voltage source of the oscillating circuit. The time constant τ is:

$$\tau = R_3(C_6 + C_7) \tag{4.8}$$

The lowest point of V_{osc} is V_{low} and when V_{osc} reaches the V_{BE} of Q1 the oscillation will be interrupted. Therefore, the voltage change during the oscillation is:

$$V_{BE} - V_{low} = (V_{control} - V_{low})(1 - \frac{1}{e^{\frac{-t_{on}}{\tau}}}) \tag{4.9}$$

The t_{on} can be defined:

$$t_{on} = -\tau ln(1 - \frac{V_{BE} - V_{low}}{V_{control} - V_{low}}) \tag{4.10}$$

From above equations the on-time is related to the control voltage derived from the feedback loop.

4.1.5. The gate signal generation
Gate drive voltage V_{cc} — The output voltage through R_4 and R_6 powers the 15 V zener with a capacitor(C_1) in parallel. C_1 eliminates the voltage fluctuation and stabilize the zener voltage. Besides, to guarantee enough charge to V_{cc}, a charge pump structure consists of C_8, D_{12} and D_{13}. This structure supplies V_{cc} through charging and discharging of C_8. At the starting stage, the two structures also speed up V_{cc} to reach 15 V.

Turn-on/turn-off methods — To generate the gate-source signal (V_{gs}), turn-on and turn-off methods need to be considered. The turn-on transition is realized by zero current detection (ZCD). When the inductor current crosses zero, C_7 will discharge and the current will be extracted from the base of Q_1. Then Q_1 is off and Q_2 is on, turning on the MOSFET. The turn-off of the switch is determined by the RC oscillation time, once the oscillation voltage reaches the turn-on voltage ($V_{be} > 0.7$ V) of Q_1. Once Q_1 conducts, Q_2 is open and MOSFET turns off.

4.1.6. Power control
Power control is achieved by the T_{on} control. The LED current is sampled by the sense resistor (R_2 and R_8). Comparing the voltage on R_8 with the reference voltage (V_{ref}) of TS431, the cathode of TS431 generates a controllable current i_k decided by the difference between the V_{R8} and V_{ref}. Consequently, the control voltage ($V_{control}$ in Equation.4.10) is gained through R_{13} times i_k.
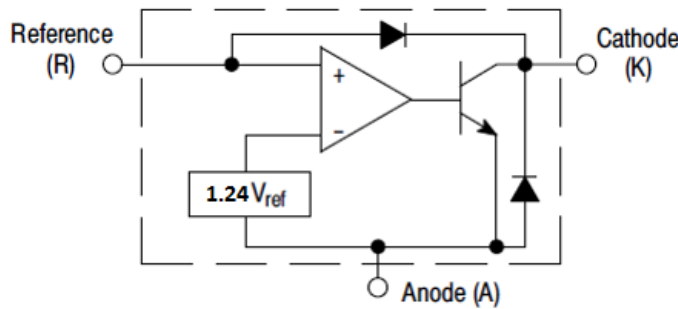
Figure 4.4: The basic structure of TS431[19]

TS431 is a low voltage adjustable shunt reference, and the simplified structure is shown in Fig.4.4. A small operating current (higher than 60 μA from datasheet) is provided through R_7 to supply the reference voltage and biasing currents for components in the chip. The output voltage can be set to any value between V_{ref} (1.24 V) and 6 V. When the difference between input voltage and V_{ref} increases but still in the operation range, more current will be extracted from the external circuit through the output (K). When i_{LED} increases, more current is extracted by TS431, and control voltage will decrease, leading to a longer oscillation time (longer T_{on}). The value of R_2 based on the desired output power.

$$P_{out} = I_{LED}V_{LED} \tag{4.11}$$

Choose the output power at the first stage.

$$I_{LED} = I_{sense} \tag{4.12}$$

The range of voltage on the sense resistor should be close to the reference voltage of TS431 (1.24 V).

$$V_{sense} = V_{ref} \tag{4.13}$$

It should be noted that these two voltage values are slightly different. However the value of R_2 can be identified according to the approximation.

$$R_{sense} = \frac{V_{ref}}{I_{sense}} \tag{4.14}$$

The control method therefore is a closed-loop control. The control range of T_{on} is limited by the value of RC oscillation (R_3 and C_6), and also the switching frequency which is related to the inductor value. Besides, the parasitic elements in the circuit need to be considered as well.

4.1.7. The start method
The start method is of importance in the circuit design. Without the start circuit, the switch will always keep off because no enough gate voltage is supplied for the gate and the circuit behaves like a rectifier with an inductor for the current regulation. The principle of the start circuit is to ensure ($V_{BE} < 0.7$ V) and the enough gate voltage to turn the switch on. Once the current flows through the switch the inductor current will go down and at the end of one cycle achieve the zero current detection to turn on the switch. The realization of the start circuit is explained: As the current flows through the circuit, the input voltage increases and clamped by the zener diodes. An instantaneous high voltage from the zener diodes is added to the control loop and supplied the gate driving voltage for the MOSFET. By means of this transition the RC oscillation starts working and leads to the turn-off of the Q1. After several cycles the system becomes stable.

4.1.8. Simulation validation
The simulation model is based on the Fig.4.3. The input is simulated as an AC current source with the ballast current operation frequency and amplitude. The inductor value is 100 μH and the LED output voltage is chosen at 150 V. Figure. 4.5 shows the waveforms of simulation results. The first plot pane to forth plot pane represent the oscillation signal, the current of C_7, the inductor current and the gate-source voltage. From the waveform of the inductor current, it can be seen that the circuit works in the boundary condition mode with 340 kHz frequency. Once zero crossing of inductor current is detected, the MOSFET is turned on. The current will be extracted from base of Q_1 and will flow up to C_7. Therefore, the gate voltage has a small oscillation below zero. The left two plots present this transition. During the oscillation time, switch keeps on (V_{gs} is high). At the end of oscillation, the MOSFET is switched off. Drain-source current goes to C_7, charging the base of Q_1 to 0.7 V.

The simulation model of TS431 is different from the LMV431 which is employed in the test. The range of operation voltage of the LMV431 is between 1.24 V and 30 V, while TS431 is 1.24 V to 6 V. In the simulation the circuit cannot work when the control voltage (also the cathode to anode voltage of TS431) is higher than 6 V. Therefore, only experimental validation of control loop function are given (see Fig. 4.7). However, the model is still reliable, if lower down the output power. To check the control loop, add an AC current to the source after the system becomes stable (30.5 ms later in
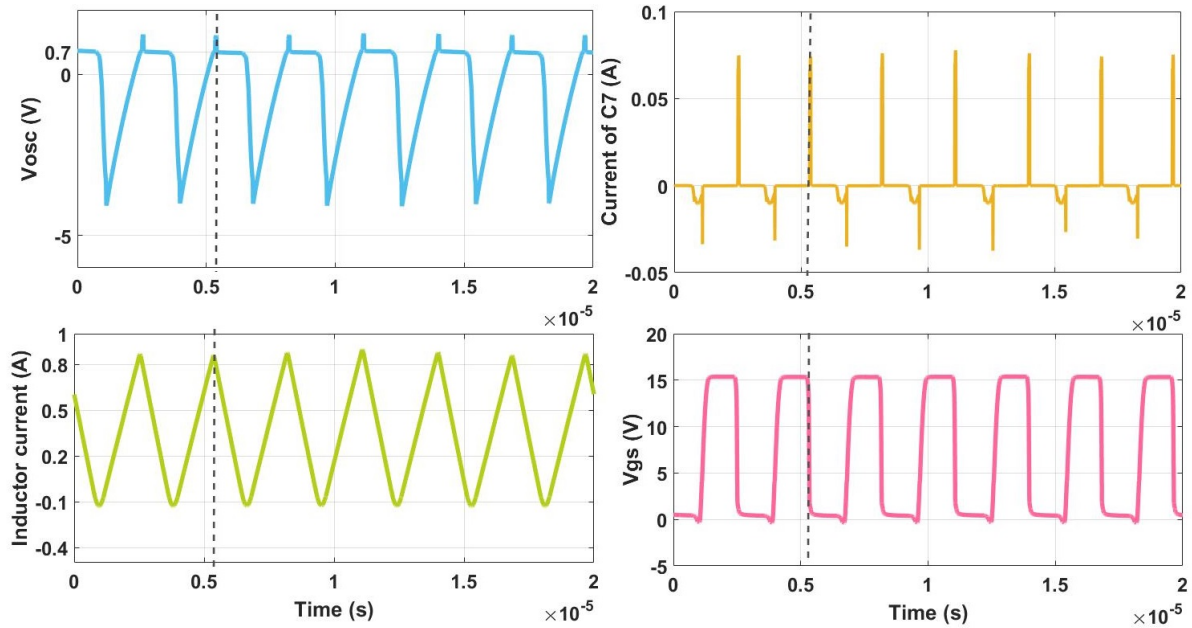
Figure 4.5: Simulation waveforms of main signals

the simulation) and change the sense resistor to 7.5 ohm (to lower down the output power). At first, the LED current is 165 mA when the input current is 530 mA AC current. Then 100 mA AC current will be injected to the input at t = 30 ms. The control voltage change is shown in Fig. 4.6(a). The LED current and input voltage is in Fig. 4.6(b).

a. Control voltage

b. Input voltage and LED current
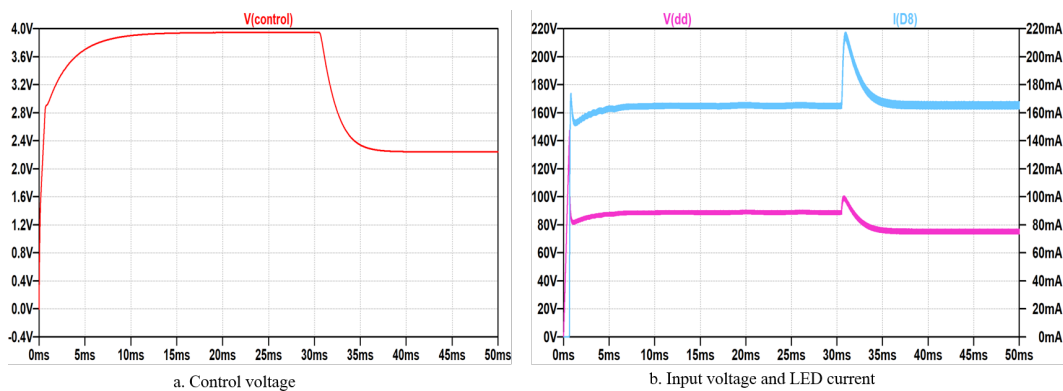
Figure 4.6: Simulation validation of the control loop

From the above figures, the control voltage changes to a lower value (from 3.9 V to 2.2 V), which means the on-time of switch is extended. More input current will flow to the switch and the LED current thus keeps constant. The blue line (higher) and purple (lower) line are the LED current and the input voltage respectively. At t = 30 ms, a disturbance shows up in the system. The LED current is 165 mA at first and then has an increase at 30 ms. After the adjustment by the control loop, the input voltage becomes lower to reduce the input power and the LED current goes back to 165 mA.

4.1.9. Experimental validation of the initial design

In this section, the main objective is to see if the practical circuit can output enough power for the LED load. The initial experimental circuit is build based on Fig. 4.3. The input of this design

is output stage of the ballast connected with the filament circuit. The LED voltage (150 V), and sense resistor (5 ohm) can be chosen for a desirable output power (35W). The test circuit is given in Appendix.A.2. Basic electrical parameters based on test are shown in Table. 4.1.

V_{out} [V]	V_{in} [V]	P_{in} [W]	P_{out} [W]	I_{in} [mA]	I_{LED} [mA]	R_{sense}[Ω]	Efficiency [%]	Frequency [kHz]
156	81.6	36.4	39.6	485	232	5	91.9	290

Table 4.1: Initial experimental results based on the 80 W ballast

The switching frequency is 290 kHz, which is lower than the simulation result. The parasitic elements in the real circuit mainly lead to this difference. In Fig. 4.7(a), the inductor current is the green triangular waveform. The yellow line and purple line (top) show the LED current and the input voltage. The circuit operates in boundary condition mode, and the output power reaches 35 W. The LED current ripple is lower than 5% of the average LED current. The input current waveform is shown in Fig. 4.7(b). Basically, the ballast current waveform matches the simulation result. The reference signal of TS431 is 1.24 V which means the control loop works. The undesirable oscillation shown in test figure happens because during the dead time of the switches in the half bridge of ballast. The time interval where both switches are off in the half bridge is so-called dead time [20]. The small resonance in the ballast output stage therefore happens, leading to an oscillation of output current. Besides, the parasitic elements in the circuit, arrangement of wiring and soldering problems. Also the test probe produces some small oscillations when connected to the circuit.

a. Input voltage, inductor current and LED current   b. Input current and reference voltage of TS431
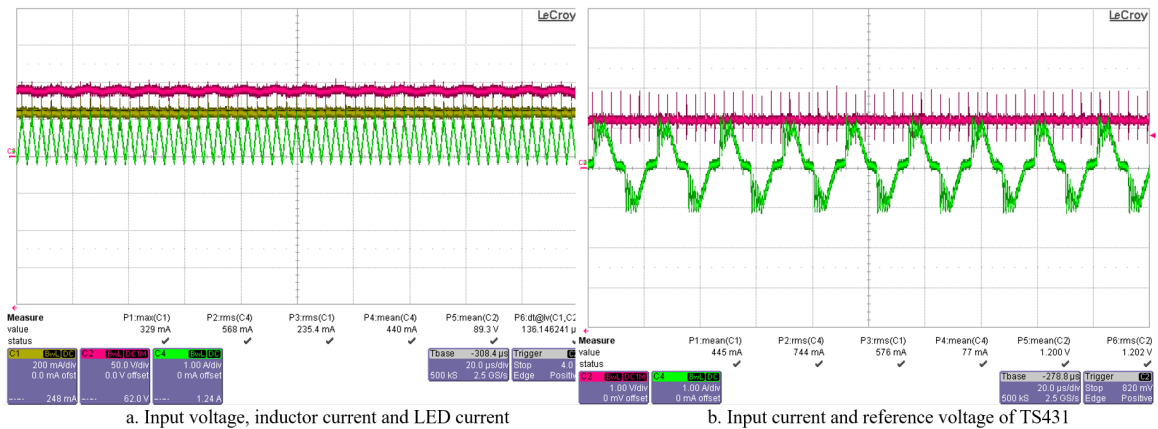
Figure 4.7: Experimental results which match to the 80 W ballast

As discussed above, this design can achieve basic requirements mentioned in Chapter 1. However, the size of the circuit needs to be reduced to fit the T5 tube. Other circuit performances also could be improved such as efficiency and high inrush current. After optimizing the initial circuit, a detailed test results will be given in later section.

4.1.10. Improvements based on initial test results

Inrush current is the maximum and instantaneous input current as the circuit starts working. The high start voltage and charging of the input capacitor at the beginning cause a high inductor inrush current, which current may result in the saturation and overheat of the inductor, potentially causing the electrical device to malfunction or breaking down. The simulation result of this problem is shown in Fig. 4.8. Furthermore, the undesirable size and efficiency should be optimized by changing the value of components and circuit structures.

Improvement of high inrush current

In the previous design, the control method in this circuit is the on-time control and the on time of the first cycle is not limited to a low inductor current. The inductor inrush current can reach 6 A which is much higher than the steady state current. The concept for dealing with this problem is to turn off the Q_1 quickly after the start, and at the mean time V_{cc} reaches a value that is enough for turn-on of the MOSFET. To solve this problem in implementation, the lower yellow part of the circuit in the Fig. 4.3 is added. During the first cycle, the oscillation signal will get a turn-on voltage by R_9 and after a short T_{on} time, Q_1 will be shut down by Q_3. The base current of Q_1 will be extracted from Q_3 when Q_3 is switched on because the start voltage is added to Q_3 by R_{12} and C_4. Once the control loop starts working, the diode (D_{18}) will prevent the Q_3 part from working. V_{cc} also should be high enough to guarantee the gate voltage. The simulation result is shown in Fig. 4.9(a). The inductor current in the first cycle is in BCM and the value lows down to 4.2 A.
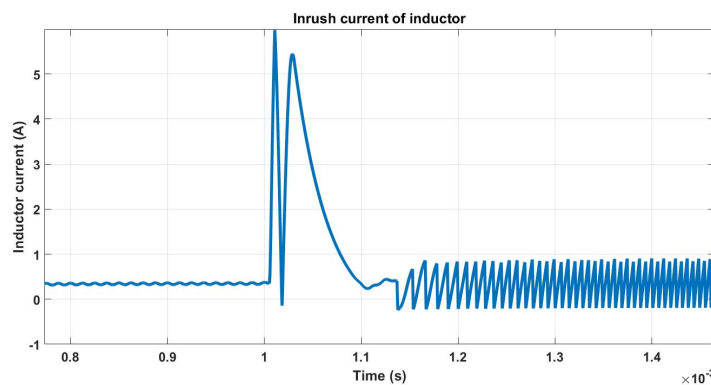
Figure 4.8: The inrush current in the inductor at the start in the simulation

The experimental validation is shown in Fig. 4.9(b). The peak value of inrush current is 4.5 A and basically matches the simulation result. The peak value in the practical is slightly higher than the simulation due to the real input current is higher than the simulation. The load impedance of this circuit is lower than the 80 W lamp resistor, resulting in a higher ballast current but still in an acceptable range (lower than 120% ballast current of fluorescent lamp).

b. The inductor current at the start after improvement in the simulation

a. The inductor current at the start after improvement in the test
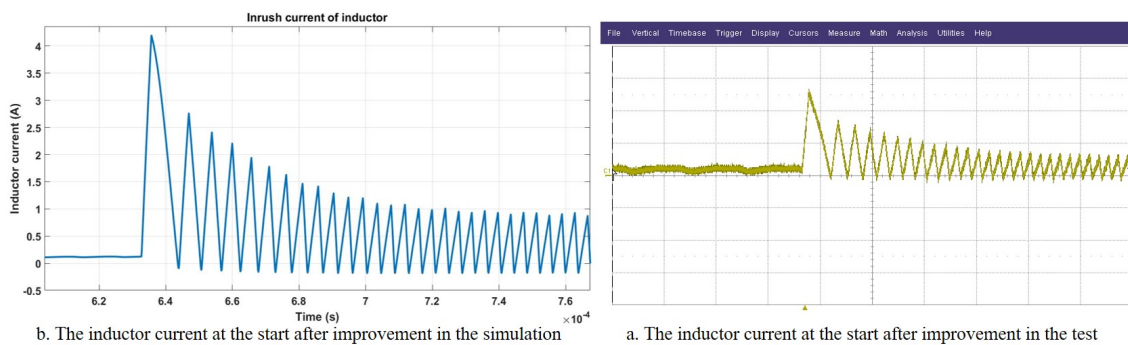
Figure 4.9: The inductor current at the start after improvement

Improvements of efficiency and size

The efficiency of the initial design is 91.9% and after the improved based on the following aspects, the efficiency reaches 93.4%. First, change the driving current of TS431 from the output voltage (V_{out}) to V_{cc}. Thus the loss on the R_7 is reduced. Second, R_4 is removed after the practical test,

because V_{cc} is build up soon by R_{15} and charge pump structure(C_8, D_{13} and D_{12}). Third, the starting circuit is changed to reduce the size of circuit, which also lowers down the conduction loss of the diodes during the start.

Although many methods have been applied to the design to reduce the circuit size in the initial design. The initial size is too large to fit in the T5 tube. In order to reduce the size of circuit, the values of input and output capacitor are reduced. The reduction of the output capacitor is based on the standard: The LED current ripple should be lower than 30% of the average LED current. Besides, R_{10}, Q_4 and D_{22} are removed, since the reduction of turn-off loss by this structure can be neglected. Additionally, the two upper zener diodes (D_{11}, D_{16}) and the diode D_{10} are removed. The start can rely on other two zener diodes according to the test result. The topology after improvements is shown in Fig. 4.10.
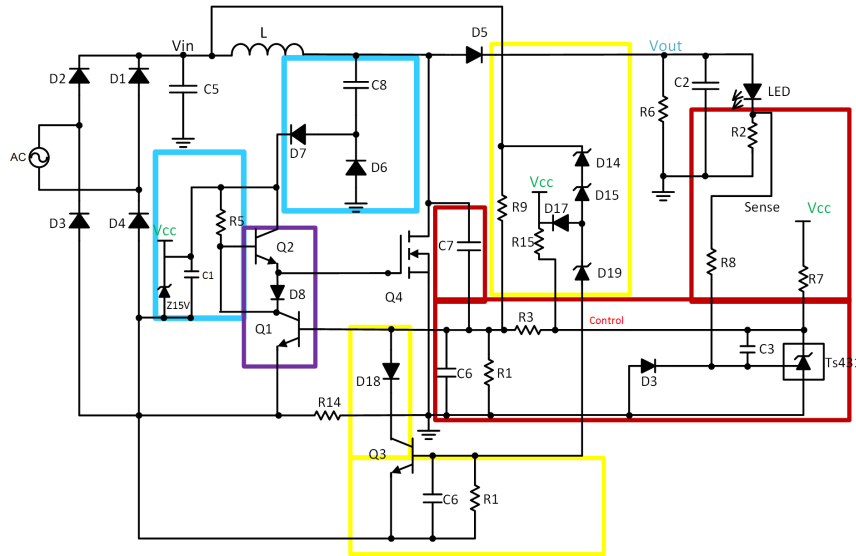
Figure 4.10: The basic schematic of the designed SMPS circuit after improvements

4.1.11. Experimental validation after improvement

The test circuit is improved based on Fig. 4.10. The related parameters are given in Table. 4.2. The difference between the initial circuit and the improved circuit is mainly due to a higher sense resistor (5.6 ohm) applied in improved circuit. The output power therefore decreases about 1 W compared with the initial circuit.

V_{in} [V]	V_{out} [V]	I_{LED} [mA]	R_{sense} [Ω]	Operation frequency [kHz]
75.68	154.52	221.7	5.6	300

Table 4.2: The related electrical specifications after improvement

In Fig.4.11(a), the yellow triangle line is the switch current (i_{ds}) and the red square line is the switch voltage (V_{ds}). The current and voltage test results of MOSFET are presented in Table. 4.3. Fig.4.11(b) shows the reference voltage (in blue) and the oscillation signal (in purple) respectively. The reference voltage is close to 1.24 V which means the control loop works normally. The oscillation in each switch turn-off transitions is caused by the disturbance when the switch current flows to Q_1 through C_7 as soon as Q_1 is on.

In Fig. 4.12, the inductor current (lower) is in yellow and LED current (higher) is in green. It can be seen that the boost converter works in BCM. The peak current of inductor is 1.17 A, which is higher

a. Switch current and voltage   b. Oscillation signal and reference voltage
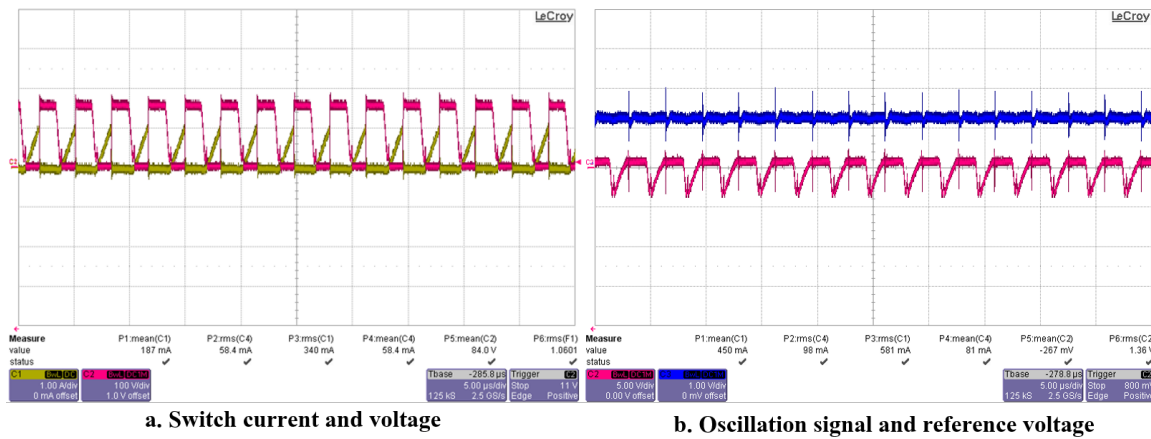
Figure 4.11: The switch current with voltage and control signals

V_{ds} [V]	$I_{sw,rms}$ [mA]	$I_{sw,ave}$ [mA]	$I_{sw,peak}$ [A]
154	371	155	1.17

Table 4.3: Electrical parameters of MOSFET

than simulation. It is because the input current in the practical is the output current of the ballast which is not an ideal AC current source. Besides, the load impedance of ballast in this condition is lower than the fluorescent lamp, increasing the ballast output current. The LED current ripple is 40 mA which is 18% of average LED current (still meet the requirement that the current ripple should lower than 30%) after reducing the output capacitor.
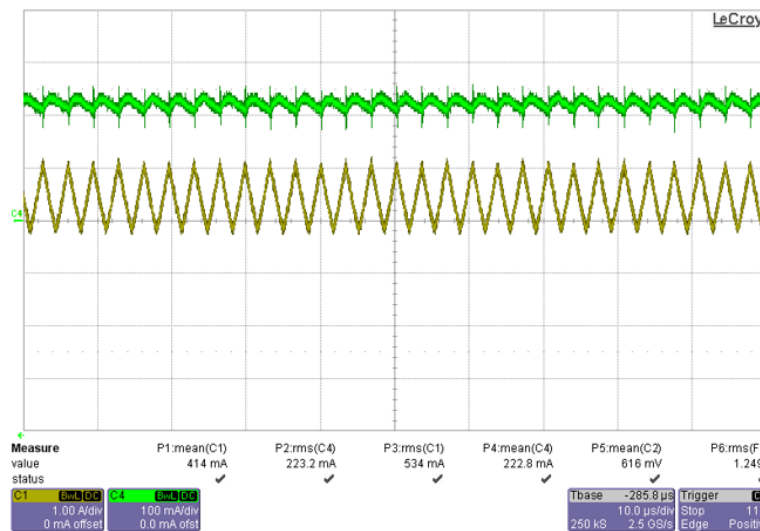
Figure 4.12: The inductor current and the LED current in the test

4.1.12. Behavior of each components

In this section, the behaviors of main components in this circuit will be shown for the loss calculation and validation with simulations.

The switching behavior

The test results of MOSFET are shown in Figure 4.13. The yellow line is drain-source current (I_{DS})

and the red line is drain-source voltage (V_{DS}).
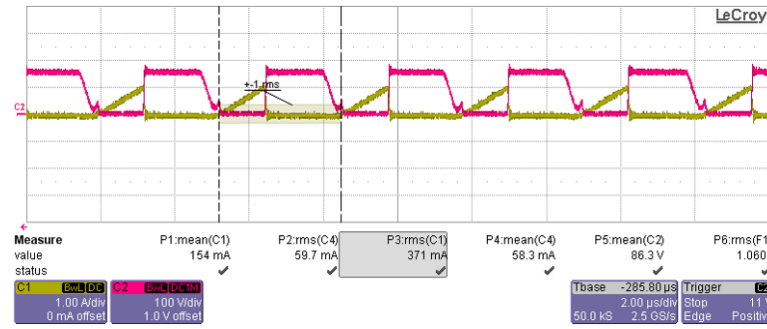
Figure 4.13: V_{DS} and I_{DS} of MOSFET in the test

The loss from MOSFET can be divided into conduction loss and switching loss. The conduction loss is derived as:

$$P_{mos,cond} = I_{sw,rms}^2 R_{DS,on} \tag{4.15}$$

$R_{DS,on}$ is the conduction resistance of MOSFET and this value can be found from datasheet. While this value is tested in a specific condition in datasheet, the calculation based on this parameter can lead to an error. The switching loss of MOSFET is more complex than the conduction loss. In BCM, the turn-on loss should be zero due to zero voltage switching(ZVS). Figure. 4.14 gives the turn-on and turn-off transition of the MOSFET. The yellow line represents I_{DS} and the red line represents V_{DS}. During the turn-on transition the V_{DS} falls to zero before the I_{DS} begins rising. Therefore the

a. v_{DS} and i_{DS} during turn-on transition   b. v_{DS} and i_{DS} during turn-off transition
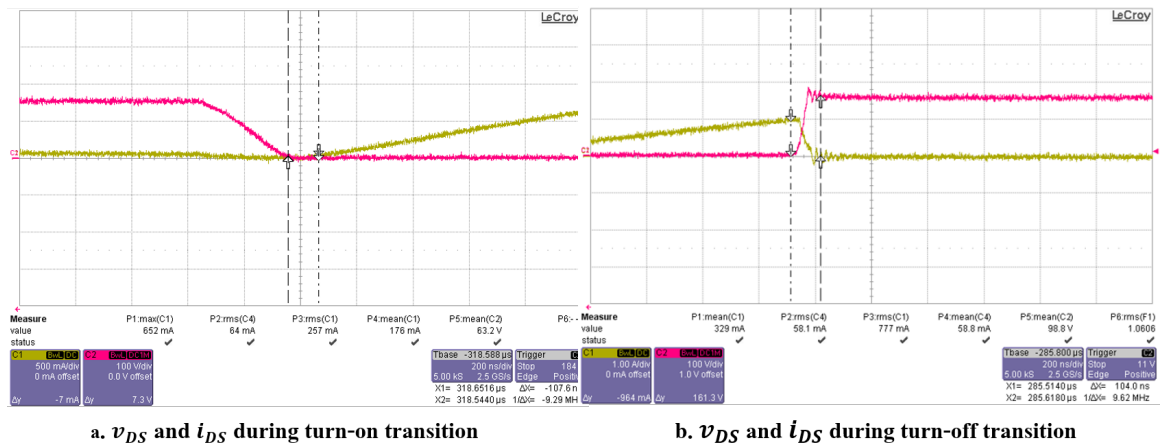
Figure 4.14: V_{DS} and I_{DS} during the turn-on and off transition in the test

switching loss in turn-on transition can be seen as zero. During the turn-off transition, the switching loss can be determined by:

$$P_{sw,loss} = \frac{1}{2} V_{out} i_{L,peak} (t_f + t_{d,off}) f_s \tag{4.16}$$

Where t_f is the fall time of drain-source current and $t_{d,off}$ is the turn-off delay time. It should be noticed that the calculation result (0.6 W) based on this equation is larger than the test loss (0.4W) tested by the power meter, because the measured $t_f + t_{d,off}$ from the oscilloscope brings errors. These two time values depends on the charging time of the the parasitic capacitors(C_{GD} and C_{GS}), the plateau voltage and the gate resistor of the MOSFET. Thus it is difficult to get accurate values of t_f and $t_{d,off}$ through the oscilloscope and calculations. The loss tested by the power meter is also not exactly the switching loss of the MOSFET even after removing the conduction loss part, but

contains the loss from other parasitic elements in the MOSFET. However the error from the power meter is less than the calculation, the result is shown in section. 4.1.13.

Diode behavior

To verify the diode behavior and calculate the diode conduction loss, the diode current is shown in Figure 4.15. The switching loss of the diode happens when the diode switches from blocking state to forward bias and vice verse[17]. While the turn-on loss is rather small compared with the turn-off loss and neglected in many boost converter application notes. The turn-off loss is related to the reverse recovery time (t_{rr}), the reverse recovery charge, the blocking voltage and the switching frequency. In order to low down the turn-off loss, a Schottky diode with very short t_{rr} is selected for the output diode and the rectifier. Besides, this circuit operates in BCM, reduce the turn-off loss further. Therefore the switching loss of the diode in this design can be negligible compared to the conduction loss.
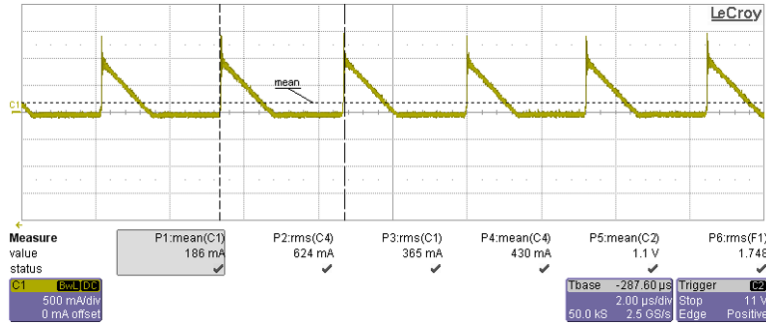
Figure 4.15: The diode current in the test

Table. 4.4 presents the test results of diode. The conduction loss of diode can be calculated by:

V_D [V]	$I_{diode,rms}$ [mA]	$I_{sw,ave}$ [mA]	$I_{sw,peak}$ [A]	$R_D[\Omega]$
0.46	365	185	1.17	0.0625

Table 4.4: Electrical parameters of diode

$$P_{Diode,loss} = R_D I_{D,rms}^2 + V_D I_{D,avg} \tag{4.17}$$

R_D is the equivalent conduction resistance of diode and V_D is the forward voltage drop on the diode. R_D can be gained from the forward voltage difference divided by difference of forward current at a specific temperature. V_D can be tested in the circuit by oscilloscope probe.

Inductor behavior

The inductor chosen in this circuit is a commercial inductor considering the size limitation. However, the related parameters of the inductor such as the core material, wiring and power density are not given in the datasheet. The inductor behavior is related to the operation frequency, the winding resistance, the operation current and voltage, and the core material of the inductor. In this design, the analysis of inductor will only focus on the power loss which is explained in the next section.

Capacitor behavior

The input capacitor is for building the DC voltage at the input stage. The output capacitor provides power for the load during the switch-on time and also works as a filter capacitor to eliminate AC components in the output stage. The loss on capacitors is defined as:

$$P_{loss} = ESR i_{c,rms}^2 \tag{4.18}$$

The ESR is the equivalent series resistance, resulting in the main loss of capacitors. This parameter is tested in a specific frequency by impedance analyzer.

4.1.13. Loss analysis

The power loss in the circuit will be discussed in this section. The power loss in the boost converter can be classified into conduction loss, dynamic loss and fixed losses [21]. Fixed loss is produced by leakage currents of transistors, diodes and capacitors, which is independent of the switching frequency or the load. This loss is much lower than other two type losses and often can be neglected [21]. Semiconductor components such as MOSFETs and diodes produce dynamic losses. Conduction loss is related to resistors, for example, the conduction resistance (R_{on}) of MOSFETs.

P_{in} [W]	P_{out} [W]	V_{in} [V]	V_{out} [V]	I_{LED} [mA]	$I_{L,rms}$ [mA]	Duty cycle	Efficiency [%]
36.6	34.2	75.7	154.5	221.7	551	0.51	93.4

Table 4.5: The basic electrical parameters of the SMPS circuit in the test

The basic electrical parameters in the practical test are shown in Table. 4.5. It can be seen that about 2.4 W loss in these components. In the circuit, the power loss in the components is calculated based on previous section. The result is shown in Table. 4.6:

	Rectifier	MOSFET	Inductor	Diode	Resistor	Cpacitor	Total
Power loss [W]	0.48	0.6	1.8	0.11	0.31	0.01	3.31
Percentage [%]	20	25	75	4.6	12.9	4.2	137.9

Table 4.6: Loss in the circuit from calculations

It can be found that about 37.9% calculation loss in the circuit is superfluous. The calculation errors should be noticed. The inductance and resistance of the inductor versus frequency are tested by the impedance analyzer and the results are shown in Fig. 4.16. According to:

$$P_{Inductor,loss} = I_{L,rms}^2 R_{AC} \tag{4.19}$$

At 300 kHz frequency, the AC resistance of this inductor is about 6 ohm which means 1.8 W inductor
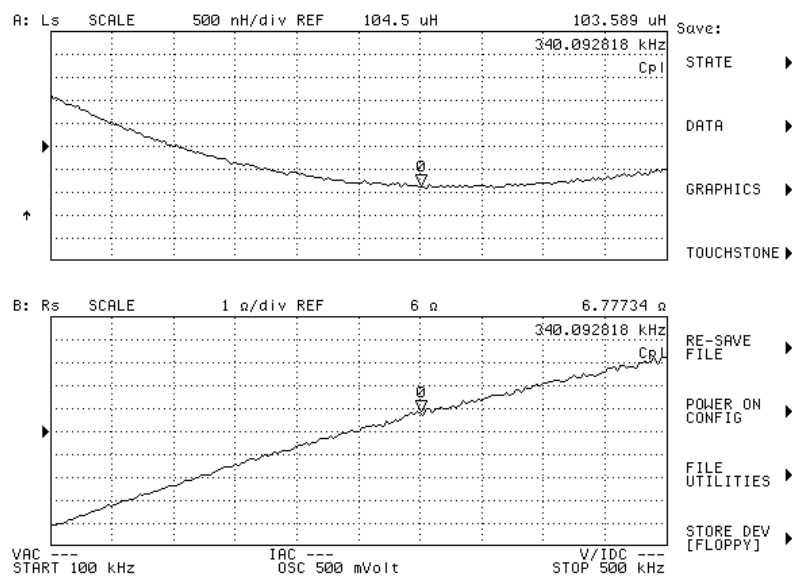

Figure 4.16: The inductance and resistance versus frequency

loss after times the inductor RMS current. The inductor AC resistance based on the inductance analyzer may not be correct. Therefore, to verify the loss in the inductor, thermal test is adopted. This method is considered as the most accurate way to test the inductor loss in the practical. The setup is shown in Fig. 4.17(a). The basic principle of this test method is: put a same inductor (as a reference inductor) in the same condition and a close position to the inductor used in the circuit, and add a DC current source to this reference inductor. Meanwhile, turn on the circuit. Afterwards, change the DC current through the reference inductor to make sure both inductors in the same temperature when they reach the stable state. In this way, the loss is transferred to the temperature. The inductor loss therefore can be defined as the DC voltage of the reference inductor times the DC current. The power loss in the inductor tested through this method is 1.1 W, with the 2.2 A DC current and 0.5 V DC voltage on the reference inductor. The power meter is applied to validate the

a. The thermal test setup of the inductor   b. Thermal test results of the circuit
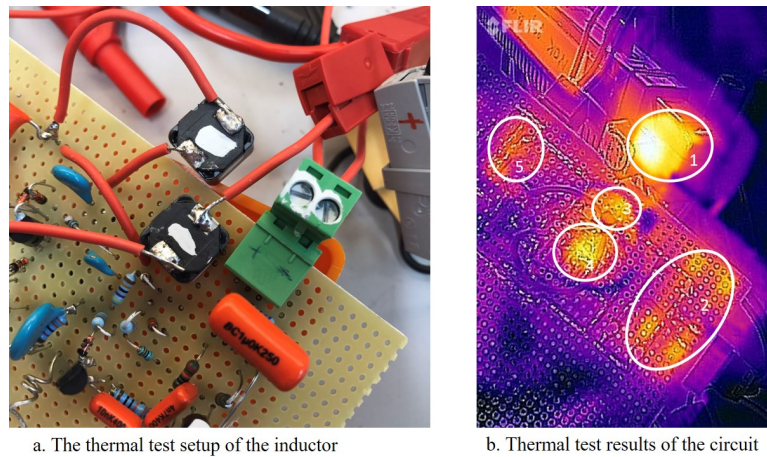
Figure 4.17: The thermal test setup of the inductor and thermal test results of the circuit

loss in each components. The loss in the circuit after this verification is shown in Table 4.7. The other loss except mentioned above this table can be generation loss in the gate signal circuit and fixed loss. Since the test circuit is not built in printed PCB board, the loss due to soldering needs to count. Besides, the errors from readings and measurements should also be considered.

	Rectifier	MOSFET	Inductor	Diode	Resistor	Cpacitor	Total
Power loss [W]	0.43	0.4	1.1	0.11	0.31	0.01	2.36
Percentage [%]	17.9	16.7	45.8	4.6	12.9	0.4	98.3

Table 4.7: Loss in the circuit after verification

4.1.14. Temperature test

The heat distribution is clearly shown in Fig. 4.17(b). The temperature of each component is measured by the thermal camera in the stable state (at least 5 minutes after the circuit starts working) and the result is shown in Table. 4.8. The part 1 to 5 presents the inductor, the rectifier, the diode, the MOSFET, and the output stage including the sense resistor and other resistors. The maximum ther-

	MOSFET	Inductor	Diode
Temperature [°C]	69	70	50

Table 4.8: The temperatures of main components

mal resistance of MOSFET is 100 (°C/W)[22] from the datasheet, Which indicates that the junction

temperature on MOSFET is about 65 °C(combine the power loss on the MOSFET and the ambient temperature). The difference can come from the influence of other components on the board.

4.1.15. Interpretations of the difference between experimental results and simulation

In this section the comparison between simulation results and test results will be introduced. The model of TS431 is not accurate in the simulation. As a result, the circuit is saturated when connected a 5.6 Ω sense resistor and the output power cannot reach 35 W. The comparison between the practical circuit and the simulation can be done when apply 25 W output power (the result is in Table. 4.9). The control loop can work in both conditions, and the difference should be similar to 35 W case.

	V_{in} [V]	V_{out} [V]	$I_{L,rms}$ [A]	I_{LED} [A]	R_{sense}[Ω]	Duty cycle	Frequency [kHz]
Simulation	73	152	0.460	0.16	7.5	0.63	350
Practical	57.6	152	0.550	0.167	7.5	0.62	290

Table 4.9: Electrical parameters in simulation and practical @ 25W

From Table. 4.9 and Table. 4.5, it can be observed that the duty cycle is 0.51 in 35 W output which is lower than 25 W condition. It is reasonable since more power goes to the load, the on-time of switch prolongs. The switching frequency is 340 kHz in simulation which is much higher than the frequency in the practical test. It is because that the parasitic elements exist in the real circuit, and the inductor value does not exactly equal to 100 $/muH$ from Fig. 4.16. In the simulation the input stage is an ideal current source, while in the test the input stage is the output of ballast with the added filament emulation. Besides, the load impedance of this circuit is lower than the 80 W lamp resistor, leading to a higher ballast current. Therefore, the real input current is higher than simulation, to get a same output power in practical the T_{on} time will increase, and more current will go to MOSFET which leads to a lower frequency. Besides, the input voltage and inductor current are different also due to different power sources applied in the simulation and the practical test.

4.1.16. Circuit volume

To match T5 tubes, the total volume of components needs to be considered. The inductor and large capacitors occupy relatively large volume beyond other components. The inductor size is chosen in 12.5(L)$\times$ 12.5(W)$\times$ 8.5(H) with B82477P4 type, according to the following reasons. Firstly, the inductor should meet the current, inductance and frequency requirements. Secondly, the saturation current decides the inductance drop while the core loss depends on the AC current ripple. Therefore, if other conditions are same, the inductor with a relatively low saturation current should be chosen in this design. A lower saturation current means that the inductor needs more turns to produce more flux, and to fit in the same volume (core) the wire will be thinner. So the DC resistance is larger within a lower saturation current. Thirdly, the inductor current ripple is large in BCM, the magnetic flux varies a lot which leads to a high core loss. More turns can distribute the flux and reduce the AC loss. (The comparison between three inductors in the test shows that the AC loss is dominate in this design, the test result is in Appendix. A.2.1). Fourthly, in order to achieve high stability and reliability, shielded inductors are considered (for the un-shielded inductor, the magnetic flux of its non-shielded counterpart is not confined to a given vicinity).

In Fig. 4.3, C_2 is the output capacitor which filters the AC component and provides the constant current for the LED load. Multi-Layer Ceramic Capacitor (MLCC) is applied in the practical products. The required package is 1206 with X7R formulations which is called "temperature stable" ceramics and adopted EIA Class II materials. In this design, the output capacitor consists of two 680 nF / 100 V capacitors in series occupying 18.432 mm^3 in total. This design saves more space in the output capacitor area compared with the exist products which take 65.536 mm^3 for the output capacitors.

The LED voltage of the released 80 W T5 products is 69 V and with 9.4 μF output capacitor. (8 * 4.7 μF/50 V (every two capacitors in series then set four groups in parallel)). The PCB schematic is shown in Appendix. Fig. A.7. The schematic shows the whole TL5 driver with the implementation of this designed circuit.

4.1.17. Conclusion of the SMPS method

The experimental test is setup on Philips HF-P 80W ballast and also other ballasts(eg. Exlc 180). In this design, the advantages are as follows. Firstly, The output of this circuit supplies the 150 V LED load and the ripple in LED current is low enough to meet the standard of Philips lighting (peak to peak LED current divided by average LED current less than 30%). Secondly, the output power can be controlled in a constant value, which makes this design could match ballasts in a widely range. Additionally, for the dimmable ballasts, this design is also adoptable. The main point is to guarantee the output power following the input power when the luminance needs to be adjusted (reduced, in general). For example, forcing the control loop saturated by adding a clamping diode which can limit the control voltage in a certain value. Therefore, the output of the circuit essentially becomes a DC current which follows various input power. Furthermore, the efficiency is acceptable for 80 W ballasts.

Although this design have above merits, there are still some limitations. The size is larger than the size required, especially after the improvement design of the inrush current. Besides, The loss from the inductor is unsatisfied if only commercial inductors are considered. The main improvement of this method in the future needs to consider the better design of the inductor. Although the frequency is chosen at a relative high level at the beginning to limit the inductor size, a suitable inductor for this design is difficult to find in the market. Building an inductor according to the requirements (size, saturated current, frequency range, etc.) could be a possible way while the cost might be high. Therefore, to eliminate the size limitation in this design, the next method comes up and also can be concerned as a potential solution in size.

4.2. Controlled charge pump method

Based on the experience from the previous solution, rectifier and inductor are removed in this design. The charge pump circuit can be considered as the inductorless DC-DC converter, which applies capacitors to storage energy and produces a higher voltage or lower voltage power source[23].

4.2.1. The design principle

The output of ballasts is a current source, the main idea of this design is to transfer required current to the load and shunt back the excess current through the switch. Moreover, no inductors means the input current should be sampled directly from the ballast output, therefore the switching frequency is synchronized to the ballast operation frequency. To control the output power, the switch is still needed to control the current through on and off states. Therefore, the controlled charge pump circuit consists of the gate signal generation part, feedback and control loop.

From the basic block diagram (shown in Fig. 4.18(a)), and waveforms of main signals including the controlled on-time, the input current (i_{in}), the diode current (i_{diode}) and the switch current (i_{switch}) (in Fig. 4.18(b)), the control method is similar to the SMPS circuit. The on - time (T_{on}) of the switch is controlled to meet the power requirement. During the positive period of the input current, the excess current goes through the switch in the controlled on-time, and the load current is delivered through the diode. During the negative period all input current flows back to the ballast through the switch. Apparently, due to the lack of the rectifier, only the half-period ballast current can be used for the load. The RC oscillation is also applicable for the on-time realization in this design. However, the gate signal generation solution is different from the SMPS circuit because there is no inductors anymore. Since the on-time control already gives a voltage signal from the feedback loop, the gate signal can be generated from a NOR gate by comparing the feedback signal and the sampled signal from drain-source voltage (V_{DS}). The NOR gate means that only both input signals are confirmed as low level, the output is high. The LED current is sensed by a resistor consisting of
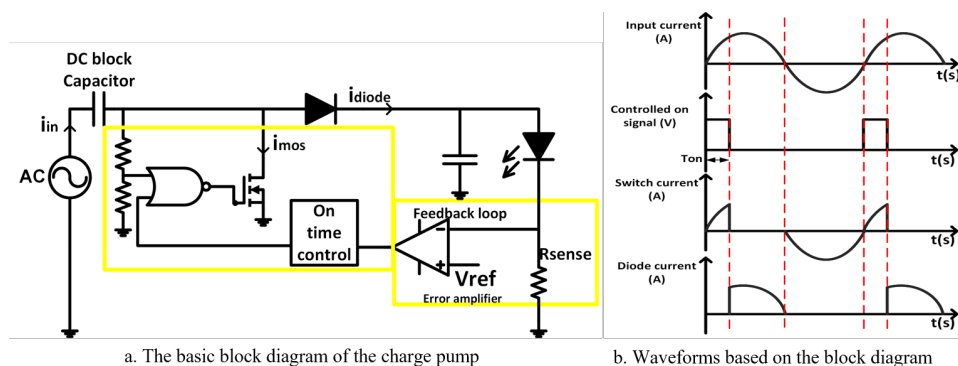

| a. The basic block diagram of the charge pump | b. Waveforms based on the block diagram |

Figure 4.18: The basic block diagram and simplified signal waveforms of the charge pump circuit

the feedback voltage (V_{sense}) which is compared to the reference voltage (V_{ref}). An error amplifier is still applied, and according to the difference between V_{ref} and V_{sense}, the output signal (can be current or voltage) of the amplifier varies to control the on-time of the switch. Through the on-time voltage signal, the gate signal is controlled. When the output current increases, the on-time of the switch becomes longer leading to a lower input voltage. As a result, the output current is brought back to the nominal value. The output current decides the input current flowing through the diode, which means the control is also a closed - loop control. A constant output power for the LED load is then realized through above methods.

Besides, since the diode current is sampled from positive periods of the ballast current and the amplitude equals to the peak current of the input current, the current ripple in the diode is also high

(similar to the previous boost in BCM). Moreover, the load power comes from capacitor when switch is on(in a part of positive period and the whole negative period). So a relatively large output capacitor (larger than the SMPS output capacitor) is needed to store energy and filter the AC components. In order to guarantee the output voltage of the NOR gate is higher than gate-source voltage, the selection of those two components need to be considered together.

4.2.2. The implementation of the charge pump design
According to the design principle, the implementation of the charge pump circuit is shown in Fig. 4.19. The circuit should satisfy the requirements mentioned in Chapter 1. The AC input represents the ballast output current.
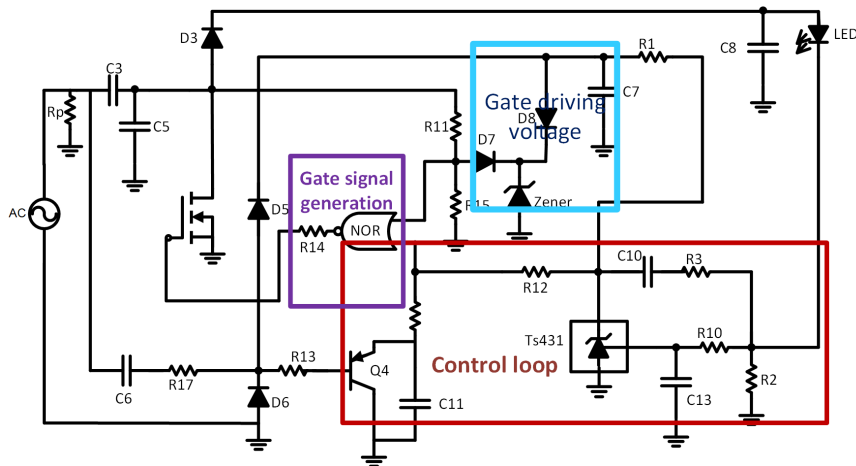

Figure 4.19: The basic schematic of the designed controlled charge pump circuit

In the practical test, it has been found that for Philips' ballasts, a DC path for charging the supply voltage of IC in the ballast is required. Besides, the output current is gained only from positive period. Thus DC components in the circuit loop resulting an unbalance input voltage seen by the ballast. When facing such a voltage, Philips' ballasts would shut down to protect the circuit. To eliminate circuit failure due to the ballast characteristics, and increase the compatibility of this solution, a resistor is added in parallel at the input stage of the circuit, which can give a grounded path for the DC component.

4.2.3. Gate signal generation
The gate signal generation part is mainly consist of the NOR gate, the transistor Q4, and the zener diode (gate voltage source). The 74LVC1G02 chip is chosen as the single 2-input NOR gate in practical, and the logical symbol is shown in Fig. 4.20(a). The maximum supply voltage of 74LVC1G02 is

Inputs	Inputs	Outputs
A	B	Y
L	L	H
L	H	L
H	L	L
H	H	L

a. Logical symbol of 74LVC1G02   b. Function table of 74LVC1G02
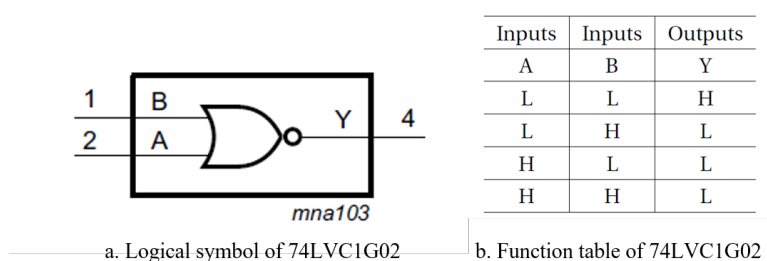
Figure 4.20: Information of 74LVC1G02[24]

6.5 V. The high-level input voltage and the low-level input voltage are defined as $0.7V_{cc}$ and $0.3V_{cc}$

respectively. In the practical test, due to the hysteresis control in this chip, the input voltage will be seen as high level when it is higher than $0.5V_{cc}$ during the rising edge. The high-level output is (V_{cc} - 0.1) V and the low-level output is 0.1 V. The function table is shown in Fig. 4.20(b). Assume A is the input of the NOR gate, sampled from V_{DS}, which follows the change of the output Y, and B is the timing input of the NOR gate, connected to the control loop. Y is the output of NOR gate, which also represents gate signal.
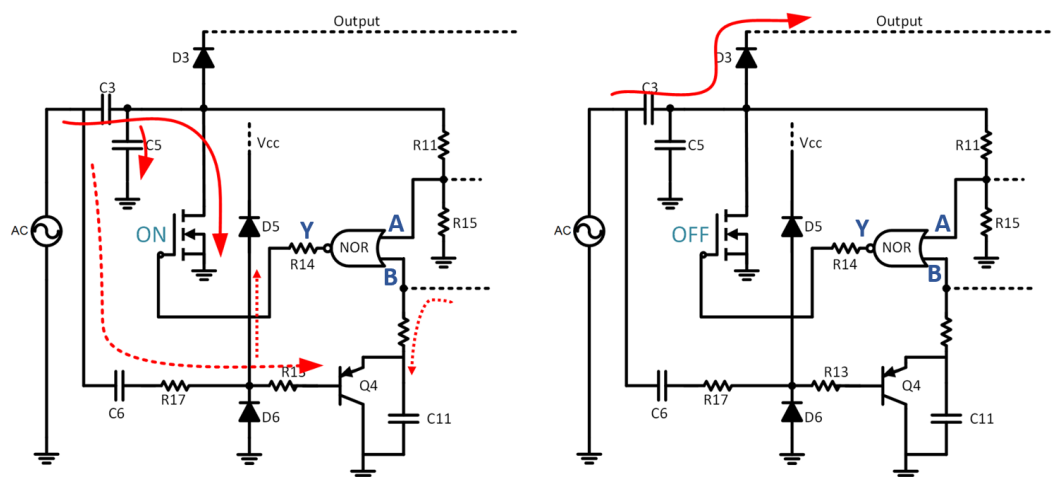

Figure 4.21: Current flow during the positive period of the ballast current

Fig. 4.21 describes the switch-on (left) and switch-off (right) transition during positive half-periods of the ballast current. At first the switch keeps on (during the previous negative period the switch is on), because the input B is at low level until it is charged to 2.7 V. After the input B becomes high, the output Y shifts to the low level which means the switch is off. Then the input A follows the high level and the input current flows to the output through the diode D_3). The T_{on} (switch-on) time can be defined similar to the previous design. During the oscillation, R_{12}, R_{16} and C_{11} are in series. The control voltage can be seen as the voltage source for oscillation. T_{on} is:

$$T_{on} = T - T_{off} \tag{4.20}$$

Where T is the ballast operation period. the T_{on} time contains the oscillation part (before the V_B reaches 2.7 V from 0 V) and the non-oscillation time (negative half-period), while switch-off time (T_{off}) is the pure oscillation time. To simplify the calculation, the T_{off} is obtained first. The time constant τ is:

$$\tau = C_{11}(R_{12} + R_{16}) \tag{4.21}$$

The T_{off} time is the time interval the oscillation voltage changes from 2.7 V to 3.4 V(2.5 V plus V_{EB}).

$$T_{off} = -\tau ln(1 - \frac{3.4 - 2.7}{V_{control} - 2.7}) \tag{4.22}$$

$V_{control}$ depends on the feedback loop and will be explained in section 4.2.3. When the ballast current changes the direction from positive to negative, the current flows from ground to the ballast through D_6, R_{17} and C_6 (see Fig.4.22(a)). During this transition, the switch keeps off before V_{EB} of Q_4 reaches 0.7 V.

The black dot square area of Fig. 4.23(a) presents the switching transition where the current will go to the ballast from the diode. Once Q_4 is on, the input B starts to fall to zero while input A is still high. The output Y then turns to the low level and next the switch turns on.

Fig. 4.22(b) shows the current flowing when the ballast current is in negative half-periods. The input A and B are low, leading to a high output, which means switch is on. During this half period,
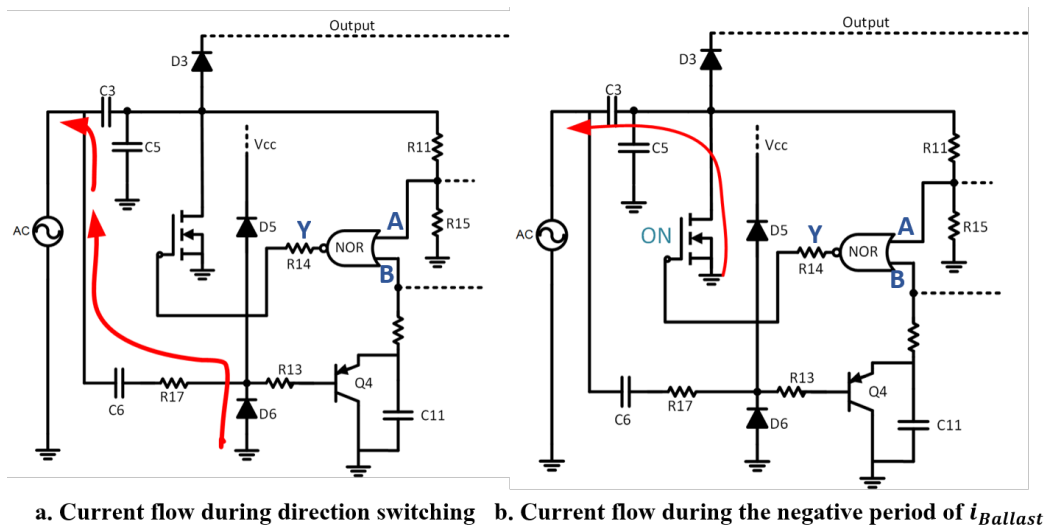
a. Current flow during direction switching   b. Current flow during the negative period of $i_{Ballast}$

Figure 4.22: The current flow during the negative half-period and switching transition

a. Currents of R17 and D6 from the simulation   b. The switch current and the ballast current from the simulation
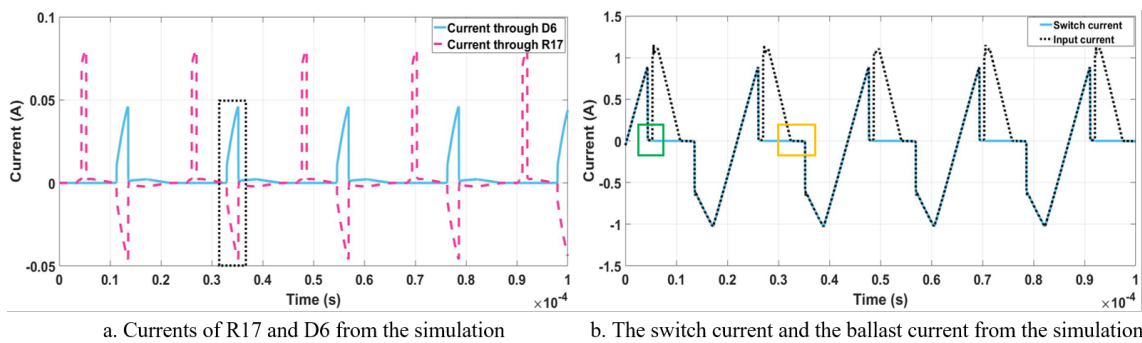
Figure 4.23: Current waveforms of mentioned parameters

no current will be used for the output power and all current will go back to the ballast through the body diode of the MOSFET. Current waveforms of the ballast current and the switch current in this transition are shown in Fig. 4.23(b). During the positive period in the green frame area, both currents are zero. It is because that the diode is reverse biased before V_{DS} reaches the LED voltage. The input current then goes to C_6 rather than the switch or the diode. The time interval (in yellow frame) where the switch current and the ballast current are both zero presents the switching transition. After gate voltage (V_{gs}) turns to a high level, the ballast current flows back through the MOSFET during the rest of negative half-periods.

4.2.4. Control method

The control method is realized similar to the previous design. The output current is sensed by a resistor, and then compare the voltage drop on the sense resistor ($I_{LED}R_{sense}$) with the reference voltage of TS431 (The structure of TS431 is in Fig. 4.4). The control voltage is derived from the output current (I_k) multiplied by R_{12}, which controls the timing part of the gate signal generation by the input B of the NOR gate. The input A and B together with output Y are given in Fig. 4.24. The red line is the input B which represents the timing part. During the charging interval the input B and A are low and the output Y is high (switch is on). Once the input B reaches 2.7 V, the output Y is reversed to a low level (switch is off). When Q4 is off, the voltage level of the timing input B increases. If the LED current increases, the control voltage becomes lower and decelerates the oscillation in R_{16}
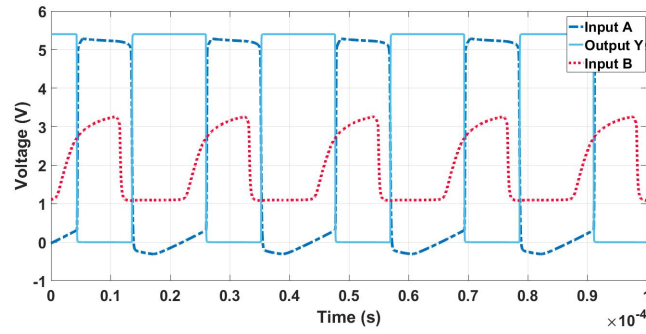
Figure 4.24: Input A and B with output Y from simulation

and C_{11}, leading to a shorter off-time of Q4. Therefore, the interval of the timing input at a low level is increased in one period, which means the on-time of the switch will prolong. More current will go back to the source through the switch, reducing the LED current and stabilizing the system. This
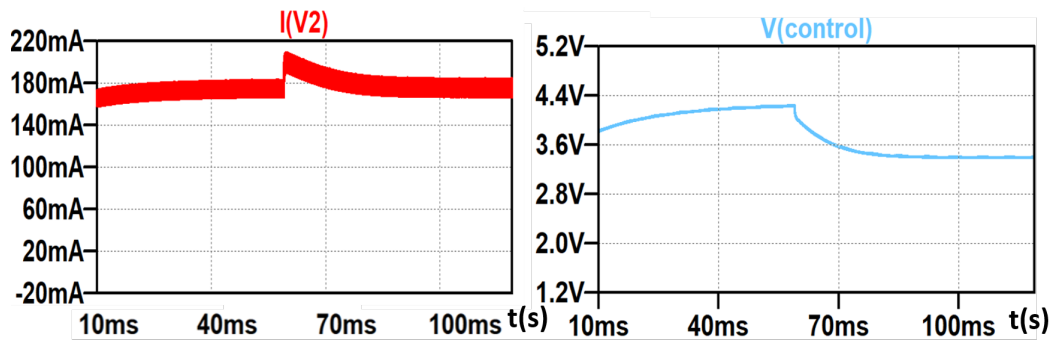

Figure 4.25: The LED current and control voltage when a disturbance added to the system in the simulation

simulation results of the control process is shown in Fig. 4.25. At t = 60 ms, an 100 mA AC current is added to the source. The LED current increases abruptly due to this disturbance and then goes back to original value. The decreasing control voltage reflects the feedback loop working normally.

4.2.5. The load Impedance
The load impedance of this design mainly depends on C_3 and C_5. The function of C_3 is applied to block the DC components and C_5 is for shunting current. From the chapter 3, adding a parallel capacitor to the ballast will low down the load impedance seen by the ballast, resulting in a higher ballast current. Besides, increasing C_5 draws more current to the C_5 rather than the load. As a result, the output power will be reduced if the LED voltage keeps constant. For a high output power, C_5 is removed from the circuit. Moreover, in order to build the input voltage as balance as possible, the DC block capacitor is chosen to close to the DC capacitor (mostly 220 nF)in the ballast.

4.2.6. Simulation validation
To get the enough power for LED load which matches 80 W ballast, a sufficient LED current or LED voltage should be provided. For the LED current, the output current is gained only from the half-period ballast current and a part of the positive current cannot be delivered to the load due to the delay from timing part charge. Thus the LED voltage is changed from 150 V to a suitable value to fit the power requirement.

$$P_c = \frac{1}{2}\Delta U_c^2 f \frac{1}{T_{on}} \tag{4.23}$$

Where P_c is the power transferred from the output capacitor and f is the operation frequency. Different from the previous design, the switching frequency in charge pump circuit is the same as the ballast operation frequency. T_{on} can be calculated by 4.20 and 4.22. According to the simulation result, the sense resistor is changed to get the maximum LED current (205 mA) where the control loop still works. If the LED current is set too high, then the ballast current cannot supply enough current for the load. Accordingly, the control loop is saturated. With the maximum LED current, the power under 150 V LED voltage is 30.5 W. Practical test also shows similar result. Therefore, the LED voltage is increased to 180 V to provide enough output power in practical.

The simulation results except the mentioned figures above are shown as below. The LTspice model is based on the Fig. 4.19. Fig. 4.26(left) corresponds to the input voltage and LED voltage. Current sampled only in half period results in the unbalance input voltage, this drawback cannot be eliminated without a rectifier. The input current, diode current and LED current are given in Fig. 4.26(right). Only in the positive period the current will be sampled from the load power. A part of the ballast current in the positive period supplies the load due to the delay of timing. The LED current is 204 mA and the ripple in LED current is small enough to meet the standard.

a. LED voltage and Input voltage   b. LED current, input current and diode current
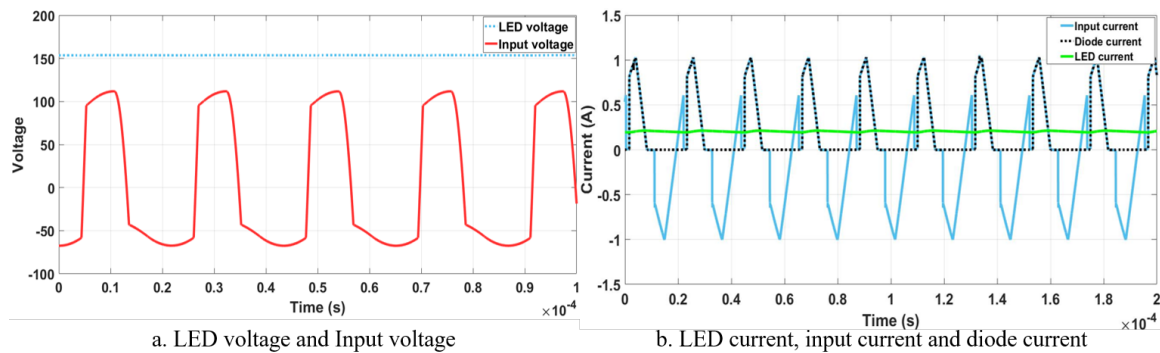
Figure 4.26: Input and output parameters in the simulation

4.2.7. Experimental validation
The practical circuit is built according to the Fig. 4.19, and the test circuit is in Appendix.A.3. In Fig. 4.27(a), the yellow line is the current through diode and the green line is the ballast current. The diode current supplies LED current, which is sampled from the positive period of ballast output current. The RMS current of ballast is 627 mA from the power meter which is more precise than the value from the oscilloscope. The currents of the switch (yellow line) and the ballast (green line) are shown in Fig. 4.27(b). It can be seen that a part of positive input current goes to the switch rather than the load as the delay of timing charge.

a. Diode current and ballast current   b. Switch current and ballast current
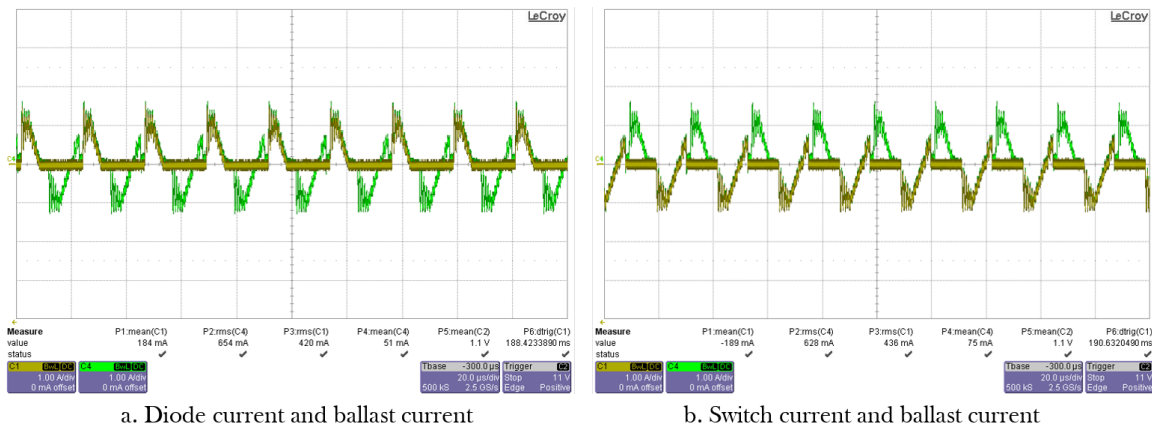
Figure 4.27: The ballast current with the diode current and the switch current

Similar to the ballast current in the SMPS tests, the oscillation in the current waveforms appears during the dead time of the switches in the half bridge of ballasts. A small resonance in the ballast output stage happens, leading to an oscillation of the output current.
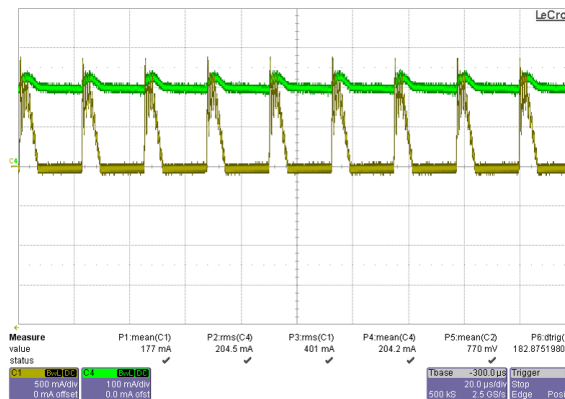

Figure 4.28: The LED current and the diode current

In Fig. 4.28, the LED current and the diode current are in green and yellow respectively. After filtered by the output capacitor the LED current ripple is 20% (peak to peak LED current divided by average LED current) which meets the standard. The basic electrical parameters of the charge pump circuit is given in Table. 4.10. The total power loss is 1.1 W which is lower than the previous boost circuit (2.4 W), mainly due to the lack of rectifier and inductor. The power loss distribution is in Table. 4.11. So it seems that this circuit features the high efficiency and a small circuit size.

P_{in} [W]	P_{out} [W]	V_{in} [V]	V_{out} [V]	I_{LED} [mA]	Efficiency [%]
38.8	37.7	92.6	181.6	208.0	97.3

Table 4.10: Basic electrical parameters of the charge pump circuit in the test

The principle of loss calculations of MOSFET, diode and capacitor are identical to the section 4.1.12. The main loss from the calculation is 1.07 W which is lower than 1.1 W from the power meter. The rest of loss is from other resistors, parasitic elements and soldering. The capacitor loss contains the input DC block capacitor (220 nF) and output electrolytic capacitor (10 μF). The loss of the power diode and MOSFET is much lower than the boost circuit mainly because of the low switching frequency(the ballast operation frequency).

	Parallel resistor	R_{sense}	MOSFET	Diode	Capacitor	Total
Power loss [W]	0.36	0.26	0.095	0.094	0.26	1.07
Percentage [%]	32.7	23.6	8.6	8.5	23.6	97.2

Table 4.11: Main loss in the circuit

4.2.8. Change based on initial test results

Due to the decreased load impedance, the RMS current of the ballast is 627 mA which is 114% higher than the original ballast current (550 mA). The increase of the ballast current produces more heat and shortens the lifetime of ballasts. To low down the ballast current, an inductor is added to increase the output impedance of ballasts. According to section 4.2.5, if the ballast current is reduced, then the LED voltage should be set a higher value to meet the power requirement. A 220 μH inductor is added to the input (see Fig.4.29). The test result is shown in Table. 4.12.
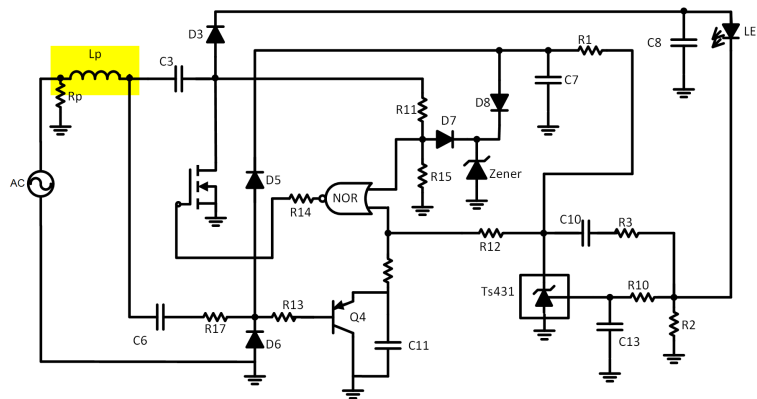

Figure 4.29: Improved charge pump topology for decreasing the ballast current

The ballast current is reduced to 570 mA according to the Table. 4.12. However, the efficiency decreases from 97.3% to 94.1% mainly due to the inductor and the parallel resistor. The input voltage increases to 104.6 V from 92.6 V because of the decreased input current. The loss distribution is shown in Table. 4.13.

P_{in} [W]	P_{out} [W]	V_{in} [V]	V_{out} [V]	I_{LED} [mA]	$I_{Ballast}$ [mA]	Efficiency [%]
39.1	36.8	104.6	204.3	180	570	94.1

Table 4.12: Basic electrical parameters of charge pump circuit after an inductor added

	Parallel resistor	R_{sense}	MOSFET	Diode	Capacitor	Inductor	Total
Power loss [W]	0.47	0.2	0.095	0.093	0.19	1.3	2.38
Percentage [%]	20	8.7	4.1	4.0	8.3	56.5	103

Table 4.13: Main loss in the changed circuit

The related information of the inductor used in the test is given in Table. 4.14. The inductor loss is relative high compared with other loss in this design. The ohmic copper loss is 0.2 W, and the winding loss due to the AC current is 0.42 W. The other loss (0.68 W) is core loss, because the inductor current ripple is high leading to a large flux change.

After the inductor is added to the circuit, the efficiency has no superiority compared with the boost circuit. Besides, with the similar inductor current but a higher inductor value than the boost design, the size advantage is weakened as well. Moreover, the inductor brings some resonance components to the circuit, which can be noticed from the inductor current (in Fig. 4.30). Although this changed

Inductance [μH]	$R_{AC}[\Omega]$	$R_{DC}[\Omega]$
215	1.3	0.59

Table 4.14: Inductor information tested in 45 kHz

circuit has been tested on other ballasts and similar results are shown, the stability and compatibility of this change still need to be discussed. The diode current and LED current are given in Fig. 4.31.
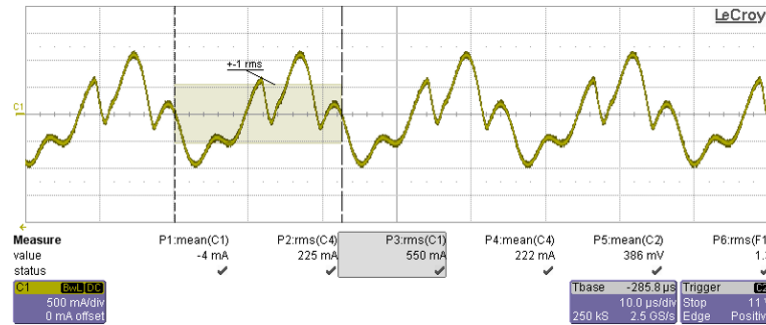

Figure 4.30: Inductor current of the changed charge pump

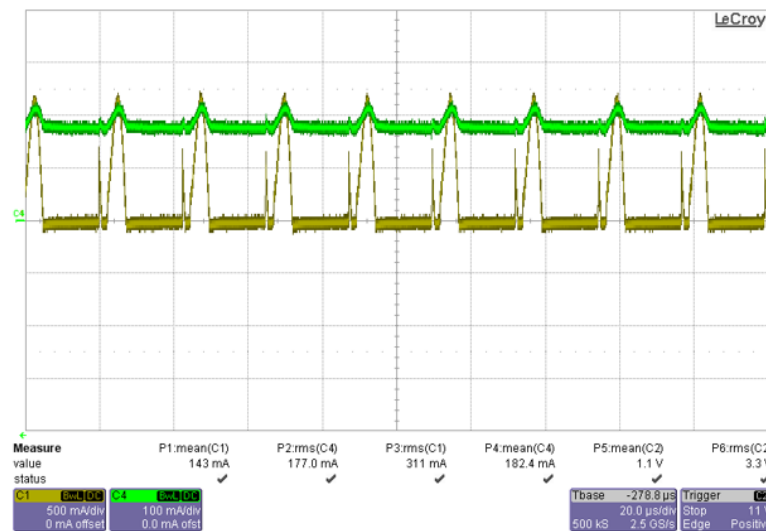The LED current ripple is around 25% of the average LED current.

Figure 4.31: The LED current and the diode current of the changed charge pump circuit

4.2.9. Conclusion of the controlled charge pump method

The experimental circuit is setup on the Philips HF-P 80W ballast and also tested on other ballasts(eg. Exlc 180). In this design, the output of the initial circuit supplies the 180 V LED load and the ripple in the LED current is low enough to meet the standard of Philips lighting (the peak to peak LED current divided by the average LED current less than 30%). The output power also can be controlled in a constant value by the close loop control. The high efficiency and small size of this design make it as a promising choice for the compatibility design.

In addition to above benefits, however, there are some drawbacks. The increase of the ballast current brings more heat and reduces the lifetime of ballasts. Although the changed circuit (with inductor in series) can reduce the ballast current, the additional loss and the increase of the circuit size are

not desirable. For the boost circuit, the size is around 335 mm^2 (Only the rectifier and the boost part are considered in the calculation for the total circuit volume). The size of the charge pump circuit is about 188 mm^2 without the inductor. While the size will be extended to 336 mm^2 after adding the inductor. Besides, the compatibility and the stability of the circuit go down due to the added inductor which inductor may bring resonant points to the system.

5

Conclusion

According to previous solutions, comparison and design suggestions come up in this chapter as a conclusion.

5.1. Comparison of compatibility designs

In previous chapters, two approaches are considered for the compatibility design between the ballasts and TLED drivers. The classification is based on if active components are applied in the design. Concerning the active method, two possible designs are shown in Chapter 4, which are the boost topology and charge pump topology respectively. The passive approach is simply speaking to put a suitable inductor in parallel with the ballast output stage. Features of each solution are listed as below.

5.1.1. The passive method

The adjustment of the ballast output impedance, specifically increasing the impedance, is the primary idea in this method. Four impedance matching structures are discussed in Chapter 3. The parallel inductor solution seems like the best one over other three solutions. The inductor loss in this structure is less than other two methods (SMPS and adapted charge pump), due to the low inductor current and low operation frequency. This solution owns the most simple structure compared with active methods. Only an inductor is added to the LED driver and the chosen inductor size is 10 mm×9 mm which is small enough to fit in T5 tubes. However, there is no control loop to regulate the output power when the ballasts are changed.

5.1.2. The boost method

According the requirements in section 1.3.1, the main topology of this design consists of a rectifier and a boost converter. With the control loop applied to this design, the output power can be kept constant when different ballasts (but in same power level) are connected. The main loss in this circuit comes from the inductor. The core loss is dominated because the boundary condition mode contains a high inductor current ripple. The efficiency is increased to an acceptable value after some improvements have been done. The key shortage of this design is the relative large size, while the reduction of output capacitor could save some space for the inductor and rectifier.

5.1.3. The charge pump method

The impressive advantages of the initial charge pump design are the high efficiency and the small circuit volume. Besides, this design also has control loop which could guarantee a constant output

power with various ballasts. Nonetheless, the high ballast current becomes an obstacle to the application of this design. The added inductor lowers down the ballast current but significantly decreases the efficiency and extends the circuit size. Besides, only less than one polarity of the ballast current is used for the output power. For ballasts which have relatively low ballast current, this solution may not supply enough power for the load.

The inductance adopted in the charge pump circuit (220 μH) is different from the boost circuit (100 μH). Nevertheless, the RMS inductor current and peak inductor current are similar in these two circuits. Although the types of inductors are different, for higher inductance and similar wiring area, the number of turns should be higher as well. Therefore, the 220 μH inductor has a higher DC resistance (Test results: 0.23 Ω in 100 μH and 0.59 Ω in 220 μH). Besides, the 220 μH inductor is non-shielded thus the flux is more divergent, causing more core losses. The suitable frequency ranges of those two inductors are also different. Despite the charge pump circuit working on a lower frequency, the resonance due to the added inductor causes more oscillations. Therefore, the inductor loss is higher in the charge pump circuit than the boost circuit.

5.1.4. Criteria definition

Requirements in section 1.3.1 are generated by the desirable system behaviors when the ballast is connected to LED loads and the circuit design criteria. To evaluate each design, the criteria list in Table. 5.1 is given based on the requirements. The importance means the significance of this criterion.

NO.	Criteria	Importance
1	Compatibility	NA
2	Size	4
3	Light consistency	5
4	Stability	6
5	Cost	1
6	Increase of ballast current	3
7	Efficiency	2

Table 5.1: List of criteria

- NA is the abbreviation for "Not Applicable". This is because compatibility must be met in each solution.

The first three criteria have been explained thoroughly in section 1.3.1. The compatibility indicates that the design can be employed in T5 LED drivers, Besides, thermal and electrical stress should be also concerned in a controlled range which guarantees the reliability and the lifetime of the products. The ballasts should be able to work normally with the added LED drivers. For this requirement, the specific value for evaluation is difficult to derive. The compatibility therefore contains many detailed but measurable indexes. Due to the time issue, this requirement is simplified based on basic circuit behaviors. In terms of the size limitation, the dimension of one side PCB for a LED driver and the filament emulation is $40 \times 10 mm^2$ (The filament emulation occupies 19.84 mm^2). All solutions should be fitted in the two sides of PCB board, and for criteria evaluation, only the area of each solution is ranked. To fit in T5 tubes the size of the circuit should be small enough. Moreover, with a smaller size, more flexible changes for heat dissipation could be done if necessary. Light consistency means a stable light level (no flickers) should be achieved. The current through LEDs needs to maintain a stabilized illumination. For stability, reliable working behavior of the LED driver should

be achieved. Moreover, different ballasts have different operation frequencies and LC stages. The judgment of stability therefore comes from the test results in different ballasts. The operation range of each design is the main criteria to assess this requirement. Concerning the increase of the ballast current, the ballast current with LED load should be limited less than 120% of the fluorescent situation. The efficiency and cost are non-functional requirements when considering the comprehensive ability of each solution. In terms of active designs in the thesis, the cost has direct proportion to the size.

5.1.5. Criteria evaluation

To compare different solutions, "weighted rating method" is adopted [25]. This method helps to evaluate every design based on the its completion of requirements mentioned in Table. 5.1. The final score is the sum of each score multiplied by the "Importance". Table. 5.2 introduces the score standard for every requirement.

NO.	Criteria	Score 1	Score 2	Score 3
1	Compatibility	/	/	/
2	Stability	NA	50% < N < 80%	N > 80%
3	Light consistency	Ripple > 30%	20 % < Ripple < 30%	Ripple <20%
4	Size	NA	>200 mm^2	< 200 mm^2
5	Cost	> 3 €	2 - 3 €	< 2 €
6	Increase of ballast current	> 120% of I_B	110% - 120% of I_B	100% - 110% of I_B
7	Efficiency	< 90%	90% - 95%	>95%

Table 5.2: Solution score standard

-I_B means the ballast current with fluorescent lamp load.
-NA is the abbreviation for "Not Applicable".

The compatibility is defined as chapter 1. The classification is based on practical test results, including current and voltage waveforms, thermal test, and etc. The initial evaluation is roughly given, since the time limitation is not enough for more detailed results. The degree of stability is gained according to the test results of the number of ballasts the circuit can match and realize the power requirement divided by the total number of ballasts . The size reference is based on released TL5 drivers (130 mm^2). Besides, the size is mainly consider the area rather than the volume, because the height of all applied components is lower than the output capacitor in released products (11 mm). The cost is an estimated value only including active components and inductors. All unite prices are under the condition of ordering 1000+ products from the Farnell website considering mass production (price of each design is in Table. 5.3).

Design	Parallel inductor	Boost circuit	Charge pump circuit2	Charge pump with inductor
Cost [€]	2.7	2.41	0.758	1.634

Table 5.3: Cost of each solutions

Table. 5.4 shows the evaluation of each solutions. The SMPS solution has the best behavior than other solutions. It should be noticed that if importance of requirements are changed according to specific requests, it is possible to choose other solutions.

Requirements	Importance	Solution 1	Solution 2	Solution 3	Solution 4
1	Compatibility	/	/	/	/
2	Stability	2	3	3	2
3	Light consistency	2	3	2	2
4	Size	3	2	2	2
5	Cost	2	2	3	3
6	Increase of ballast current	3	3	1	3
7	Efficiency	3	2	3	2
Total	/	51	56	48	46

Table 5.4: Evaluation of solutions

- "Solution 1" is the parallel inductor method
- "Solution 2" is the boost converter method
- "Solution 3" is the charge-pump circuit without inductor
- "Solution 4" is the charge-pump circuit with inductor

5.2. Conclusions and suggestions

This thesis works on the compatibility design of T5 LED drivers to the electronic ballasts. The possibilities and behaviors of the passive method and the active method are investigated in Chapter 3 and 4 respectively. In the comparison part, to simplify and clarify the explanation, "weighted rating method" is adopted to rank each solution. The boost solution shows more potential over other solutions based on the criteria in Table. 5.1 and the PCB demo of this design is in Fig. 5.1. It should be noted that all tests and simulation results are done on 80 W ballasts, which have the highest power requirement but the size limitation is the same as the T5 ballasts in the lower power level. For T5 ballasts of different powers, the solutions above could still make functions by means of parameters adjustment.
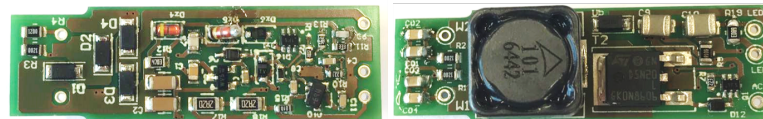

Figure 5.1: The demo of the boost method

Concerning the future work, there are several suggestions. For the passive method, the mathematical analysis of the second order system (the parallel inductor case) and the third order system (series solutions) could be done to provide a more precise description of the system. Besides, the range of ballasts can be extended in the experimental test, leading to a complete conclusion for the function of passive components. In terms of active methods, the optimizations of the boost design may focus on the over-voltage protection and shrinking circuit volume. Additionally, the selection of the inductor has a promising space to improve. For the charge pump circuit, the improvement should be concentrate on reducing the ballast current. Furthermore, those solutions could be extended to ballasts in other power levels. The validation and experimental research could be done based on this thesis.
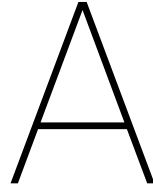
A
Appendix

A.1. Mathcad model

Mathcad is a popular software for verification, validation, documentation of engineering calculations. For second order resonant system, a mathematical model is built in Mathcad. The definition part is shown in Fig. A.1.
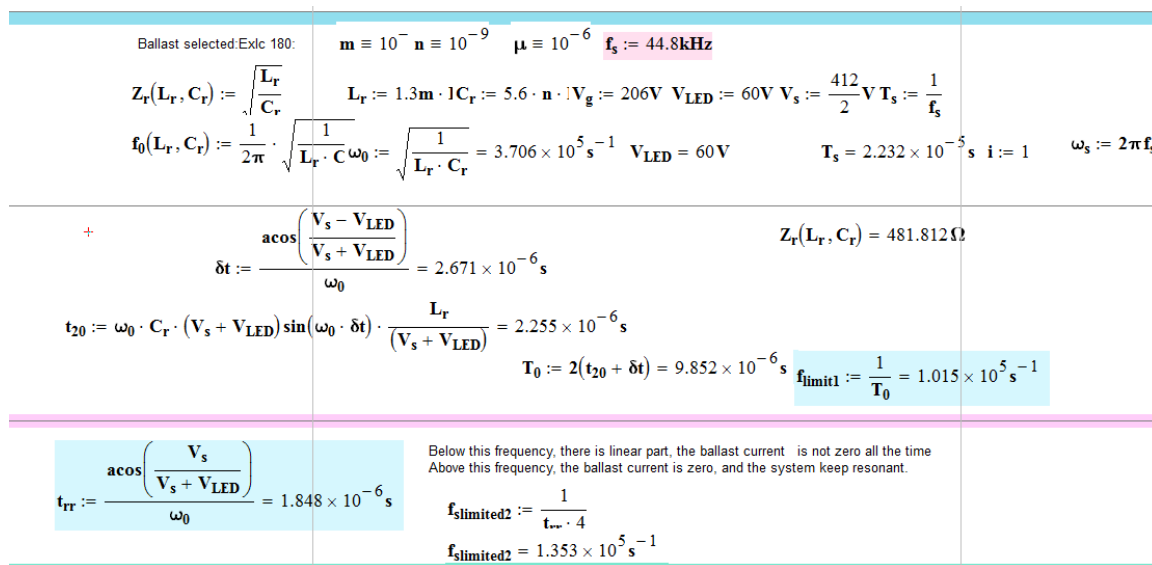

Figure A.1: Mathcad model definition

The model above is shown the parallel capacitor condition. For parallel inductor V_s is replaced by V_{eq} and ω_0 is consist of L_e and C_r. V_{eq} and L_e are defined as follow.

$$V_{eq} = \frac{L_p}{L_p + L_r} V_s \tag{A.1}$$

$$L_e = \frac{L_p L_r}{L_p + L_r} \tag{A.2}$$

In different conditions, the equations of each variables are different. The main functions is in Fig. A.2.

Main function

$$u_c(t, C_r, V_{LED}, f_s) := \begin{cases} u_{c1}(t, C_r, V_{LED}, f_s) & \text{if } 0 < f_s < \frac{1}{T_0} \\ u_{c2}(t, C_r, V_{LED}, f_s) & \text{if } \frac{1}{T_0} \le f_s < \frac{1}{t_{rr} \cdot 4} \\ u_{c3}(t, C_r, V_{LED}, f_s) & \text{if } f_s = \frac{1}{t_{rr} \cdot 4} \end{cases}$$

$$i_L(t, C_r, V_{LED}, f_s) := \begin{cases} i_{L1}(t, C_r, V_{LED}, f_s) & \text{if } 0 < f_s < \frac{1}{T_0} \\ i_{L2}(t, C_r, V_{LED}, f_s) & \text{if } \frac{1}{T_0} \le f_s < \frac{1}{t_{rr} \cdot 4} \\ i_{L3}(t, C_r, V_{LED}, f_s) & \text{if } f_s = \frac{1}{t_{rr} \cdot 4} \end{cases}$$

$$u_L(t, C_r, V_{LED}, f_s) := \begin{cases} u_{L1}(t, C_r, V_{LED}, f_s) & \text{if } 0 < f_s < \frac{1}{T_0} \\ u_{L2}(t, C_r, V_{LED}, f_s) & \text{if } \frac{1}{T_0} \le f_s < \frac{1}{t_{rr} \cdot 4} \\ u_{L3}(t, C_r, V_{LED}, f_s) & \text{if } f_s = \frac{1}{t_{rr} \cdot 4} \end{cases}$$

$$i_{ballast}(t, C_r, V_{LED}, f_s) := \begin{cases} i_{ballast1}(t, C_r, V_{LED}, f_s) & \text{if } 0 < f_s < \frac{1}{T_0} \\ i_{ballast2}(t, C_r, V_{LED}, f_s) & \text{if } \frac{1}{T_0} \le f_s < \frac{1}{t_{rr} \cdot 4} \\ i_{ballast3}(t, C_r, V_{LED}, f_s) & \text{if } f_s = \frac{1}{t_{rr} \cdot 4} \end{cases}$$

$$i_{LED}(t, C_r, V_{LED}, f_s) := \begin{cases} (-i_{ballast}(t, C_r, V_{LED}, f_s)) & \text{if } i_{ballast}(t, C_r, V_{LED}, f_s) \le 0 \\ i_{ballast}(t, C_r, V_{LED}, f_s) & \text{if } i_{ballast}(t, C_r, V_{LED}, f_s) \ge 0 \end{cases}$$

$$i_{ballast\_rms} := \begin{cases} i_{ballast1\_rms} & \text{if } 0 < f_s < \frac{1}{T_0} \\ i_{ballast2\_rms} & \text{if } \frac{1}{T_0} \le f_s < \frac{1}{t_{rr} \cdot 4} \\ i_{ballast3\_rms} & \text{if } f_s = \frac{1}{t_{rr} \cdot 4} \end{cases}$$

Figure A.2: Main functions of Mathcad model

The main function is defined according to operation frequency. With listing the functions in each operation frequency range, all variables can be expressed ($i_L(V_{LED}, C_p, f_s)$, $u_c(V_{LED}, C_p, f_s)$. V_{LED}, $I_{Ballast}(V_{LED}$, etc.).

A.2. SMPS test circuit

The test board of SMPS circuit is shown in Fig. A.3. The front is in the left side. The MOSFET and other SMD components are in the other side for soldering and testing convenience. The soldering shortage brings some parasitic problems (especially in the control part) during the test. The circuit behavior can be better when PCB board is applied.
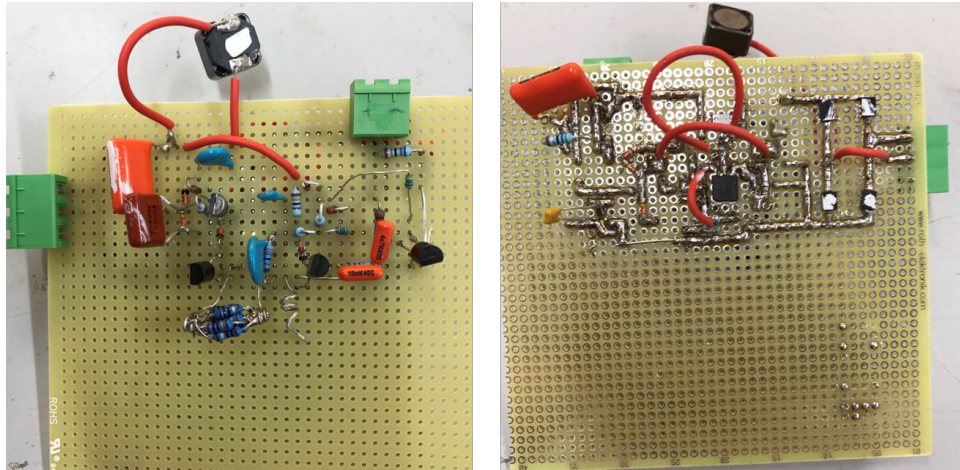

Figure A.3: Test circuit of SMPS method

The wire should be as short as possible between diode, switch and inductor, to reduce the parasitic influence of the circuit behavior. The LED load is shown in Figure. A.4. Each LED strip is for 50 V LED load, and the structure is two half LED strips (every LED is in series) in parallel. The load can be flexible when different LED voltages are needed.
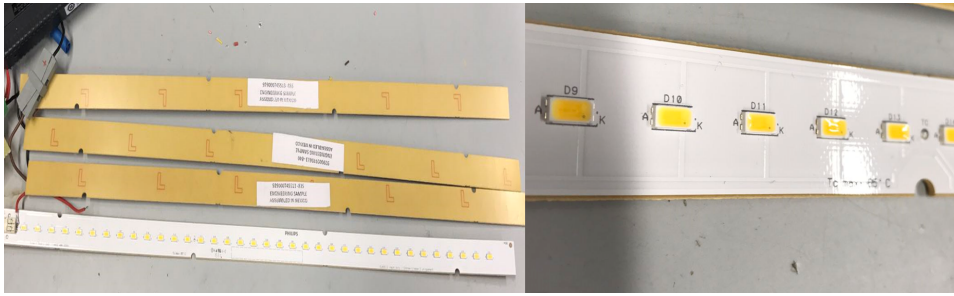
Figure A.4: LED load in the test

This LED load is applied in the all tests, and the LED voltage is changed by the number of LED. The test set up diagram is presented in Fig. A.5.
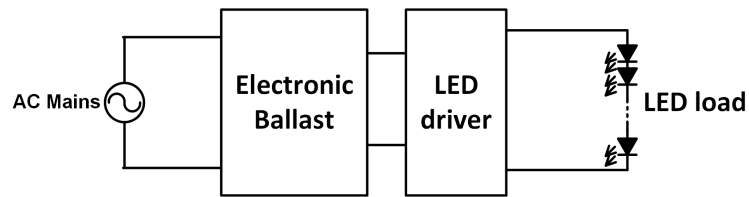

Figure A.5: Test structure

A.2.1. Inductor selection
The inductor selection is based on the test results of three available inductors in the Lab. The test result is shown in Table. A.1.

Inductance [μH]	$I_{sat,typ}$[A]	$R_{dc,typ}$ [mΩ]	Loss in the test [W]	Type
100	3.25	112	1.6	B82477R4
100	3.12	135	1.4	MSS12787
100	1.95	138	1.1	B82477P4

Table A.1: Test results of three inductors

A.3. Charge pump test circuit
The test board of charge-pump circuit is given in Fig. A.6. The power resistor in the back side is added to give the DC path.
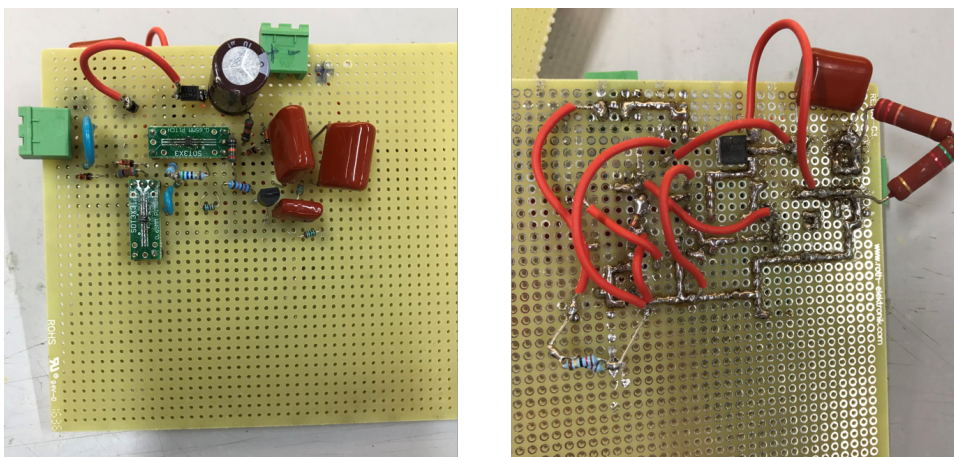

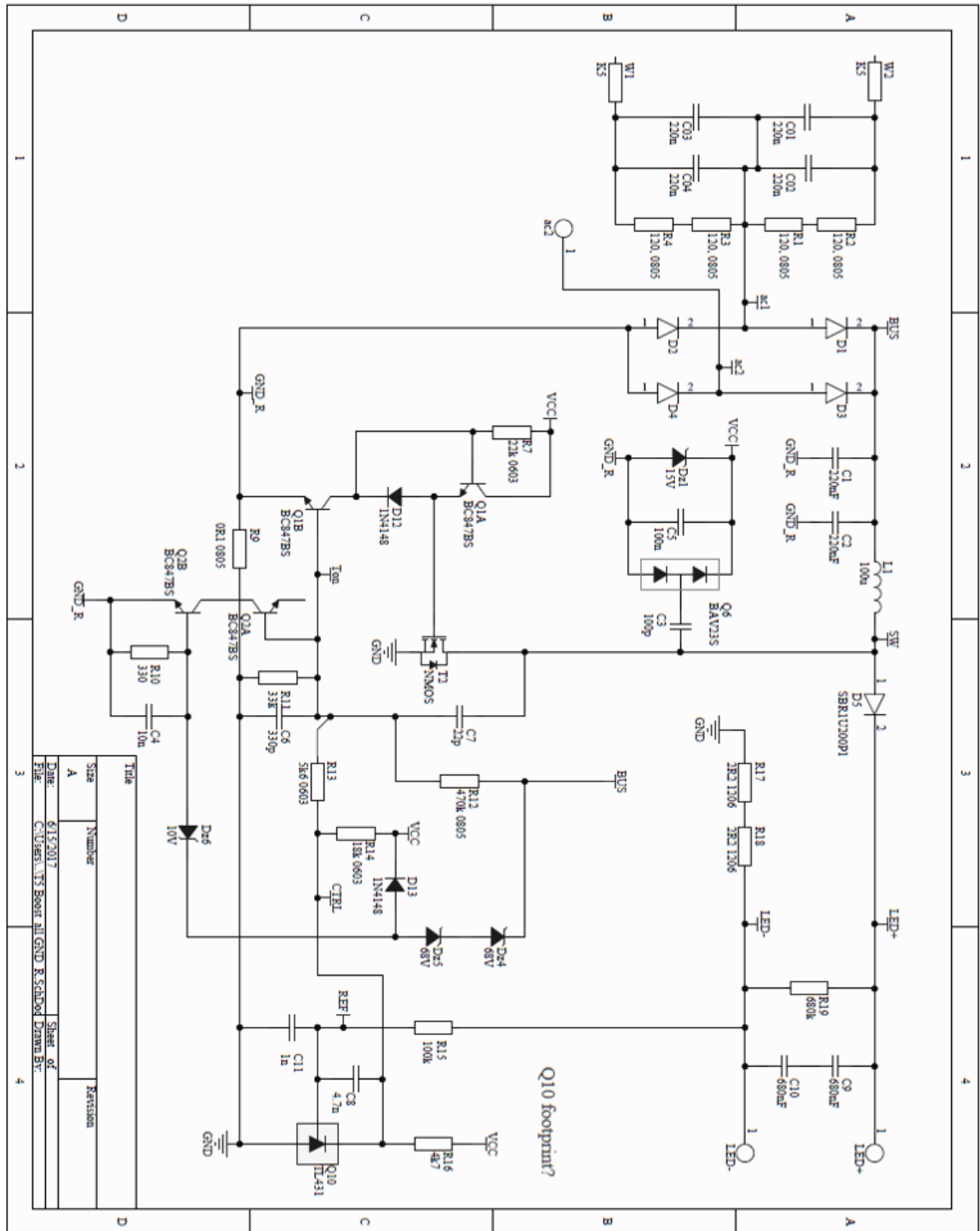Figure A.6: Test circuit of charge pump

A.4. PCB board

Figure A.7: The PCB schematic of implementation in TL5 driver

Bibliography

[1] T.J Keefe. "the nature of light", April. 23, 2012.

[2] Current powered by GE. "cfl vs halogen vs led".

[3] Energy saving trust. "the right light selecting low energy lighting – introduction for designers and house builders", 2016.

[4] Haimin Tao. "emea hf compatible tled obelix development, ", Aug, 2013.

[5] Park Jong-Yeon and Jung Dong-Youl. "electronic ballast with constant power output controller for 250 w mhd lamp", Proceeding of IEEE ISIE, 2001, pp. 46 – 51.

[6] N. Chen and Henry Shu-Hung Chung. "a driving technology for retrofit led lamp for fluorescent lighting fixtures with electronic ballasts", Feb, 2011.

[7] Philips Lighting. "philips master tl5 lamps".

[8] W. M. Ng S. Y. (Ron) Hui, D. Y. Lin and Wei Yan. "a "class-a2" ultra-low-loss magnetic ballast for t5 fluorescent lamps—a new trend for sustainable lighting technology", Feb, 2011.

[9] Haimin Tao. "nam hf compatible tled asterix development", 2013.

[10] Robert W. Erickson and Dragan Maksimovic. "fundamentals of power electronics (2nd edition) new york: Kluwer academic publishers", 2004.

[11] Tom Ribarich. "how to design a dimming fluorescent electronic ballast", Sep, 2006.

[12] S.Riaz-ul-Hasnain D. Shahwar S. Ahmed, F. Amir and S. Jamil. "electronic ballast circuit configurations for fluorescent lamps", Oct, 2015.

[13] Azlan Kamil B Mohammad Fauzy. "self oscillating dimmable electronic ballast", Mar, 2006.

[14] Pedro Luis Dias Peres Ivanil Sebasti~ao Bonatti and Jos´e Antenor Pomilio. "first harmonic analysis: A circuit theory point of view", IEEE TRANSACTIONS ON EDUCATION, VOL. 42, NO. 1, FEBRUARY 1999.

[15] Vishay. "high current, surface mount inductors - wirewound molded datasheet".

[16] Power Sources Manufacturers Association Edited for PSMA by Joseph J. Stockert. "handbook of standardized terminology for the power sources industry, 2nd edition", 1995.

[17] Tore M. Undeland Ned Mohan and William P. Robbins. "power electronics: Converters, applications, and design", 3rd edtion.

[18] ON-semiconductor. "design consideration for boundary conduction mode power factor correction (pfc) using fan7930".

[19] ST life.augmented. "low voltage adjustable shunt reference, ts 431 datasheet".

[20] Arun D Selva Kumar R, Karthick V. "a review on dead-time effects in pwm inverters and various elimination techniques", 2008.

[21] Mladen Knezic Zeljko Ivanovic, Branko Blanusa. "power loss model for efficiency improvement of boost converter", 2011.

[22] ST life.augmented. "std5n20l n-channel 200v - 0.65ω 5a dpak, datasheet", 2004.

[23] Steyaert. M Wens. M. "design and implementation of fully - integrated inductive - dc-dc converters in standard coms", 2011.

[24] Nexperia. "74lvc1g02 single 2-input nor gate, datasheet".

[25] Theodor Stewart Valerie Belton. "multiple criteria decision analysis: An integrated approach", page 321-322, 2002.